

ABSTRACT

Title of Document: THE ROLE OF SPERMIDINE IN THE
REGULATION OF DEVELOPMENT AND
DIFFERENTIATION IN SPERMATIDS OF
MARSILEA VESTITA

Faten Deeb, Doctor of Philosophy, 2009

Directed By: Professor Dr. Stephen M. Wolniak
Department of Cell Biology and Molecular Genetics

Spermiogenesis in the microspore of the water fern, *Marsilea vestita*, is a rapid process where a dry microspore containing a single cell undergoes nine successive mitotic divisions to produce 32 spermatids and seven sterile cells. Immediately after the dry microspore is placed into water, cytoplasmic movements precede the first mitotic division; a number of proteins and mRNAs aggregate into zones that later become the spermatogenous initials of the gametophyte. Development is driven by the regulated translation of stored mRNA with little or no new transcription (Hart and Wolniak, 1999). The pattern of translation in the gametophyte is ordered precisely spatially and temporally, which indicates that certain proteins are required in specific locations at specific stages of development. Spermatid differentiation involves the *de novo* synthesis of 140 basal bodies, the remodeling and condensation of nuclear chromatin and then, nuclear elongation. A complex cytoskeletal structure, the multilayered structure (MLS), is formed at the anterior end of the cell and extends the length of the elongated gamete,

and apparently functions in cell and nuclear elongation. This document focuses on the role of kinesin motor proteins and spermidine in the regulation of gametophyte development and spermatid differentiation. Blocking the translation of various kinesin isoforms with RNA interference (RNAi) resulted in arrested development at distinct time points. Centrin and tubulin immunolabeling showed different defects in basal body and microtubule ribbon formation, respectively, with the silencing of specific kinesins. The reduction of spermidine levels in the gametophytes by silencing proteins responsible for its synthesis and transport reveals the involvement of the polyamine in gametophyte cell cycle regulation and in spermatid maturation. In addition, drug inhibition of spermidine synthesis later in development highlighted the importance of its involvement in chromatin remodeling and nuclear elongation. Immunolabeling of spermidine and *in situ* hybridization assays for its synthesizing enzyme, spermidine synthase, indicated that spermidine levels are controlled in gametophytes by the regulated translation of spermidine synthase. The regulated levels of spermidine in the gametophyte is key to its function as a developmental regulator; spermidine appears to participate in multiple cellular processes in a concentration dependent manner.

THE ROLE OF SPERMIDINE IN THE REGULATION OF DEVELOPMENT AND
DIFFERENTIATION IN SPERMATIDS OF *MARSILEA VESTITA*

By

Faten Deeb

Dissertation submitted to the Faculty of the Graduate School of the
University of Maryland, College Park, in partial fulfillment
of the requirements for the degree of
Doctor of Philosophy
2009

Advisory Committee:
Professor Stephen M. Wolniak, Chair
Professor Todd Cooke
Professor Ian Mather
Assistant Professor Lian-Yong Gao
Associate Professor Douglas Julin, Dean's Rep.

© Copyright by
Faten Deeb
2009

Dedication

This dissertation is dedicated to my family for their endless love and support especially to my parents for their tremendous sacrifices.

Acknowledgements

I would like to thank my advisor, Dr. Stephen M. Wolniak for his guidance, support and patience during this journey. I thank him for teaching me to keep an open mind and allowing me to experiment with different ideas and projects in the lab. This helped me stay motivated and expanded my knowledge and skills. I would like to extend special thanks to Dr. Corine Van der Weele for her helpful discussions and critiques of my research. I am thankful to her for creating an enjoyable environment in the lab, one that I wanted to come to everyday. I also would like to thank my committee members: Dr. Todd Cooke, Dr. Ian Mather, Dr. Lian-Yong Gao, and Dr. Douglas Julin in addition to previous members: Dr. Eric Baehrecke, and Dr. Eric Haag for taking the time to support my project. Their critical comments and valuable advice improved my project and helped me become a better researcher. I thank Dr. Matt Thompson for sharing his particle knowledge and tips about cloning. I also would like to thank Dr. Michael Keller for providing the Lac-Z vectors and his helpful comments on my research. Furthermore, I thank Amy Beaven for her help with the sequencers and the deconvolution microscope. I would like to acknowledge the USDA for the financial support through the Food and Agricultural Science National Needs Graduate Fellowship, and I thank Dr. Heven Sze and Dr. Caren Chang for their efforts to make this fellowship available to the department. Finally, I thank all my family and friends for their unconditional love and support that were great assets for me on this journey.

Table of Contents

Dedication.....	ii
Acknowledgements.....	iii
Table of Contents.....	iv
List of Figures.....	vii
List of Abbreviations.....	x
Chapter I: Introduction.....	1
Rapid development is driven by the regulated translation of stored mRNA.....	2
The role of the cytoskeleton in mRNA localization and translational regulation.....	6
Polyamines and spermiogenesis.....	7
<i>Marsilea vestita</i> , an endosporous, heterosporous fern.....	8
Spermiogenesis in <i>Marsilea vestita</i>	9
Microspore development in <i>Marsilea vestita</i>	14
Patterning and cell fate determination during <i>M. vestita</i> gametophyte development.....	16
<i>Marsilea vestita</i> as an experimental system.....	18
Purpose and significance of this dissertation.....	23
Chapter II: The Role of Spermidine in Microspore Development and Spermatid Nuclear Remodeling.....	25
Introduction:.....	25
Materials and Methods:.....	28
Microspore culture and fixation.....	28
RNAi experiments.....	30
<i>In situ</i> hybridization.....	32
Cytology and immunocytochemistry.....	32
Spermidine Synthase Inhibition.....	33
Results:.....	34
Spermidine localization pattern in the developing microspore.....	34
Development is arrested early after spermidine synthase silencing.....	34
The effect of spermidine synthase silencing on spermatid differentiation.....	39
The effects of spermidine depletion on spermatid differentiation.....	41
The effects of inhibition of microtubule polymerization on nuclear remodeling.....	44
The regulation of SPD distribution during the microspore development.....	48
Discussion:.....	59
The effects of SPD depletion on spermatid differentiation:.....	59
Regulation and control of SPD levels in the microspore:.....	62
Conclusion:.....	63
Chapter III: The Regulation of Transcript Unmasking: The Likely Involvement of Spermidine and Other Cytoplasmic Factors.....	65

Introduction:.....	65
Materials and Methods:.....	68
Microspore culture and fixation.....	68
RNAi experiments	70
<i>In situ</i> hybridization	70
Cytology and immunocytochemistry	71
Addition of polyamines.....	72
Results:.....	72
Spermidine Synthase transcripts have a distinct localization pattern in the developing gametophyte.....	72
Added SPD affects the release of several transcripts during development	78
Transcript abundance is affected differently with different polyamines	84
The EJC complex is involved in the regulation of transcript masking.....	90
Discussion:.....	90
mRNA masking controls translational patterns the male gametophyte of <i>M. vestita</i> ...	92
SPD plays a role in transcript unmasking.....	93
Different polyamines exert different effects on transcript unmasking	95
Several cytoplasmic factors are involved in the control of transcript masking and unmasking in the developing gametophyte.....	98

Chapter IV: The Role of Kinesin Motors in the Gametophyte Development.....101

Introduction:.....	101
Materials and Methods:.....	104
Microspore culture and fixation.....	104
RNAi experiments	105
Cytology and immunocytochemistry.....	106
Results:.....	107
Isolation of kinesin isoforms from <i>M. vestita</i> cDNA library	107
The effects of different kinesin proteins on development and differentiation.....	107
The some kinesin motors are required for early stages of development.....	109
Kinesin II knockdown alters divisions and centrin translational patterns	114
Kinesin encoded by MvU2336 affects cell divisions and basal body positioning.	119
Discussion:.....	124
Different kinesin motors are needed at different developmental stages	125
Kinesin II is needed for the establishment of cell identity.....	126
MvU2336 encodes a kinesin protein required for the orientation of the division plane.	128

Chapter V: Conclusions and Perspectives.....132

Conclusions:.....	132
Future experiments:	139

Appendix I142

Programmed Cell Death in the Jacket Cells.....	142
Introduction:.....	142
<i>In situ</i> cell death detection assay.....	142
LR White embedding.....	142
<i>In situ</i> cell death assay.....	143
Results:.....	144
<i>In situ</i> cell death assay on control gametophytes.....	144
The effects of RNAi treatment for MvU271 on development.....	150
Centrin translation and localization patterns in gametophytes treated with MvU271 dsRNA.....	150
Cell death in MvU271 RNAi.....	154
Appendix II.....	158
Transient Translation in the Developing Gametophytes	158
Introduction:.....	158
Transient Translation of β -galactosidase	159
Generation of LacZ RNA:	159
Transient translation of lacZ-His, color development and imbedding:	159
Results:.....	161
Color detection for lacZ-His:	161
Immunofluorescence staining for lacZ-His:	163
Transient Translation of Centrin.....	163
Centrin constructs:	163
Transient translation of centrin:	165
Results:.....	166
Discussion and conclusions:	168
Appendix III	172
<i>M. vestita</i> cDNA Clones Used in This Study	172
Bibliography	185

List of Figures

Chapter I

Figure I - 1: Cell division patterns during development of male gametophyte of <i>M. vestita</i>	11
Figure I - 2: Differentiation of spermatozoid of <i>M. vestita</i>	12
Figure I - 3: The formation of basal bodies from the blepharoplast.....	13
Figure I - 4: The multilayered structure (MLS) in a developing spermatid of <i>M. vestita</i>	15
Figure I - 5: Distribution of PRP19, a spliceosome component, mRNA during spermiogenesis.....	17
Figure I - 6: Cytoplasmic Poly A-RNA polymerase distribution during spermiogenesis.....	19
Figure I - 7: RNAi effects are sequenc specific and concentration-dependent.....	22

Chapter II

Figure II - 1: Polyamine biosynthetic pathway in mammals and plants.....	26
Figure II - 2: Immunofluorescence localization of SPD during normal gametophyte development.....	35
Figure II - 3: Localization patterns of spermidine synthase mRNA during normal gametophyte development.....	37
Figure II - 4: Spermidine synthase dsRNA treatment successfully reduced the levels of spermidine synthase mRNA in the affected gametophytes.....	38
Figure II - 5: Toluidine Blue-O staining for spermidine synthase silencing showing a range of severity of developmental anomalies.....	40
Figure II - 6: The silencing of spermidine synthase resulted in arrested cell divisions, failed nuclear elongation, and scattered microtubule ribbon.....	42
Figure II - 7: The silencing of spermidine synthase resulted in reduced numbers of cell divisions, anomalously clustered basal bodies and a failure of nuclear elongation in the spermatogenous cells.....	43
Figure II - 8: The inhibition of spermidine synthase enzyme at the onset of the differentiation phase resulted in a failure to form the microtubule ribbon, and produced round nuclei in the spermatogenous cells.....	45
Figure II - 9: The inhibition of the spermidine synthase enzyme at the start of the differentiation phase prevented the localization of centrin into the basal bodies in the spermatogenous cells.....	46
Figure II - 10: Treatment with microtubule depolymerizing drug (oryzalin) prevented the formation of microtubule ribbon but not the MLS.....	50
Figure II - 11: In the presence of a microtubule depolymerizing drug (oryzalin), the basal bodies failed to separate and become evenly distributed.....	52
Figure II - 12: The silencing of spermidine transporter resulted in altered positioning of the division planes and reduced numbers of cell divisions.....	53
Figure II - 13: Spermidine synthase RNAi treatment resulted in reduced levels of spermidine transporter mRNA in the affected gametophytes.....	55

Figure II - 14: The silencing of spermidine transporter prevented the increase in SPD levels in the spermatogenous cells.....	56
Figure II - 15: The silencing of spermidine transporter disrupted cell divisions and the formation of the microtubule ribbons.	57
Figure II - 16: The silencing of spermidine transporter affected basal body formation. ..	58

Chapter III

Figure III - 1: The localization patterns of spermidine synthase transcripts in the developing gametophyte.....	74
Figure III - 2: Spermidine synthase transcripts are detected only in the jacket cells of gametophytes treated with spermidine transporter dsRNA.	75
Figure III - 3: Toluidine Blue-O staining for gametophytes developed in the presence of SPD and fixed at 4 h.	77
Figure III - 4: The addition of spermidine at the time of hydration affects the distribution patterns of spermidine synthase mRNA.	79
Figure III - 5: The normal localization patterns of spermidine synthase mRNA shortly after the activation of development.....	80
Figure III - 6: The addition of spermidine at the time of hydration affects the distribution patterns of several mRNAs.	82
Figure III - 7: The premature release of centrin mRNA does not result in elevated levels of centrin translation.	83
Figure III - 8: Spermidine synthase transcripts show different localization patterns in gametophytes treated with different polyamines.	85
Figure III - 9: Different polyamines have different effects on the distribution patterns of PRP19 mRNA.....	86
Figure III - 10: Immunolocalization of SPD on RNAi treatments for centrin and cyclin B.	88
Figure III - 11: Spermidine synthase mRNA is restricted to the jacket cells in gametophytes with arrested cell cycles.....	89
Figure III - 12: Silencing of any of the core components of the exon-exon junction complex (EJC) alters the distribution patterns of spermidine synthase mRNA.	91
Figure III - 13: The structures of polyamines.	97

Chapter IV

Figure IV - 1: Different kinesin proteins are apparently required at different developmental stages.	108
Figure IV - 2: The silencing of kinesin 5 (Kin5) homolog, (MvU99) does not show detectable effects on cell divisions and differentiation.....	110
Figure IV - 3: Gametophytes treated with POK1 kinesin protein (MvU130) dsRNA show no detectable defects after 8 h of development.....	111
Figure IV - 4: Several different kinesin knockdowns show similar defects in basal body formation.....	112
Figure IV - 5: Several different kinesin knockdowns inhibit the formation of the microtubule ribbon.....	113

Figure IV - 6: The effects of MvU629 (Kinesin II) silencing on cell divisions and centrin translational patterns.	115
Figure IV - 7: The effects of MvU629 (Kinesin II) silencing on the formation of the microtubule ribbon.	117
Figure IV - 8: The effects centromeric kinesin-like protein (MvU2336) silencing on cell division and centrin translational patterns.	120
Figure IV - 9: The effects centromeric kinesin-like protein (MvU2336) silencing on the formation of the microtubule ribbon.	122
Figure IV - 10: Spermatid of <i>R. americana</i> treated with drugs that disrupt the microtubule organizing centers showing paired-MLS structures.	130

Chapter V

Figure V - 1: A model linking the changes in spermidine distribution patterns in the gametophytes to developmental events.	134
---	-----

Appendix I

Figure AI - 1: <i>In situ</i> cell death assay on untreated gametophytes embedded in LR White.	145
Figure AI - 2: <i>In situ</i> cell death assay on untreated gametophytes embedded in LR White and treatment with RNase.	148
Figure AI - 3: Toluidine Blue-O staining for MvU271 RNAi treatment.	151
Figure AI - 4: Centrin immunofluorescence staining after MvU271 RNAi treatment. ...	152
Figure AI - 5: β -tubulin immunofluorescence staining after MvU271 silencing.	155
Figure AI - 6: <i>In situ</i> cell death detection assay on spores treated with MvU271 dsRNA.	156

Appendix II

Figure AII - 1: LacZ-His vector.	160
Figure AII - 2: Transient translation of lacZ-His in the microspores: Color development.	162
Figure AII - 3: Transient translation of lacZ-His in the microspores: immunofluorescence staining with anti- β -galactosidase antibody.	164
Figure AII - 4: Western blots for samples treated with ssRNA encoding tagged-centrin (UTR-) without 5'Cap and a poly(A) tail.	167
Figure AII - 5: Western blots for samples treated with ssRNA encoding tagged-centrin (UTR-) with 5'Cap and a poly(A) tail.	169
Figure AII - 6: Western blots for samples treated with ssRNA encoding tagged-centrin (UTR+).	169

List of Abbreviations

ADC	Arginine decarboxylase
AdoMeth	s-Adenosylmethionine
bb	Basal Bodies
BCIP	5 bromo-4 chloro-3 indolyl-phosphate
Cent	Centrin
CHA	Cyclohexylamine
DAPI	4',6-diamidino-2-phenylindole
DC AdoMeth	Decarboxylated s-Adenosylmethionine.
dsRNA	Double stranded RNA
JC	Jacket Cells
mt	Microtubule Ribbon
N	Nucleus
NBT	Nitro-blue tetrazolium
ODC	Ornithine decarboxylase
P	Plastid
PBS	Phosphate Buffer Saline
PBST	Phosphate Buffer Saline with Tween
Put	Putrescine
RNAi	RNA interference
SP	Spermatogenous Cells
SPD	Spermidine

SPD	Spermidine
SPDT	Spermidine transporter
SPM	Spermine
Tub	Tubulin

Chapter I: Introduction

Biological systems exhibiting rapid developmental patterns have inherent complexity that has intrigued and fascinated biologists for decades and have been the focus of intensive studies since the middle of the twentieth century (*e.g.*, Stavy and Gross, 1969; Raff *et al.*, 1972; Davidson, 1986). Although they give rise to dramatically different organisms, the processes of early embryogenesis in invertebrates and seed and spore germination in plants, all depend on similar developmental mechanisms including protein and mRNA localization, regulated translation, and precise control over rapid cell cycle progression in order to progress normally. In these systems, development is complex, rapid, and mainly dependent on sets of stored proteins and stored mRNAs to give rise to different cell types that are quite distinct from their progenitors. Once development is initiated with specific developmental cues in different systems, rapid development is driven by the coordinated protein localization and the spatial and temporal regulation of mRNA modification and translation.

Male gametophyte development in *Marsilea vestita* provides a unique opportunity to address several questions related to the regulation of rapid cell division, translational regulation and cellular differentiation. The single celled microspores are meiotic products, and their rapid development relies on the utilization of stored proteins and the translation of stored mRNAs to undergo a series of precise mitotic divisions that produce two distinct kinds of cells within the spore wall, and then, in the spermatids, to produce highly differentiated motile gametes that are far different from the cells that gave rise to them. The microspore development resembles early metazoan embryonic development in

that it is rapid and takes place with no or little transcription. However, unlike animal embryos, the microspores of *M. vestita* require very little transcription to support the entire developmental process that culminates the release of motile male gametes. The microspores have all of the necessary molecules needed for the activation of development, the mitotic division cycles, and gametogenesis. The spermatids require the *de novo* formation of complex cellular structures, such as the basal bodies and the elaborate cytoskeleton known as a multi-layered structure (MLS), but they rely only on the presynthesized mRNAs and proteins of the dry spores. Once development is initiated, upon hydration of the dry microspore, rapid development is executed with striking levels of coordination between the different stored molecules to accomplish precise localization of proteins and spatial and temporal translation of mRNA.

In this dissertation, the microspores of *Marsilea vestita* were used as an experimental system to study two of the fundamental regulators of development and differentiation: the polyamine spermidine and kinesin motors. The aims of the studies presented here were as follows: First, investigate the role of spermidine as an essential molecule for spermatid differentiation and morphogenesis and as a developmental regulator. Second, determine the roles of different kinesin proteins in protein and mRNA localization to establish cell polarity, fate and differentiation. These studies were focused on the formation of basal bodies and microtubule ribbon as markers for cell identity and differentiation.

Rapid development is driven by the regulated translation of stored mRNA

“During the development of plants and animals, morphogenetic processes are prepared at the molecular level long before morphological changes can be perceived”

(Eiden, 1982). In resting stages such as in eggs, cysts, and in dormant structures such as pollen, spores and seeds, proteins and mRNAs are stored for utilization when development is triggered. mRNA is stabilized and can be stored for prolonged periods of time. The concept of dormant maternal mRNA was first established in sea urchins; experiments showed that fertilization induced changes in protein synthesis even in the presence of transcriptional inhibitors (Davidson, 1986). Since then, there have been numerous studies on the role of maternal mRNA in early development (Telford *et al.*, 1990; Dworkin and Dworkin-Rastl, 1990; Gandolfi and Gandolfi, 2001). The regulated translation of the stored mRNA allows the utilization of different pools of mRNA at different time points of development. In addition, it allows the establishment of protein localization and protein gradients even when the mRNA is distributed uniformly. Protein localization can also be established by the translation of localized transcripts, for example, the *bicoid* RNA is localized to the anterior pole of the fly embryo and as a result, bicoid protein is translated at the anterior pole (St. Johnston *et al.*, 1989). In this case, translation is activated upon the proper localization of mRNA (McDonald and Smibert, 1996). The asymmetric localization of specific proteins results in cell polarity and gives rise to developmental patterning and cell fate. A classical example is the specification of the germ cells in different organisms, amphibians, nematodes and insects; they are all accomplished through the localization of mRNAs to specific daughter cells (Kloc *et al.*, 2002). Therefore, the precise spatial and temporal translation of specific messages in the cell gives the cells their correct identities at the appropriate stage of development.

During development, mRNA translation can be modulated on several levels: first, by controlling the rate of translational initiation. Functional ribosomes are assembled onto the mRNA in a stepwise procedure. In short, mRNA is first capped at the 5' end with 7-methyl guanosine cap, which is a part of a large protein complex that includes the cap-binding protein eIF-4E and the RNA helicase eIF-4A. The small ribosomal subunit binds to initiation factors on the RNA and forms a new ribosomal subunit-initiation factor complex. This complex scans the 5' UTR of the mRNA until it finds the start codon (AUG), then the large ribosomal subunit joins the complex and protein translation starts (reviewed by Hershey, 1991). The rate of translation is affected by both the concentration of active initiation factors and the primary sequence of the 5' UTR (Parkin *et al.*, 1988; Lazaris-Karatzas *et al.*, 1990; Koromilas *et al.*, 1992; Thach, 1992; Hess and Duncan, 1994). Stable secondary structures in the 5' UTR can block ribosome scanning; therefore, the sequence of the 5' UTR can provide an intrinsic control of mRNA translational initiation (Kozak, 1989).

Second, mRNA translation can be controlled by RNA masking, where RNA is associated with RNA-binding proteins and sequestered into mRNP (mRNA-Protein complex) particles that are inaccessible to the translational machinery. Masked mRNA can be translated efficiently once the masking proteins are disassociated and the poly(A)-tail is reconstituted (Richter and Smith, 1984). RNA masking has been demonstrated to play an essential role in mRNA storage during early embryogenesis (Richer, 1991) and spermatogenesis (Kleene, 1995). There are two types of masking proteins, those that repress the translation of specific mRNAs by binding to specific sequences or secondary structure; and those that have general effects and repress several different mRNAs

(Sommerville and Ladomery, 1996). The general repressor proteins are widely studied in several systems. They are members of highly conserved nucleic acid binding proteins, known as Y-Box family proteins. YB proteins were first identified as transcription factors that bind to a conserved Y-box sequence in the promoter region of some genes (Didier *et al.*, 1988). The YB family proteins were later found to bind a wide variety of templates including mRNA. Now, YB proteins are known to be the most abundant proteins found that bind stored mRNA in *Xenopus* oocytes and male gametes (Sommerville, 1992; Kown and Hecht, 1991; Tafuri *et al.*, 1993). YB proteins were shown to bind to pre-mRNA in the nucleus and then to exit the nucleus to bind other mRNP proteins to establish the complete repression of mRNA (Sommerville and Ladomery, 1995). Although the mechanisms of mRNA masking are dissected and masking proteins are well characterized, there is still no consensus on the exact mechanism of RNA unmasking. Several factors were demonstrated to play a role in mRNA unmasking, such as ubiquitination of the masking proteins (Hochstrasser, 1996) or phosphorylation of mRNP complex proteins, possibly by cell cycle kinases (Paris *et al.*, 1991, Walker *et al.*, 1996). Specific sequences at the 3' UTR are needed for the unmasking of mRNAs at specific time points (Curtis *et al.*, 1995). The studies in chapter III were conducted to shed some light on the possible mechanisms and cytoplasmic factors involved in mRNA unmasking in *M. vestita*.

Finally, mRNA translation can be repressed or activated by modulating the length of the poly(A) tail through specific sequences of the 3' UTR. The length of the poly(A) tail is closely correlated to rates of translation. Most newly transcribed mRNAs are polyadenylated in the nucleus. Once they are exported to the cytoplasm, their poly(A)

tails are either shortened or lengthened by cytoplasmic enzymes. A long poly(A) tail, between 150-200 nucleotides, increases mRNA stability and translational rates; it can also promote the formation of the cap-binding complex (Gallie, 1991). However, mRNA with either short or long poly(A) tails can initiate translation with similar efficiencies when they are not in competition for limited components of the translational machinery (Proweller and Butler, 1994).

The role of the cytoskeleton in mRNA localization and translational regulation

Development is regulated through the localization of proteins and regulated translation of mRNAs, which are mainly accomplished by cytoskeletal transport. In eukaryotic cells, the cytoskeleton and its motors are responsible for most transport processes. Cells can move and localize their chromosomes, organelles and proteins through the rearrangements of cytoskeletal fibers and their active transport via their motors. mRNA localization and anchoring and the regulation of its spatial translation is also accomplished by active transport. The correct localization of proteins and mRNAs is essential for cell polarity, fate and differentiation. In the *Drosophila* oocyte, the localization of specific mRNAs to the poles is a cytoskeletal-dependent process. For example, kinesin motor proteins were shown to be responsible for the localization of *oskar* mRNA to the posterior pole of the oocyte (Brendza *et al.*, 2000). Kinesins are either attached directly to RNAs or through RNA–protein particles. They utilize ATP to generate sufficient force to ‘walk’ along the microtubules and overcome the resistance exerted on the transported molecules by the viscosity of the gel-like cytoplasm. Different motors are involved in moving different molecules and protein complexes. Motor

proteins are also needed for the formation of complex cytoplasmic structures. During ciliogenesis and flagellar formation, kinesin motor proteins are used to transport proteins needed for the assembly of the cilia and flagella. Recently, motor proteins have been shown to play additional roles to active transport. Several kinesins were found to bind to scaffolding proteins that are part of signaling complexes (Verhey *et al.*, 2001). This indicates that kinesins and possibly other motors can play a role in the spatial regulation of signaling pathways.

Polyamines and spermiogenesis

Another group of regulators of cell development and differentiation is the polyamines. Polyamines (spermidine, putrescine and spermine) are ubiquitous organic compounds with two or more primary amino groups. They are involved in many important biological processes such as cell growth, and differentiation (Tabor and Tabor, 1984). *In vitro*, polyamines can form tight, noncovalent complexes with DNA, RNA and proteins. The synthesis of polyamines is stimulated prior to the synthesis of DNA, RNA or proteins (Tabor and Tabor, 1976, 1984; Janne *et al.*, 1978). They have also been implicated to play an important role in spermiogenesis (Oliva *et al.*, 1982). High expression levels of polyamine biosynthesis enzymes are observed during early spermiogenesis (Hakovirta *et al.*, 1993; Kaipia *et al.*, 1990). Polyamines are thought to play an essential role during histone replacement and chromatin compaction. The presence of polyamines is thought to help diminish the energy needed to bring the negatively charged DNA molecules into close proximity for chromatin compaction (Oliva *et al.*, 1982). In addition, they can increase the stability of nucleosomes

(Quemener, 1992). Spermidine and spermine are trivalent cations, and they are the most effective in condensing DNA (Bloomfield, V.A, 1997). The concentration of the polyamine spermidine increases during spermatid maturation in the rat (MacIndoe and Turkington, 1973). In humans, spermidine concentrations increase in the spermatid nuclei during histone replacement while spermine levels decrease (Quemener *et al.*, 1992). Spermidine is also known to stabilize condensed chromatin and repress transcription (Igarashi and Kashiwagi, 2000).

In addition to their involvement in spermiogenesis, polyamines are known to participate in many different cellular processes, such as cell division, protein synthesis, and programmed cell death. Different polyamines have different effects on these processes. It is still unclear how these simple polycations can affect so many different cellular functions and processes.

***Marsilea vestita*, an endosporous, heterosporous fern**

Marsilea vestita is a water fern. Its life cycle alternates between a diploid sporophyte and a haploid gametophyte. The sporophyte is a green, macroscopic plant, and it consists of a rhizome, leaves and roots. *M. vestita* is heterosporous. Two different kinds of spores, microspores and megaspores, are produced by meiosis, which occurs within the sporangia. In turn, hundreds of sporangia are enveloped in a modified leaf structure known as a sporocarp. The mature sporocarp is a desiccated structure that resembles a dried lentil. Spores are contained within sporangia that reside inside the sporocarp where they can remain dormant for many years. Over time, the sporocarp wall degrades and exposes the sporangia. Development in the spores is only initiated when they are placed

into water. Upon hydration, a fertile frond bearing the megasporangia and microsporangia expands dramatically and the structure emerges from the sporocarp. The spores then germinate to initiate gametophyte development, which is endosporous. Megaspores give rise to female gametes, and microspores give rise to ciliated, free-swimming male gametes known as spermatozoids. Fertilization occurs soon after the spermatozoids mature. Primary roots and leaves of new sporophytes can be established within few days of fertilization (Laetsch, 1967).

Spermiogenesis in *Marsilea vestita*

Male gametophyte development in *M. vestita* is synchronous, and is activated by placing dry microspores into water (Hepler, 1976; Wolniak *et al.*, 2000). Development requires 11 h at 20 °C, and it has two distinct phases, a division phase for the first 5.5 h and a differentiation phase for the next 5.5 h. Upon hydration, significant cytoplasmic movements take place within the spore resulting in plastid rearrangement into one side of the cell and the nucleus into another. After ~90 min, the first asymmetrical division takes place generating a germ cell and a prothallial cell. The prothallial cell, a presumptive remnant of gametophytic thallus, stops dividing and eventually disintegrates. The germ cell proceeds with development; about 30 minutes after the first division is complete, it divides symmetrically giving rise to two antheridial initials. The antheridial initials undergo a series of three asymmetric divisions to produce 6 sterile cells, jacket cells, and 2 large, centrally-placed spermatogenous initials. While jacket cells do not divide and develop further, the spermatogenous initials undergo four additional symmetrical divisions to generate a total of 32 spermatids. The spermatids undergo an elaborate

synchronous differentiation process to give rise to 32 freely swimming spermatozooids (Figure I-1), each of which possesses a ciliary apparatus comprising ~140 cilia (Figure I-2) (Sharp, 1914; Hepler, 1976; Myles and Hepler, 1977). As in all plants, there is no movement of cells during development of the gametophyte of *M. vestita*. Thus, the positioning of division planes is extremely important for the development of this gametophyte because cell position and cell size determine cell fate. Since there is no cell movement, and since there are only sterile and spermatogenous cells produced in precise places within the spore, these gametophytes provide an excellent system for the study of mechanisms that define cell fate.

The differentiation and maturation phase of the spermatid involves the *de novo* formation of basal bodies in cells that lack preexisting centrioles, in a particle known as the blepharoplast (Sharp, 1914, Mizukami and Gall, 1966; Klink and Wolniak, 2001). The blepharoplast first appears as a cytoplasmic particle localized to a small indentation on the distal side of the nucleus after the seventh division (Hepler, 1976). The blepharoplast disappears between the 7th and 8th divisions. It reappears again, essentially in the same position in the cytoplasm, as a double structure after the 8th division, and it persists through the ninth, last, division. The blepharoplast becomes positioned at the spindle poles, and it serves as a centrosome for the last mitotic division (Figure I-3A). At this stage, the blepharoplast is 0.8 μm in diameter and is hollow. After the last division, the blepharoplast breaks up into a cluster of procentrioles near the nucleus (Figure I-3B) (Mizukami and Gall, 1966). In the newly formed spermatids, the procentrioles will be transformed into basal bodies, which later serve as templates for ciliary axonemes (Mizukami and Gall, 1966, Hepler 1976, Wolniak *et al.*, 2000). The basal bodies

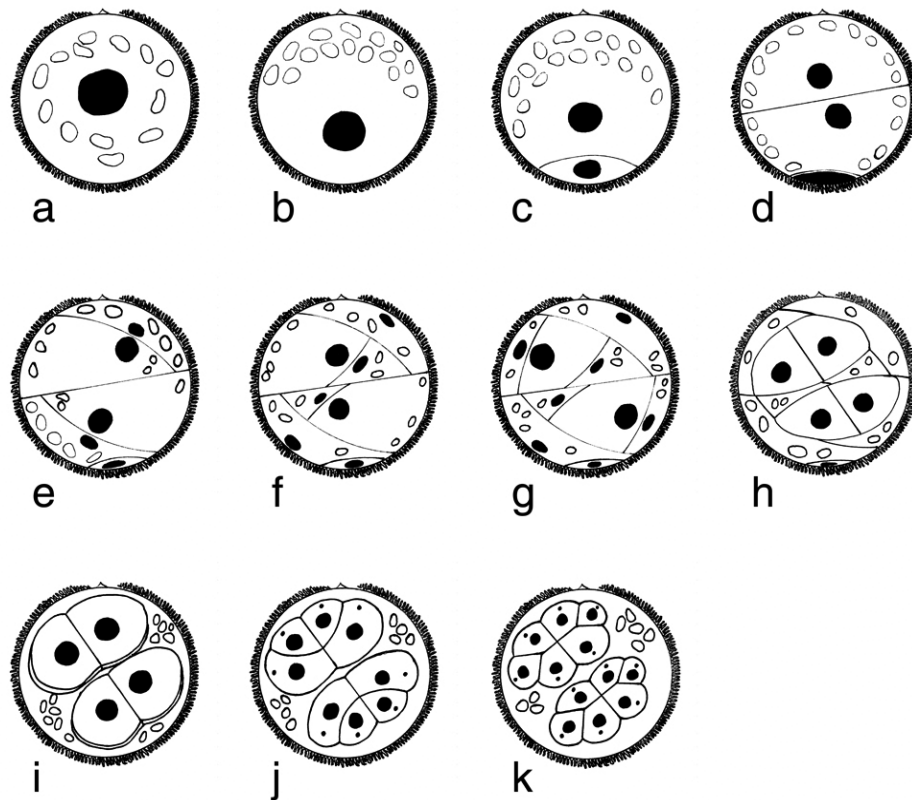


Figure I - 1: Cell division patterns during development of male gametophyte of *M. vestita*.

(a) Microspores at the time of imbibition: The black solid circle is nucleus and the surrounding open circles are plastids. (b) Prior to the first division, cytoplasm reorganize with plastids move to one side of the cell and nucleus migrates to the other side. (c) First mitotic division is asymmetric and produces a prothallial cell that loses the ability to go through further divisions. (d) The second division gives rise to two antheridial initials. (e- g) Each antheridial initial undergoes three more asymmetric divisions that produce three sterile jacket cells and one primary spermatogenous cell. (h-k) Each primary spermatogenous cell undergoes symmetric division to produce 16 spermatids. Jacket cells degenerate at this stage. (Drawing by Dr. S.M. Wolniak, adapted from Sharp, 1914 and Hepler, 1976).

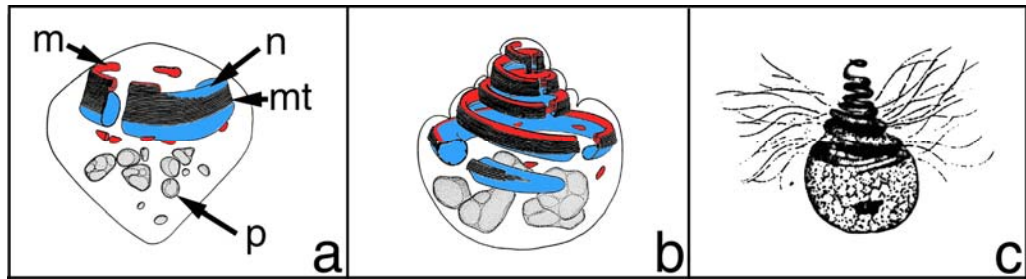


Figure I - 2: Differentiation of spermatozoid of *M. vestita*.

(a) The spermatid initiation the synthesis of MLS. Nucleus and mitochondrion are associated with microtubule ribbon and started to elongate. (b) Spermatid after nuclear shaping is completed. (A, &b are modified from Myles and Hepler, 1982). (c) Mature spermatozoid after emerging from the antheridium.

m: mitochondrion (red); **mt:** microtubule ribbon; **n:** nucleus (blue); **p:** plastid.

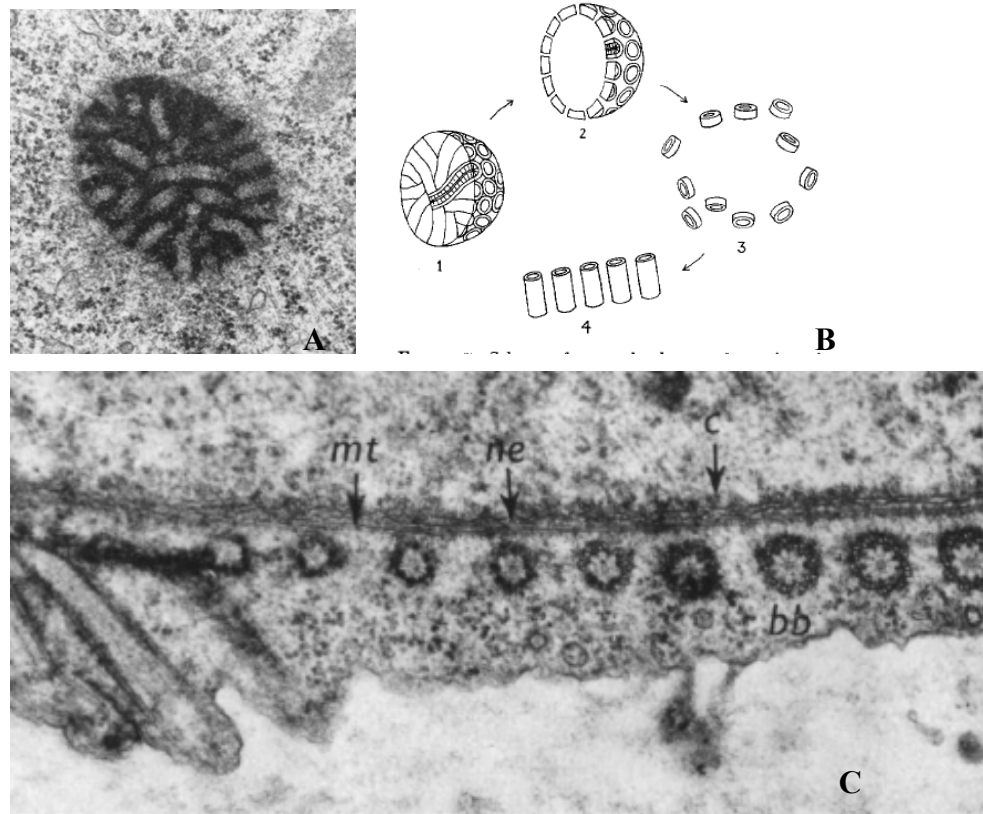


Figure I - 3: The formation of basal bodies from the blepharoplast.

(A) The mature blepharoplast before the last mitotic division as observed by electron microscopy. It consists of cylindrical channels (From Hepler, 1976). (B) Representation of the transformation of the blepharoplast into basal bodies. 1- Mature blepharoplast. 2- Hollow blepharoplast found after the last mitosis. It consists of radially arranged procentrioles. 3- Break up of the blepharoplast. The procentrioles align along the nuclear envelope and elongate to form basal bodies (From Mizukami and Gall, 1966). (C) Cross section of a spermatid after 6.5h. Basal bodies are positioned along the microtubule ribbon and the elongated nucleus. **mt**: microtubule ribbon. **ne**: nuclear envelop. **C**: condensed chromatin. **bb**: Basal bodies. (Myles and Hepler, 1977).

eventually line up along the nuclear envelope (Figure I-3C). After the basal bodies are formed, an elaborate microtubular structure called the multi-layered structure (MLS) starts to form ventral to the basal bodies (Figure I-4). The MLS consists of four stacked layers of vanes and fins positioned under a ribbon of cross-linked microtubules known as a “spline” (Wolniak *et al.*, 2000). As the microtubule ribbon of the MLS grows, it becomes associated with basal bodies (Hepler, 1976, Wolniak *et al.*, 2000). The spline is attached to the nucleus and mitochondrion on its ventral side and the basal bodies and cilia attach on the dorsal side, beneath the plasma membrane (Figure I-4). The chromatin of the spermatid nucleus undergoes substantial remodeling and condensation. The nucleus elongates and takes a spiral shape (Figure I-2). The growth of the microtubule ribbon is thought to be responsible for driving the elongation of the nucleus to giving it its final coiled shape (Myles and Hepler, 1977, 1982).

Microspore development in *Marsilea vestita*

Development of *M. vestita* microspore is similar to the rapid development of many organisms in that it depends on little or no transcription (Raff *et al.*, 1972; Capco and Jeffery, 1979; Davidson, 1986; Richer and Smith, 1984; Rosenthal, *et al.*, 1993; Curtis *et al.*, 1995). The dry microspores of *M. vestita* contain large quantities of stored proteins and stored mRNAs (Hart and Wolniak, 1998, 1999). Newly synthesized proteins become detectable after 2 h of hydration and reach their maximal labeling after 8 h. Immunoblots for specific proteins show that some proteins, such as γ -tubulin, are maintained at the same abundance level throughout development. Other proteins, such as α - and β -tubulin, show little increase at specific stages of development (Klink and Wolniak, 2001, 2003).

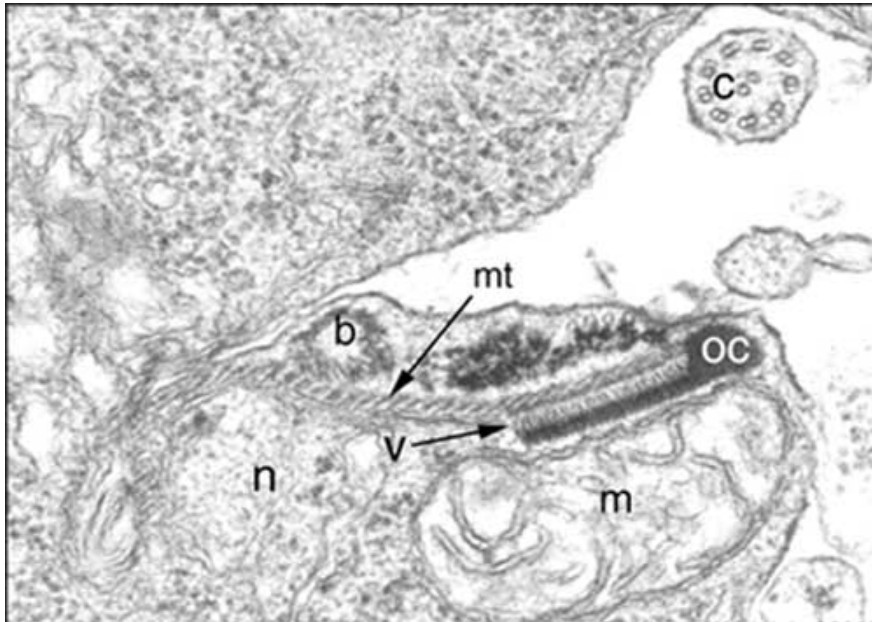


Figure I - 4: The multilayered structure (MLS) in a developing spermatid of *M. vestita*.

The MLS consists of a series of vanes (v) and fins positioned under a ribbon of microtubules (the spline) (mt). The mitochondrion (m) is positioned on the ventral side of the MLS and appears to be attached to the lowermost side of the MLS. Basal bodies (b) are positioned on the dorsal side of the spline (Klink and Wolniak, 2000 from Myles and Hepler, 1977). C: Cilia.

Finally, some proteins are not present in the dry spore but are synthesized during development, such as centrin and other ciliary proteins (Hart and Wolniak, 1998; Wolniak *et al.*, 2000). *In vitro* translation of isolated mRNAs at different time intervals reveals that messages isolated up to 30 min of hydration can not be translated (Hart and Wolniak, 1998). However, messages isolated after 30 min of development could be translated. In addition, some transcripts would decrease and sometimes disappear after 8-10 h (Hart and Wolniak 1998, 1999). These results suggest that development in the spore is driven by processes of translational regulation, and a big part of mRNA processing takes place during the first 30 min of development.

Patterning and cell fate determination during *M. vestita* gametophyte development

Protein and mRNA localization is crucial for cell fate determination in the gametophyte. Early cytoplasmic movements, prior to first divisions, allow certain proteins to become aggregated into cytoplasmic domains that predict the locations of the spermatogenous initials. In contrast to proteins, most mRNAs do not become aggregated into these domains; but rather, remain dispersed in the cytosolic compartments of all cells in the gametophyte throughout the 11 h developmental process. However, a few, specific mRNAs aggregate into zones that later become the spermatogenous initials of the gametophyte (Tsai *et al.*, 2004). These mRNAs include a transcript that encodes a PRP19-like protein, which is part of a spliceosome (Figure I-5), an RNA helicase, and several mRNAs that encode regulators for DNA replication.

Although mRNAs are present in both the spermatogenous and jacket cells, polyadenylated transcripts are abundant only in the spermatogenous cells. The reason for

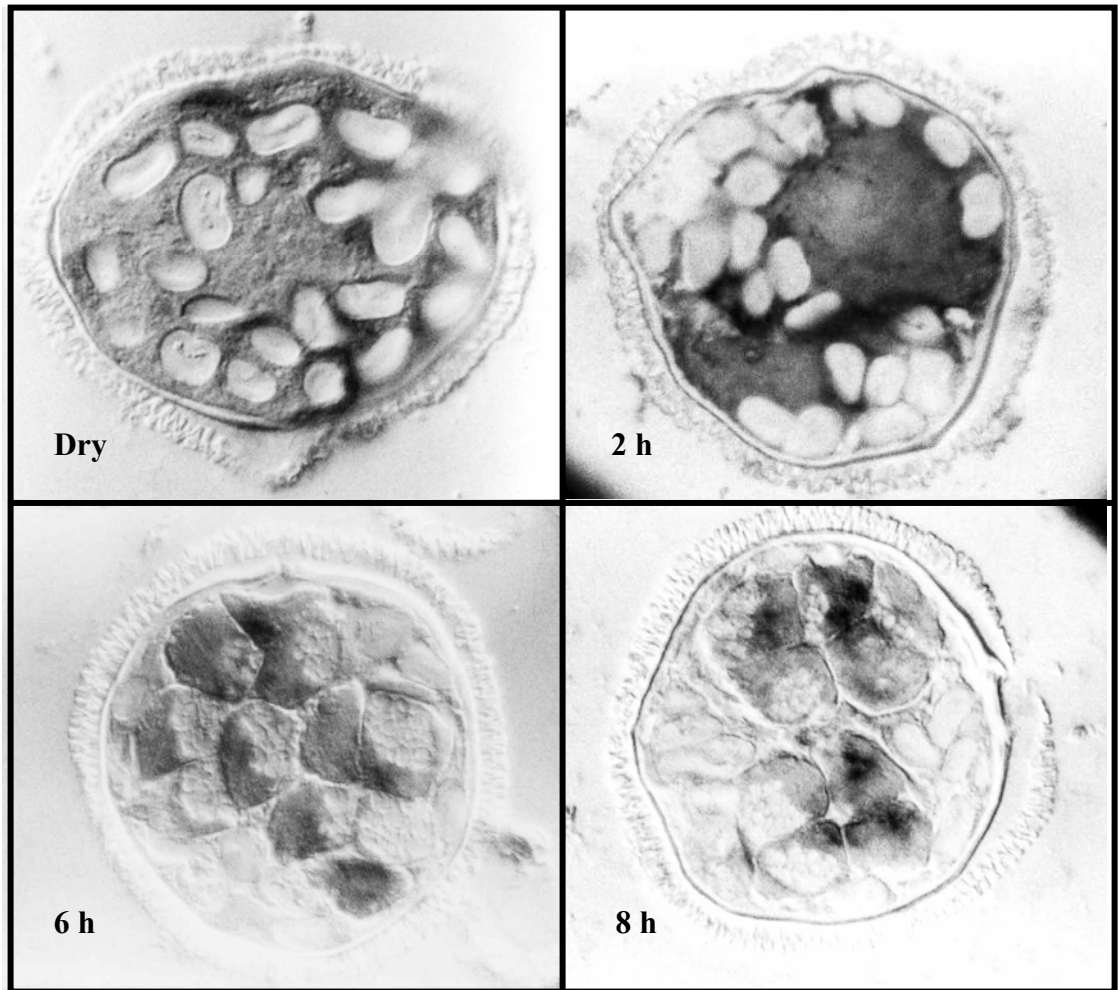


Figure I - 5: Distribution of PRP19, a spliceosome component, mRNA during spermiogenesis

mRNA was uniformly distributed in the cell prior to the first mitotic division (dry) and then segregated into spermatogenous cells (2 h- 8 h). (8 h) mRNA labeling was concentrated in the anterior end of the spermatogenous cells with little detectable in the jacket cells (From Tsai *et al.*, 2004).

this difference appears to be the consequence of asymmetric distribution of cytoplasmic poly-A-polymerase, which accumulates (as a protein) almost exclusively in spermatogenous cells (Tsai *et al.*, 2004) (Figure I-6). As a result, translation of stored mRNAs occurs primarily in spermatogenous cells where the bulk of RNA processing and translation machinery is localized (Myles and Hepler, 1977). Cell fate in the gametophyte is established first through the localization of the existing cytoplasmic proteins and certain mRNAs. Remarkably, translation appears to continue normally in the gametophyte, even after inhibition of the cell division cycles (Tsai and Wolniak, 2001), but in these cells, fate determination is anomalous. The movement of these molecules is carried out and controlled by the cytoskeleton and its motors (Molk and Wolniak, 2001; Swamy and Wolniak, unpublished results). Second, cell fate is accomplished through localized translation of certain messages in the gametophytes at specific locations.

***Marsilea vestita* as an experimental system**

Marsilea vestita provides a unique opportunity to study several developmental questions that are relevant to a variety of other multicellular organisms. The male gametophyte development resembles early embryonic development in a number of different animals. The microspores of *M. vestita* have proven to be particularly amenable to experimental manipulations, and are ideally suited for the study of rapid differentiation of motile cells. *M. vestita* microspores were used for cytological and ultrastructural studies to provide an understanding of the *de novo* formation of basal bodies from a precursor structure, the blepharoplast (Sharp, 1914; Mizukami and Gall, 1966; Hepler,

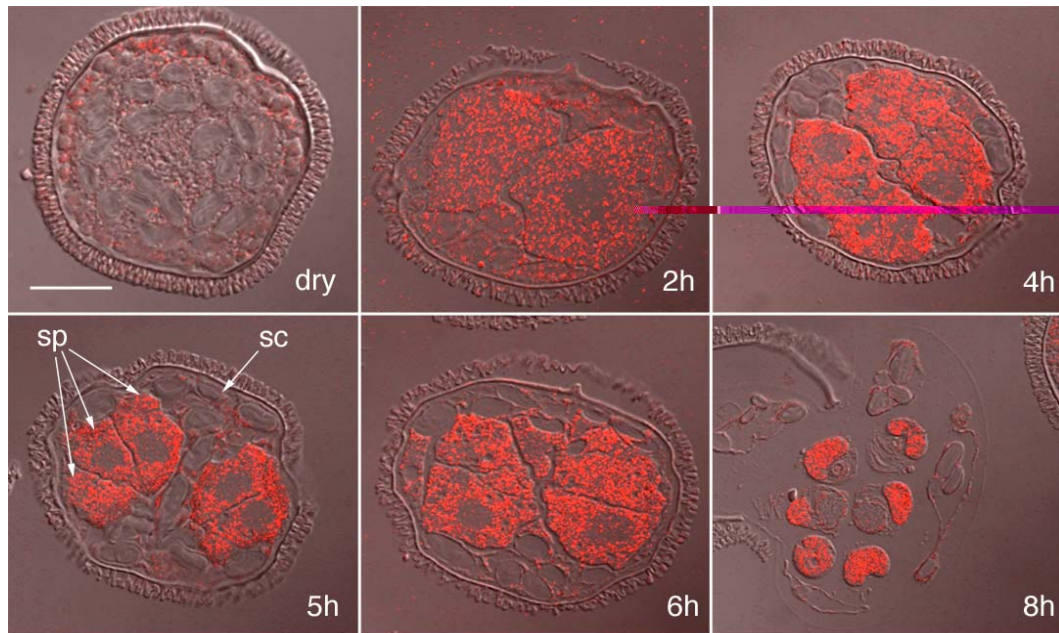


Figure I - 6: Cytoplasmic Poly A-RNA polymerase distribution during spermiogenesis.

Poly A-RNA polymerase was uniformly distributed in the cell prior to the first mitotic division (dry). With more divisions it started to segregate into spermatogenous cells (2 h, 4 h). Staining was concentrated in the anterior portion of the spermatogenous cells (5 h, 6 h) and later in the spermatids (8 h). (Confocal imaging of immunogold localization patterns in fixed, sectioned gametophytes, from Tsai *et al.*, 2004). **SP:** Spermatogenous Cells. **SC:** Sterile jacket Cells

1976; Myles and Hepler, 1977; Hart and Wolniak, 1998, 1999). Biochemical techniques were carried out to dissect the composition of the blepharoplast and basal bodies (Hyams *et al.*, 1983; Pennell *et al.*, 1986, 1988). Developmental studies focusing on gene expression, cell fate and ciliogenesis started in the nineteen nineties (Hart and Wolniak, 1998, 1999; Wolniak *et al.*, 2000; Klink and Wolniak, 2001; Tsai and Wolniak, 2001; Tsai *et al.*, 2004).

There are several factors that make *M. vestita* useful as an experimental system. First, the sporophytes are easily grown at the university green house facilities. The collected sporocarps can be stored for an extended time while remaining viable. Second, populations of spores hydrated at the same time develop in synchrony, allowing more accurate and comprehensive analysis. Third, at the time of hydration, the spores readily take up various molecules, drugs, labels and RNA probes of different sizes, which provides flexible and uninvasive methods for experimental manipulations (Tsai and Wolniak, 2001; Klink and Wolniak, 2000). Finally, development of the gametophyte is endosporous; it takes place within the spore wall. Development is supported by molecules stored and made in the microspore.

With the previous observations in mind, Wolniak and others have developed several tools to help understand key developmental processes in the gametophyte. One tool is an RNA interference (RNAi) protocol (Klink and Wolniak, 2000, 2001). Since gene knockout experiments can not be performed, RNAi is used to create a null phenocopy. RNAi provides the means for the targeted destruction of specific mRNAs in developing gametophytes (Klink and Wolniak, 2000, 2001; Tsai and Wolniak, 2001). The disruption of different messages by RNAi results in altered patterns of development. In addition,

development can be arrested at different time points dependent on the specific dsRNA used and the time point at which the translation of the mRNA of interest becomes limiting (Klink and Wolniak, 2001, 2003). For example, the silencing of centrin arrests development at 4 h when centrin is needed for blepharoplast and basal body formation. However, α - and β -tubulin knockdowns arrest development later at 8-10 h, when the production of additional tubulin is required for the formation of ciliary axonemes. With adequate levels of α - and β -tubulin present up through 8 h, these knockdowns do not affect development at all.

The efficiency of RNAi treatments was determined in previous studies by Klink and Wolniak, (2001). RNAi treatments showed concentration dependent effects. High concentrations of dsRNA (2 mg/ml) arrested development early in the one-cell stage while low dsRNA concentrations (2-20 μ g/ml) affected only few gametophytes. The best effects were obtained when intermediate concentrations (100-200 μ /ml) of dsRNA were used. At these intermediate concentrations, the majority of the gametophytes were affected, and they exhibited consistent anomalies.

The specificity of RNAi treatments in the gametophytes was also established in previous published studies (Klink and Wolniak, 2001; Tsai and Wolniak, 2001; Tsai *et al.*, 2004). Series of western blots and *in situ* immunolocalization assays were performed for different proteins on different RNAi treatments. Western blots for protein samples isolated at 8 h from gametophytes treated with different concentrations of centrin dsRNA showed reduced levels of centrin protein, but the levels of other protein such as β -tubulin and P28 were not affected (Figure I-7: A). In addition, western blots for proteins samples isolated at 8 h from gametophytes treated with different concentrations of β -tubulin

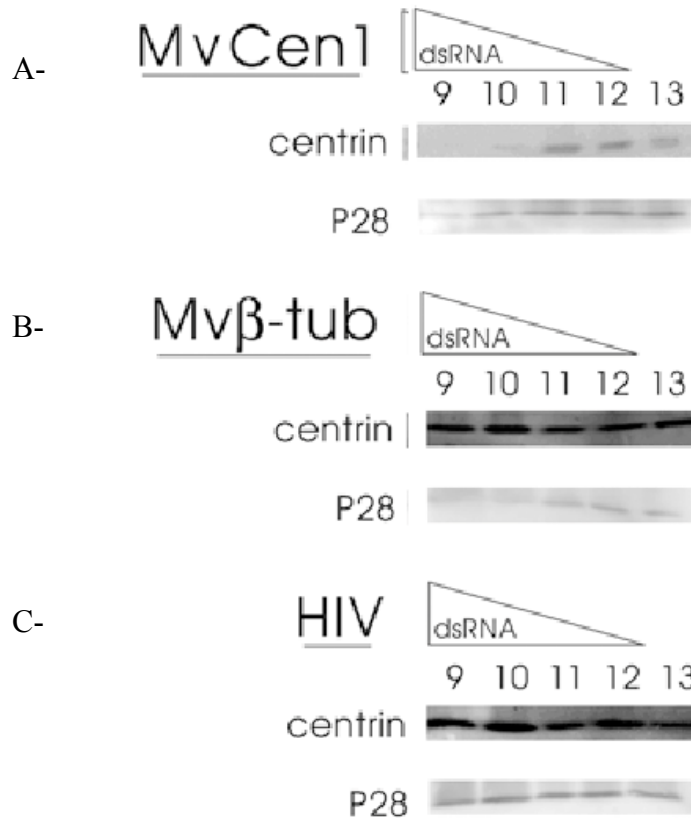


Figure I - 7: RNAi effects are sequence specific and concentration-dependent.

Immunoblots of protein isolates obtained after 8 h of development from gametophytes treated with different concentrations of dsRNA (lanes 9–12). RNA probes were made from cDNA encoding centrin (A) (Hart and Wolniak, 1998), β -tubulin (B), and from a 250 bp random sequence present in the viral genome of HIV (provided by Dr. J. DeStefano, University of Maryland) (C). The concentration of dsRNA used was 2 mg/ml in lane 9, 200 mg/ml in lane 10, 20 mg/ml in lane 11 and 2 μ g/ml in lane 12. Lane 13 represents protein isolate that was obtained from untreated gametophytes at 8 h. The immunoblots were performed for either centrin protein (upper blot) or P28 protein (lower blot). The immunostaining was detected by ECF fluorescence imaging with the STORM PhosphorImager. (A) Centrin silencing reduced the amount of the translated centrin protein in the gametophytes in a concentration dependent manner. P28 translation was not affected by the presence of centrin dsRNA probes. (B and C) dsRNA encoding either β -tubulin or HIV had no significant effect on the abundance of either centrin or P28 after 8 h of development. (This figure was modified from Klink and Wolniak, 2001, with permission).

dsRNA showed that β -tubulin protein levels did not increase after 8 h, unlike the untreated controls (Klink and Wolniak, 2001). On the other hand, the abundance levels of centrin and p28 proteins were not affected (Figure I-7: B). Developmental defects were only observed when the dsRNA probes used encoded proteins needed for gametophyte development. When the gametophytes were treated with dsRNA encoding a random fragment of the HIV genome, development was not affected at all and protein abundance patterns for centrin and P28 were unaltered as detected with western blots (Figure I-7: C) and on sections of treated gametophytes (data not presented) (Klink and Wolniak, 2001). On the other hand, introducing dsRNA probes that contained a conserved domain such as an ATP binding domain common to a number of kinesin isoforms (and other proteins) to the gametophytes arrested development very early on, as a result of the silencing of all transcripts that contained the conserved sequence (Deeb and Wolniak, unpublished observations). In contrast, dsRNAs encoding unique sequences from those several different kinesin isoforms that contain the ATP-binding site resulted in developmental arrest at distinct stages of development. Later, Van der Weele *et al.* (2007) showed that treating the gametophytes with dsRNA encoding mago nashi reduced the levels of mago protein, but it did not affect the abundance levels of α -tubulin protein as detected on western blots. These studies demonstrate the efficiency and specificity of RNAi knockdowns in affecting development in gametophytes of *M. vestita*.

Purpose and significance of this dissertation

The aim in this dissertation is to provide an understanding of how development is regulated and differentiation is established during spermiogenesis of *Marsilea vestita*. In

the second chapter, insight are provided into how spermidine is involved in development and differentiation of the spermatids. Spermidine clearly plays different roles at successive stages of gametophyte development and it appears that the effects of spermidine are linked to the changing concentration of the polyamine in the cells as the gametophyte matures. In Chapter III, the role mRNA unmasking is highlighted as a new mechanism of translational regulation in the gametophyte. Spermidine appears to function as a developmental regulator that affects mRNA availability and translation by affecting transcript unmasking. In addition, several other cytoplasmic factors are shown to be involved in the control of mRNA unmasking. Finally, in chapter IV, several kinesin motor proteins are investigated to determine when each kinesin participates in development and how it regulates development and differentiation and affects the establishment of cell fate. The studies in this chapter focus on microtubule assembly, regulated translation and localization of centrin to determine the role of each kinesin in the formation of the motile apparatus.

Chapter II: The Role of Spermidine in Microspore Development and Spermatid Nuclear Remodeling.

Introduction:

Spermidine (SPD) is a polyamine found in both prokaryotic and eukaryotic organisms (Tabor and Tabor, 1984). In plants, SPD is involved in many cellular processes such as cell division, development of reproductive organs, embryogenesis, development of floral bud, root growth, and leaf senescence (Kaur-Sawhney *et al.*, 2003). The precise mechanisms by which polyamines function to regulate cellular processes are still not well understood. SPD is synthesized through a conserved pathway that gives rise to other polyamines (Figure II-1) (Kaur-Sawhney *et al.*, 2003; Yatin, 2002). The intracellular concentration of SPD is established through the regulation of its synthesis, degradation and transport (Covassin *et al.*, 2004; Igarashi and Kashiwagi, 1999). In addition to *de novo* synthesis, cells acquire SPD from exogenous sources through a transmembrane transporter, the potA-D protein complex. Mutations in any subunits of this complex disrupt SPD transport (Igarashi and Kashiwagi, 1999).

High levels of SPD and other polyamines are correlated with spermatogenesis in many systems, such as newts (Matuski *et al.*, 1981), roosters (Oliva *et al.*, 1982), rats (Watts *et al.*, 1987), sea star (Sible *et al.*, 1990) and humans (Quemener *et al.*, 1992). In mice, ODC transcripts are found in high levels in mid- and late-pachytene spermatocytes in round spermatids, thus linking polyamines with the process of early spermatogenesis. In rooster spermatogenesis, SPD and other polyamines were found to play a protective

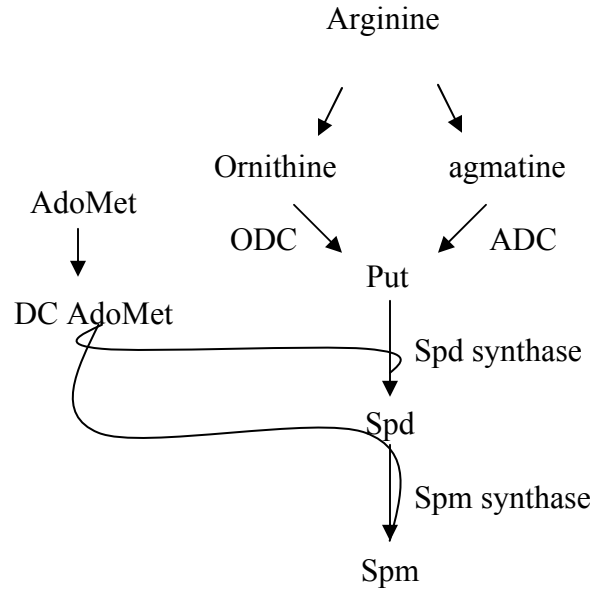


Figure II - 1: Polyamine biosynthetic pathway in mammals and plants.

In mammalian cells, polyamine synthesis starts by converting Arginine to Put by ODC. In some plants and bacteria, Put synthesis is initiated by ADC. Spd synthase transfers aminopropyl group from DC AdoMeth to Put to generate Spd. Similarly, Spm synthase transfers aminopropyl group from DC AdoMeth to Spd to generate Spm. (Modified from Yatin, 2002). **Put:** Putrescine, **Spd:** Spermidine, **Spm:** Spermine, **ODC:** Ornithine decarboxylase, **ADC:** Arginine decarboxylase, **AdoMeth:** s-Adenosylmethionine, **DC AdoMeth:** decarboxylated s-Adenosylmethionine.

role for DNA during histone replacement by protamines (Oliva *et al.*, 1982). Similarly, it is likely that SPD plays a role in the chromatin remodeling and spermatid differentiation in *Marsilea vestita*.

The water fern *Marsilea vestita* provides a useful system to study the role of SPD during spermiogenesis. The endosporous development of the male gametophyte consists of two phases, an early division phase, where both sterile and spermatogenous cells are formed, followed by a differentiation phase, where chromatin remodeling, ciliogenesis, and morphogenesis occur in the spermatids. Gamete differentiation commences as soon as division cycles are completed. The multi-layered structure (MLS) is a large, complex cytoskeletal array that is assembled in the newly formed spermatid. The MLS is present in the spermatozooids of all embryophyte plants, and is, in effect, a signature organelle for these gametes (Carothers, 1975). A microtubule ribbon, comprising approximately 40 crosslinked microtubules grows out of the MLS and associates with the nucleus through a line of dense material along the nuclear envelope (Myles and Hepler, 1977). Basal bodies, previously assembled at the blepharoplast, are present in clusters and then become distributed along the dorsal face of the growing microtubule ribbon (Myles and Hepler, 1977). In *M. vestita*, nuclear shaping precedes chromatin condensation. There is a long-standing notion (Myles and Hepler, 1977; Myles and Bell, 1975; McIntosh & Porter, 1967; Turner, 1970) that nuclear elongation is guided by the microtubule ribbon, which could provide mechanical support for directional growth. The dense material connecting the MLS with the nucleus is thought to play a role in coordinating events between the microtubule ribbon and the nucleus.

The close association between the different structures formed during differentiation, basal bodies, MLS and the condensed nucleus, implies that there is coordination among the synthesis and assembly processes. Therefore, a defect in one of these structures will most likely affect the formation of others. In this chapter, the relationship between chromatin condensation and basal body and MLS formation is examined. First, the role of spermidine during development of the gametophyte is examined, and the developmental stage at which spermidine synthase is needed is determined. Next the role of spermidine in chromatin condensation and nuclear elongation is investigated. It is likely that spermidine depletion would prevent chromatin condensation. The experiments performed in this chapter permit the analysis of the effects of blocking chromatin condensation on the formation of basal bodies and microtubule ribbon. Finally, the patterns of SPD distribution and abundance in the gametophyte are determined, and an explanation to how and why these changes occur during development is provided.

Materials and Methods:

Microspore culture and fixation

Marsilea vestita sporophytes were raised in 7 ponds in the greenhouse facilities at the University of Maryland. The original spores were obtained from Dr. P. Hepler (University of Massachusetts; Amherst, MA). Sporocarps, the dried structures containing the microspores and megaspores, were collected from *M. vestita* sporophytes. To obtain microspores, sporocarps were ground with three one-second bursts using a commercial coffee grinder (Braun, model KSM2; Lynnfield, MA) and sifted through a series of wire sieves of 425 μm and 212 μm (Hepler 1976; Klink and Wolniak, 2001; Tsai and

Wolniak, 2001). In a 2 ml centrifuge tube, 4 mg of microspores were combined with 1 ml of commercial spring water (Dannon). The microcentrifuge tubes were placed on an Orbitron Rotator (model 260200, Boekel Scientific, PA) with aeration at 20 °C. After 1 h, the gametophytes were transferred to 50 ml flasks; the volume was brought to 8 ml with Dannon commercial spring water in each flask. The flasks were placed in a temperature-controlled water bath shaker at 20 °C (New Brunswick model RM6, New Brunswick, NJ), (Hepler, 1976; Klink and Wolniak, 2001; Tsai and Wolniak, 2001). The gametophytes were allowed to develop for different time increments and then fixed with paraformaldehyde using modified protocols from Klink and Wolniak (2001) and Tsai and Wolniak (2001) (Van der Weele *et al.*, 2007). In summary, at the time of fixation, the gametophytes were first collected onto a polyester filter (BioDesign Cell Micro Sieves, BioDesign Inc., Carmel, NY) on a Buchner funnel with a mild vacuum. 1 ml of fixative (4% paraformaldehyde in 50 mM PIPES, pH 7.4) was used to wash the gametophytes on the filter. The filter with the gametophytes was transferred to a metal mortar. Two 50 µm thick brass spacers were placed in the mortar above the filter to prevent complete squashing of the gametophytes (Hepler, 1976; Kink and Wolniak, 2003). The gametophytes were then cracked by a mechanical force from one or two hammer blows onto the metal pestle. The gametophytes were washed from the filter into a 50 ml conical centrifuge tube with fixative and then placed at 4 °C for 2 h. The gametophytes were then transferred into 2 ml tubes and rinsed 3 x 15 min in 1X PBS (phosphate buffered saline, pH 7.4). Next, gametophytes were dehydrated with a graded ethanol series of 10, 25, 50, 75 and 90% ethanol for 2 h each followed by 4 x 100% ethanol for 30 min each. The gametophytes were infiltrated with ethanol-methacrylate mixture (3:1, 1:1, 1:3) for 2 h

each followed by 5 washes of 100% methacrylate mixture for 1 h each. The gametophytes were transferred into BEEM capsules, and the samples were polymerized for 5 h in ultraviolet light at 4 °C. Semi-thin (1-2 µm) sections were made using glass knives on an ultra-microtome. The sections were transferred onto a microscope slide and relaxed by holding a chloroform-saturated swab in close proximity to the sections. The slides were placed on 40 °C heating block, to allow the sections to adhere to the glass.

RNAi experiments

cDNA clones encoding spermidine synthase and a spermidine transporter were isolated from our gametophyte cDNA library. The construction of our cDNA library and isolation and sequencing of the cDNA clones is described in Hart and Wolniak (1998, 1999). Blast searches indicate that MvU185 (GenBank accession# NM-202171) encodes a spermidine synthase I, and MvU2596 (GenBank accession# CP000800) encodes a spermidine transporter (*potC*). Single stranded RNAs were transcribed *in vitro* as described by Tsai and Wolniak (2001), and Van der Weele *et al.* (2007). To generate the dsRNA, the concentration of ssRNA was adjusted to 1 µg/µl with RNase free water. Equal amounts of the sense and the antisense RNA were added together in microcentrifuge tube. The RNA mixture was heated to 80 °C for 10 min, placed at 50 °C for 5 min and later at 37 °C for 30 min. The quality of dsRNA was checked by gel electrophoresis prior to each experiment. For each RNAi treatment, 4 mg of microspores were added to 200 µg/ml dsRNA in 1ml total volume in a 2 ml microcentrifuge tube. For control samples, 4 mg of microspores were placed in Dannon water. The tubes were placed on orbiting shaker at 20 °C (Klink and Wolniak, 2001 and Tsai and Wolniak,

2001). After 5-10 min, the gametophytes were released from the sporangia by pipetting against the tube wall using 1 ml pipette tips. After 1 h, the gametophytes were transferred to 50 ml sterile flasks, and the total volumes were brought up to 10 ml with commercial spring water (Dannon). The flasks were placed in a shaking water bath at 20 °C as described above. The gametophytes were allowed to develop for the desired length of time and then fixed and embedded in Methacrylate for microscopic observations as described above. Each of the treatments was performed at least twice with newly transcribed dsRNA (most were performed on three different populations of microspores). Thin sections (1-2 μm) of the fixed gametophytes were obtained, and the sections were examined with light microscope. Since the analysis depended on the observation obtained from sectioned material, the observation of hundreds of sections was essential to construct a sense of three dimensional representation of the phenocopy. The phenocopies were clustered into groups based on the severity of the effects; the percentage of each phenocopy was estimated. The phenocopy with the highest percentage of occurrence, representing the majority of the affected gametophytes, was included in the analysis. Images for at least 30 different gametophytes were obtained for each treatment and assay that was carried out on the treated gametophytes to ensure the accuracy of assessments of the RNAi effects. The images chosen to be presented in this document were most representative of the effects of the different treatments and assays performed on the gametophytes. The same strategy was applied to other pharmacological treatments that were performed on the gametophytes.

In situ hybridization

Probes used for *in situ* hybridization were made from cDNA clones centrin (MvU184), β -tubulin (MvU518) spermidine synthase I (MvU185), and spermidine transporter-potC (MvU2596). *In situ* hybridizations were performed according to protocols described by Tsai and Wolniak (2001) and modified by Van der Weele *et al.* (2007). To label the RNA probes with digoxigenin, half of the dUTP was substituted with digoxigenin-11-dUTP (Roche Diagnostics, Indianapolis, IN). Thin sections were placed on silanated slides (KDMedical, Columbia, MD) and relaxed holding a chloroform saturated cotton swab in close proximity to the sections; slides were dried on a heat block at 40 °C. Slides were treated with acetone, proteinase K, glycine, paraformaldehyde and triethanolamine according to procedures by Steel and coworkers (1998). Probes were hybridized and visualized with Nitro-blue tetrazolium (NBT) and 5 bromo-4 chloro-3 indolyl-phosphate (BCIP) according to procedures described by Tsai and Wolniak (2001).

Cytology and immunocytochemistry

Sections were stained with Toluidine Blue O and viewed with bright field microscopy (O'Brien and McCully, 1981). Immunofluorescence cytochemistry was employed to localize proteins in the gametophytes. Immunocytochemistry was performed as described by Baskin and Wilson (1997), except that sections (1-2 μ m) were etched in chloroform followed by acetone for 15 min each, blocked with blocking solution (Hardin and Wolniak, 1998) for 1 h, washed with PBST 0.05%. Primary antibodies used were polyclonal anti-spermidine (1:100) (Abcam), anti-centrin monoclonal 20H5 directed

against *Chlamydomonas reinhardtii* (1:100) (kind gift from Dr. J. Salisbury, Mayo Clinic, Rochester, MN) and monoclonal anti α -tubulin (1:100) (CalBioChem, DM1A). Primary antibodies were added to the slides after a rinse series with 1X PBS and 0.01% PBST after blocking. The sections were incubated with these antibodies for 1 h at room temperature. The secondary antibody used was an Alexa Fluor 594-conjugated goat-anti-mouse (Molecular Probes, Invitrogen Detection Technologies). All antibodies were diluted in PBS. Fluorescence microscopy was performed with a Zeiss Axioskop with a standard Texas Red filter set. Paired fluorescence and phase contrast images were made of at least 30 gametophytes from each sample.

Spermidine Synthase Inhibition

Four milligrams of microspores were placed in 2 ml microcentrifuge tube, and 1 ml of water was added. The tubes were placed on orbiting shaker at 20 °C (Klink and Wolniak, 2001 and Tsai and Wolniak, 2001). After 5-10 min, the gametophytes were released from the sporangia by pipetting against the tube wall using 1 ml pipette tips. The gametophytes were allowed to develop for 6 h on the orbitron at 20 °C. Cyclohexylamine (CHA), spermidine synthase inhibitor, stock solution (1 M in water) was added to tubes in the appropriate volumes to bring the final concentrations to 1 μ M, 10 μ M, 100 μ M, 1 mM, 10 mM and 100 mM. The gametophytes were allowed to develop for two additional hours and then fixed after a total of 8 h of development and embedded in Methacrylate for microscopic observations as described above.

Results:

Spermidine localization pattern in the developing microspore

SPD immunolabeling of untreated gametophytes fixed at different time points revealed a distinct localization pattern. During early stages of development, up to 4 h, SPD was present mainly in the jacket cells (Figure II-2: B, C). By 6 h, low levels of SPD were detected in the spermatogenous cells, and high levels of SPD were still detected in the jacket cells (Figure II-2: E, F). However, by 8 h, SPD became abundant in the differentiating spermatids (Figure II-2: H, I). SPD in the spermatids was localized along the anterior side of the elongated nuclei, the location of the multilayered structure (MLS) and the microtubule ribbon. The localization pattern for spermidine synthase transcripts was similar to that of SPD (Figure II-3). Spermidine synthase mRNA was detected in the jacket cells only up to 4 h of development (Figure II-3: A, B). Between 4- 6 h, the transcripts were first detected in the spermatogenous cells in a distinct punctate (Figure II-3: C, yellow arrowhead). By 8 h, the transcripts became abundant throughout the microspore (Figure II-3: D).

Development is arrested early after spermidine synthase silencing

RNAi treatments were performed to examine when and how SPD participates in gametophyte development and differentiation. DsRNA probes were introduced to the spores at the time of hydration. The gametophytes were fixed after 8 h of development. *In situ* hybridization assays showed a significant reduction in spermidine synthase mRNA staining in the affected gametophytes (Figure II-4: B) when compared to the untreated controls (Figure II-4: A). The majority of the treated gametophytes (>60%) were arrested

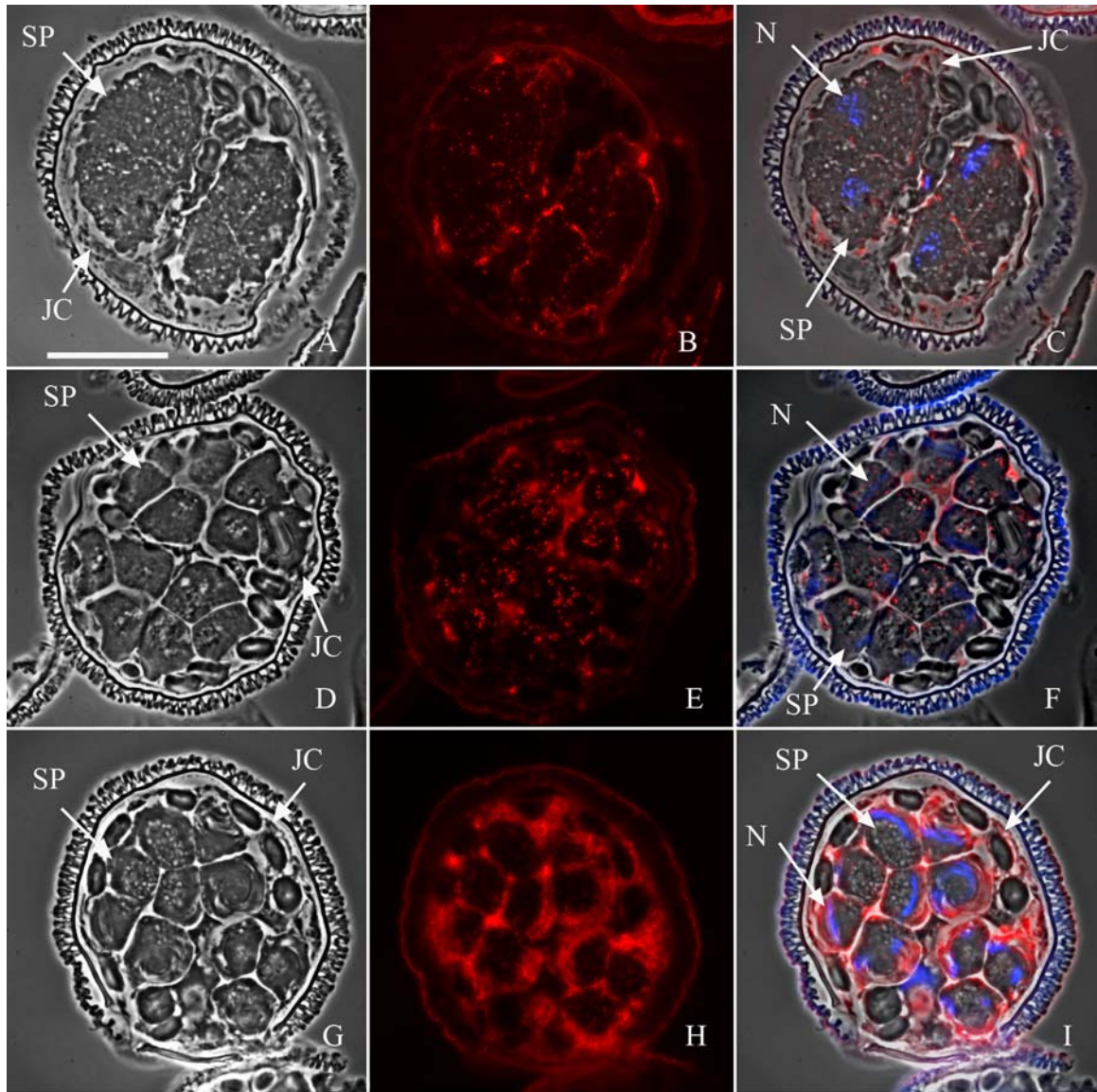


Figure II - 2: Immunofluorescence localization of SPD during normal gametophyte development.

SPD levels increase gradually in the spermatogenous cells during development. Gametophytes were allowed to develop normally for various time intervals and then fixed, embedded in methacrylate and sectioned. (A, D, G) Phase contrast images showing the morphology of the gametophytes. (B, E, H). Immunolabeling with anti-SPD primary antibody and Alexa fluor 594 conjugated secondary antibodies (red). (C, F, I) Images of phase contrast, antibody staining and DAPI nuclear staining (blue) were overlaid to establish the relative localization of SPD in the gametophyte. (A-C) In 2 h controls, SPD

is mainly localized in the jacket cells. (D-F) After 6 h of development, SPD is mainly localized to the jacket cells and some SPD is detected in the spermatogenous cells. (G-I) At 8 h of development, SPD is more abundant throughout the microspore, in both spermatogenous and jacket cells. The spore wall autofluoresces brightly (i=intine). **SP:** Spermatogenous cells. **JC:** Jacket cells. **SPD:** Spermidine. **N:** Nucleus. Bar = 20 μm .

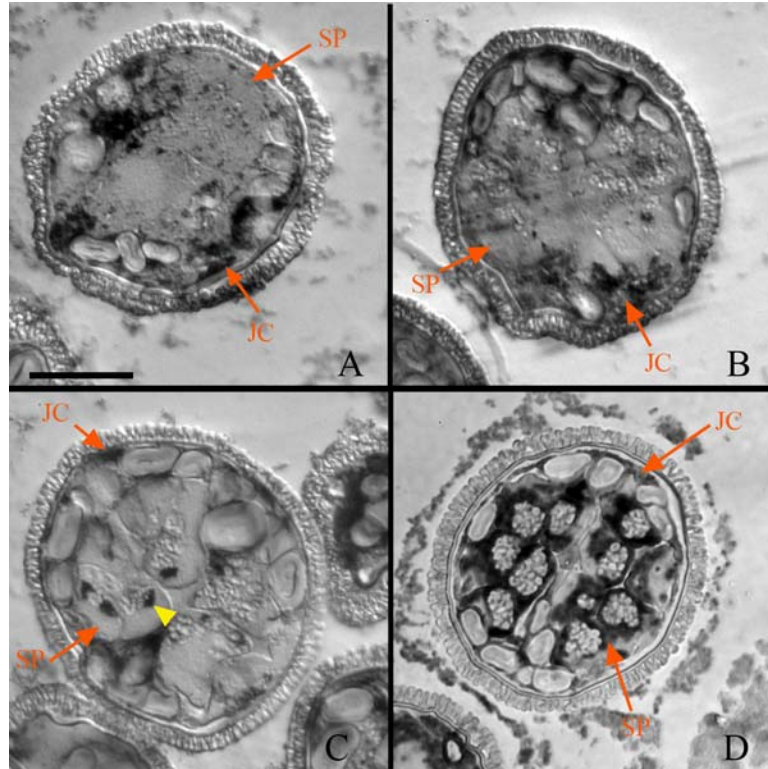


Figure II - 3: Localization patterns of spermidine synthase mRNA during normal gametophyte development.

Gametophytes were allowed to develop normally for variable time increments, fixed, embedded in methacrylate and sectioned. *In situ* hybridization assays for spermidine synthase were performed on thin sections (1-2 μm). Images were acquired with a bright field microscope. (A) 2 h sample. (B) 4 h sample. (A, B) Spermidine synthase transcripts were detected in the jacket cells only up until 4 h of development. (C) 6 h sample. Spermidine synthase transcripts became detected in distinctly localized dots in the spermatogenous cells (yellow arrowhead). (D) 8 h sample. Transcripts were detected throughout the microspore. **SP**: Spermatogenous cells. **JC**: Jacket cells. Bar = 20 μm .

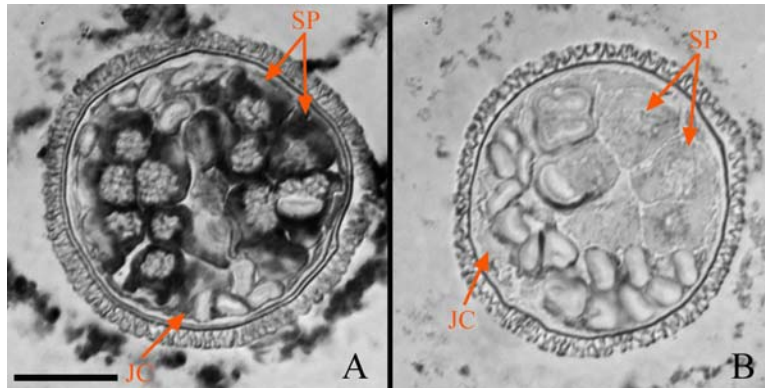


Figure II - 4: Spermidine synthase dsRNA treatment successfully reduced the levels of spermidine synthase mRNA in the affected gametophytes

Gametophytes were treated with dsRNA probes encoding spermidine synthase, fixed after 8 h of development and embedded in methacrylate. *In situ* hybridization for spermidine synthase were performed on semi-thin sections (1-2 μm). (A) Control gametophyte at 8 h showing normal dark staining for spermidine synthase transcripts. (B) Affected gametophytes in the treated sample showed significant reduction in the staining for spermidine synthase mRNA. **SP:** Spermatogenous cells. **JC:** Jacket cells. Bar = 20 μm .

after 4- 5 h of development (Figures II-5: C). The gametophytes in this population had fewer and bigger spermatogenous cells, compared to controls, while the jacket cells appeared normal in both size and position. This indicates that the last round of divisions, which produce the spermatids, was blocked. In addition, only a few of the spermatogenous cells exhibited elongated nuclei. A small percentage of the treated gametophytes, (20%), showed severe defects with developmental arrest between 2- 4 h (Figure II-5: B). In this population, incomplete cell plates prevented the normal partitioning of jacket cells from the spermatogenous domain. The cells in the spermatogenous domains failed to divide further. Finally, less than 10% of the gametophytes were very similar to the untreated controls with subtle anomalies (Figure II-5: D). In this category, gametophytes exhibited the correct positioning and numbers of both spermatogenous and jacket cells. Nevertheless, the spermatogenous cells looked larger than their counterparts in the untreated gametophytes. The nuclei of these cells were elongated and coiled as in the controls. The phenocopy cluster with the highest percentage of occurrence (>60% in this RNAi treatment) and the most consistent effects was considered as the effect of spermidine synthase silencing. This phenocopy was considered as the most important outcome of the treatments in the consequent analyses performed on the samples.

The effect of spermidine synthase silencing on spermatid differentiation

After 8 h of normal development, α -tubulin antibody staining shows microtubules arranged in one bundle on the outer side of the spermatogenous cells. This microtubule bundle denotes the proper formation of the microtubule ribbon and the multilayered

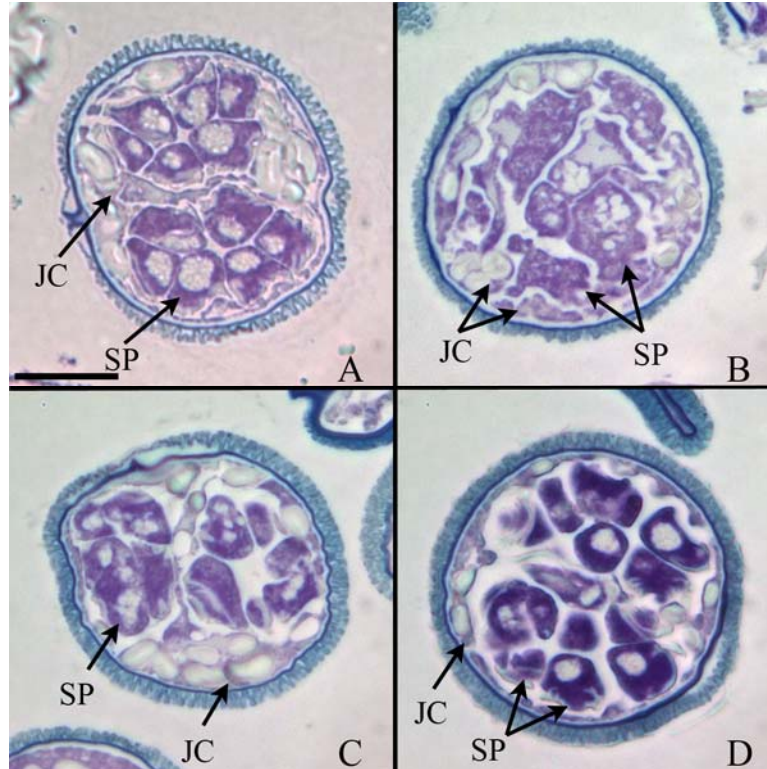


Figure II - 5: Toluidine Blue-O staining for spermidine synthase silencing showing a range of severity of developmental anomalies.

Gametophytes were treated with dsRNA encoding spermidine synthase and fixed after 8 h of development. Thin sections (1-2 μm) were stained with Toluidine Blue-O and observed with bright field microscopy. (A) Control gametophyte at 8 h. (B) Severe effects of SPDS RNAi. Development was arrested at an early stage around 4 h. (C) Majority of the treated gametophytes were arrested before the last division cycle was completed (D) Few treated gametophytes looked almost normal with subtle anomalies in the spermatogenous cells. Some spermatids looked bigger than normal and more elongated. The spermatids seemed to condense and elongate their nuclei. **SP:** Spermatogenous cells. **JC:** Jacket cells. Bar = 20 μm .

structure (MLS) (Figure II-6: B, C). In gametophytes treated with spermidine synthase dsRNA, α -tubulin immunostaining showed the microtubules formed in close association with the nucleus; however, they were organized into scattered arrays instead of the coherent bundles observed in the untreated gametophytes. α -tubulin was also localized into aggregates, possibly as a result of failing to form the microtubule ribbon correctly. In addition, nuclear shaping was affected in the treated gametophytes (Figure II-6: F, arrowhead). In the same gametophyte, some spermatids had elongated nuclei while others were spherical. However, chromatin condensation failed to occur in all of silenced gametophytes.

In normally developing gametophytes, after 8 h, centrin antibody staining shows the basal bodies as evenly spaced dots placed in close proximity to the nucleus on the dorsal side of the developing gametes (Figure II-7: B, C) (Carothers, 1975; Myles and Hepler, 1977; Marc and Gunning, 1986; Hoffman and Vaughn, 1995). After spermidine synthase silencing, centrin was translated and localized into basal bodies-like structures close to the nucleus (Figure II-7: E arrowhead, F). However, these basal body-like structures showed anomalous positioning relative to each other. Some affected spermatocytes had basal bodies sporadically positioned in the cell, while others had basal bodies formed in clusters, in contrast to the linear pattern of dorsally-placed organelles observed in the untreated controls.

The effects of spermidine depletion on spermatid differentiation

To investigate the direct effects of SPD on chromatin remodeling and spermatid differentiation, cells were treated with cyclohexylamine (CHA), a SPD synthase

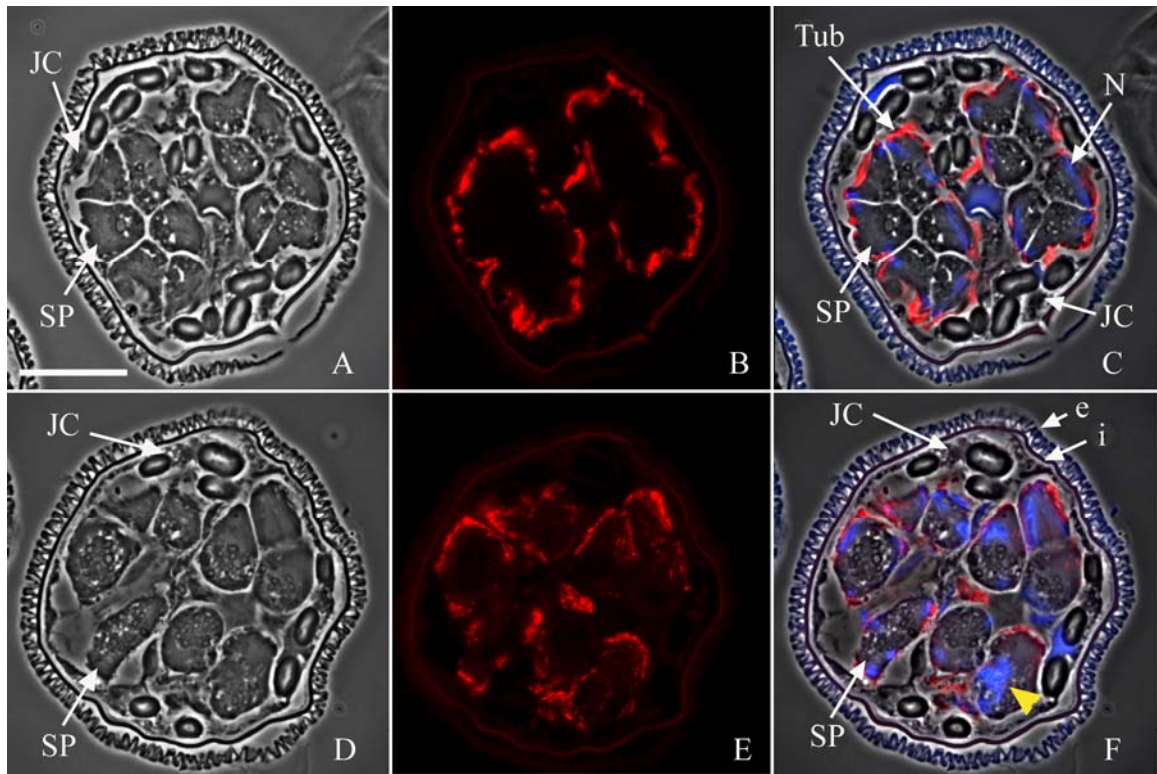


Figure II - 6: The silencing of spermidine synthase resulted in arrested cell divisions, failed nuclear elongation, and scattered microtubule ribbon.

Gametophytes were treated with dsRNA encoding spermidine synthase. The gametophytes were fixed after 8 h of development, embedded in methacrylate and sectioned. (A, D) The morphology of the gametophytes was examined with a phase contrast microscope. (B, E) Labeling of the microtubule ribbon with anti- α -tubulin primary antibody and Alexa fluor-594 conjugated secondary antibody (red). (C, F) Images of phase contrast, α -tubulin labeling (red), and DAPI nuclear staining (blue) were overlaid to establish the relative positioning of the microtubule ribbon in the gametophyte. (A-C) In 8 h controls, the spermatogenous cells form the microtubule ribbon (red) along the elongated nuclei (blue). (D-F) Gametophytes treated with dsRNA encoding spermidine synthase had spermatogenous cells of altered sizes and shapes. The microtubule ribbon failed to form in well organized bundles. The spermatids nuclei were unelongated, and the chromatin was uncondensed (yellow arrowhead). The spore wall autofluoresces brightly (i=intine, e=exine). **SP**: Spermatogenous cells. **JC**: Jacket cells. **Tub**: Microtubule ribbon. **N**: Nucleus. Bar = 20 μ m.

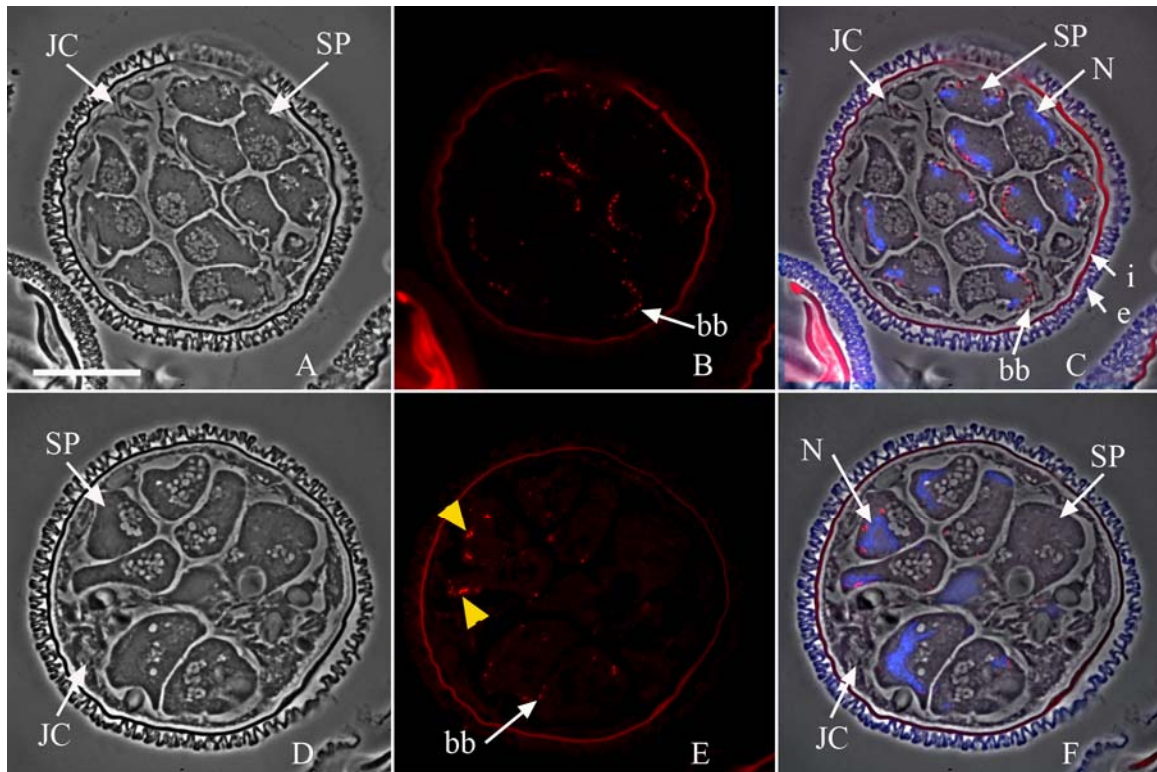


Figure II - 7: The silencing of spermidine synthase resulted in reduced numbers of cell divisions, anomalously clustered basal bodies and a failure of nuclear elongation in the spermatogenous cells.

Gametophytes were treated with dsRNA encoding spermidine synthase, fixed after 8 h, embedded in methacrylate and sectioned. (A, D) Phase contrast images were acquired to compare the effects of spermidine synthase silencing (D-F) to normal development (A-C) at 8 h. (B, E) Immunofluorescence labeling with anti-centrin primary antibodies and Alexa fluor-594 conjugated secondary antibodies (red). (C, F) Images of phase contrast, centrin labeling (red), and DAPI nuclear staining (blue) were overlaid to establish the relative cellular localization of centrin in the gametophytes. (A-C) At 8 h, normally developing gametophytes had basal bodies positioned in even intervals (red, bb). (D-F) Gametophytes treated with spermidine synthase dsRNA; the basal bodies became anomalously clustered after RNAi treatment (E, yellow arrowheads). The spermatids failed to elongate their nuclei after spermidine synthase silencing (F, N, blue) unlike the controls where the spermatids had condensed and elongated nuclei at 8 h (C, N, blue). The spore wall autofluoresces brightly (i=intine, e=exine). **SP:** Spermatogenous cells. **JC:** Jacket cells. **bb:** basal bodies. **N:** Nucleus. Bar = 20 μ m.

inhibitor, to reduce SPD levels in the gametophytes after the completion of the division rounds. As expected, gametophytes treated with CHA had completed divisions and produced spermatogenous cells of comparable size and number to that of the untreated controls. The striking difference, however, was the shape of the spermatid nuclei. DAPI staining of the treated gametophytes showed round or elliptical nuclei with uncondensed chromatin (Figure II-8: F, Figure II-9: F) instead of the highly elongated nuclei with condensed chromatin observed in the untreated control spermatids (Figure II-8: C, Figure II-9: C). Alpha-tubulin protein was distributed uniformly throughout the cytoplasm and no microtubule ribbon was detected (Figure II-8: E, F). In addition, centrin protein was translated and uniformly distributed throughout cytoplasm of the spermatids. CHA treated spermatids failed to aggregate centrin into discrete blepharoplasts and the basal bodies were not detected in these cells (Figure II-9: E, F).

The effects of inhibition of microtubule polymerization on nuclear remodeling

To investigate the relationship between the MLS formation and nuclear shaping further, oryzalin, a plant microtubule depolymerizing drug, was added to developing gametophytes at the onset of spermatid differentiation. The gametophytes were then fixed at 8 h. At 1 μ M oryzalin, almost 50% of the gametophytes were affected; approximately 40% showed normal development and 5- 10% of the gametophytes did not develop. At 10 μ M oryzalin, 90% of the gametophytes were affected, and a small population (< 10%) of the gametophytes either did not develop or underwent few divisions with altered cell plate positioning; the later population was not included in the analysis. Treatments with either 1 μ M or 10 μ M oryzalin showed similar effects in the affected gametophytes. The

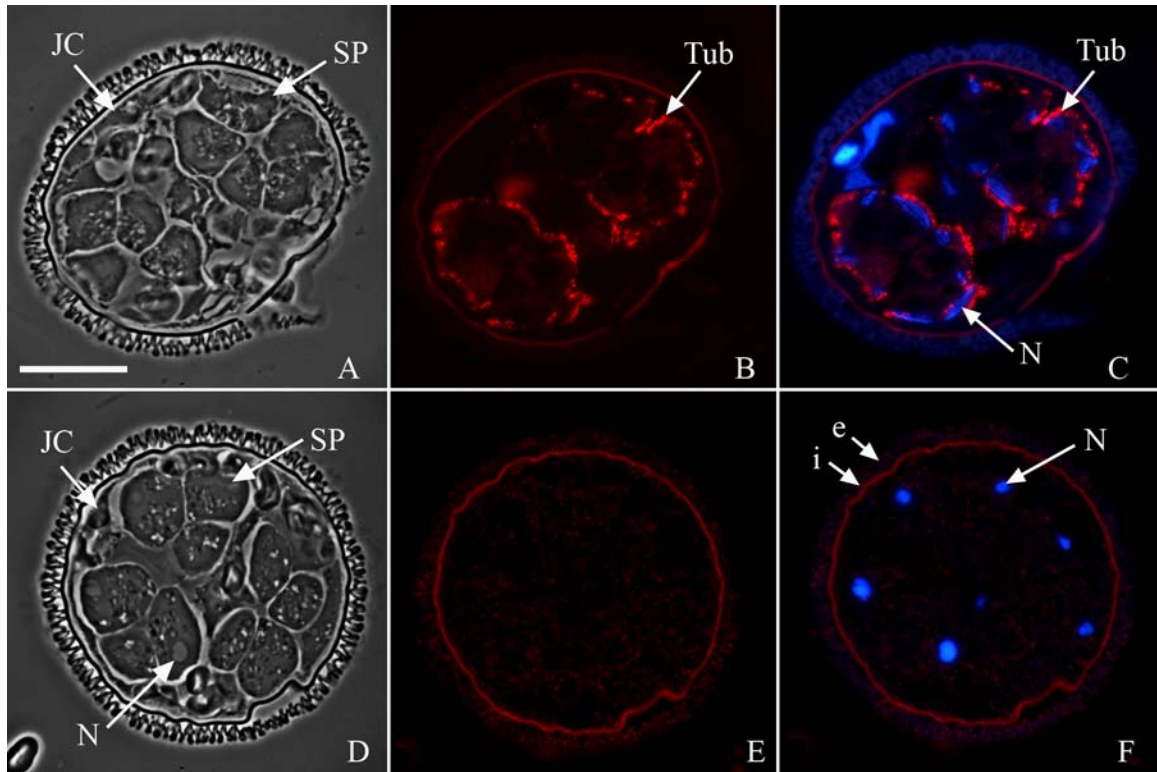


Figure II - 8: The inhibition of spermidine synthase enzyme at the onset of the differentiation phase resulted in a failure to form the microtubule ribbon, and produced round nuclei in the spermatogenous cells.

Gametophytes were treated with spermidine synthase inhibitor (CHA) after 6 h of normal development and fixed after 8 h. (A, D) Phase contrast images were acquired to compare the effects of spermidine synthase inhibition (D-F) to normal development (A-C) at 8 h. (B, E) Labeling of the microtubule ribbon with anti- α -tubulin primary antibody and Alexa fluor-594 conjugated secondary antibody (red). (C, F) Images of phase contrast, α -tubulin labeling (red), and DAPI nuclear staining (blue) were overlaid to establish the relative positioning of the microtubule ribbon in the gametophyte. (D) The spermatids in CHA treated gametophytes showed similar morphology to that of 8 h controls (A). (B, E) Anti- α -tubulin antibody staining showing the normal formation of the microtubule ribbon (B), but the ribbon failed to form in the gametophytes treated with CHA (E). (C) The microtubule ribbon was formed along the elongated nuclei in the spermatogenous cells. (F) Spermatids treated with CHA had round nuclei with uncondensed chromatin (blue). No microtubule staining of the ribbon was observed next

to the nuclei. The spore wall autofluoresces brightly (i=intine, e=exine). **SP:** Spermatogenous cells. **JC:** Jacket cells. **Tub:** Microtubule ribbon. **N:** Nucleus. Bar = 20 μm .

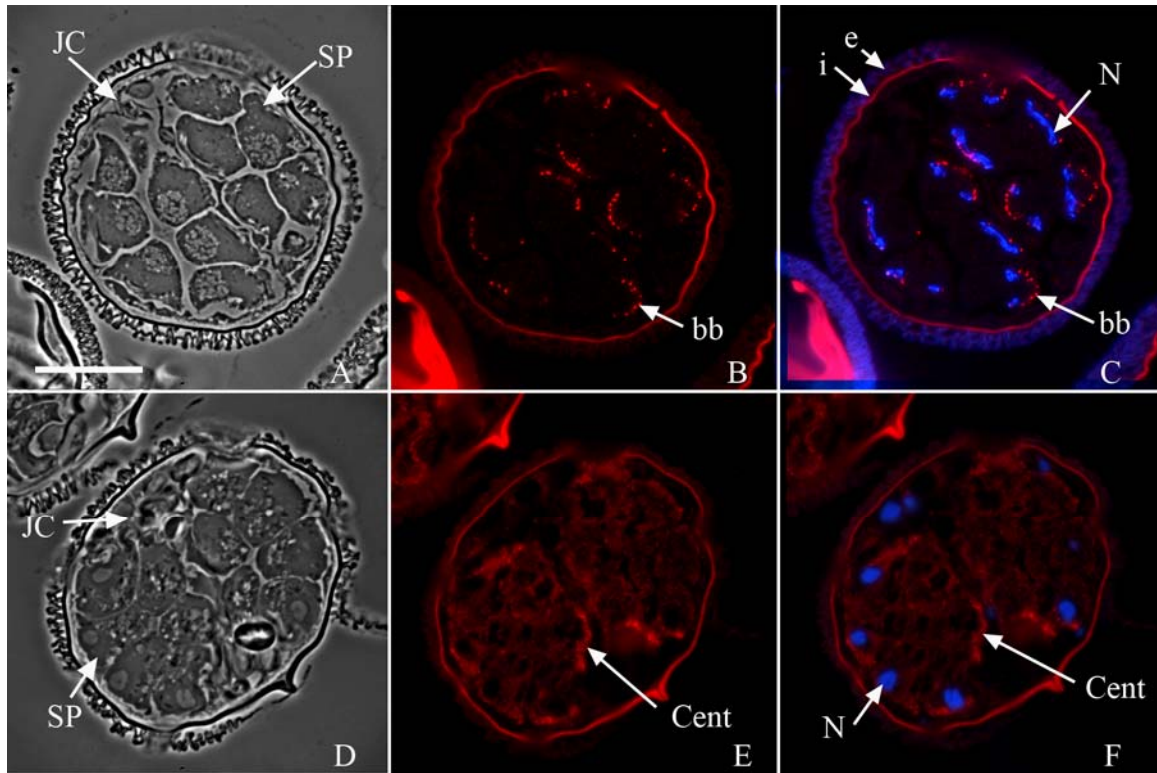


Figure II - 9: The inhibition of the spermidine synthase enzyme at the start of the differentiation phase prevented the localization of centrin into the basal bodies in the spermatogenous cells.

Gametophytes were treated with spermidine synthase inhibitor (CHA) after 6 h of normal development and fixed after 8 h. (A, D) Phase contrast images were acquired to compare the effects of spermidine synthase inhibition (D-F) to normal development (A-C) at the same time point, 8 h. (B, E) Labeling of the basal bodies with anti-centrin primary antibody and Alexa fluor-594 conjugated secondary antibody (red). (C, F) Images of phase contrast, centrin labeling (red), and DAPI nuclear staining (blue) were overlaid to establish the relative positioning of the basal bodies to the nuclei in the gametophyte. (A, D) Phase contrast imaging showed spermatogenous cells of the treated

gametophytes (D) having similar size and shape to that of the controls (A). (C) In 8 h controls, the basal bodies (red) had an evenly spaced positioning next to the elongated nuclei (blue). (E) Centrin (red) was not localized into basal bodies in the spermatids of gametophytes treated with CHA. (F) The nuclei failed to elongate and condense their chromatin as a result of the inhibition of spermidine synthase. The spore wall autofluoresces brightly (i= intine, e= exine). **SP:** Spermatogenous cells. **JC:** Jacket cells. **bb:** basal bodies. **N:** Nucleus. **Cent:** centrin. Bar = 20 μm .

spermatid nuclei were elongated and the chromatin condensed, but the nuclei failed to stretch properly when compared to the untreated controls (Figure II-9: D, F, yellow arrowhead). The different oryzalin concentrations showed similar effects on the formation of the microtubule ribbon and basal bodies. Anti- α -tubulin antibody staining showed abnormally thin lines of microtubules in close association with the nucleus (Figure II-10: H, F, white arrowhead). Centrin immunolabeling showed few basal bodies forming in clusters (Figure II-11: D, F, white arrowhead) unlike the controls where basal bodies had linear arrangement (Figure II-11: B).

The regulation of SPD distribution during the microspore development

A clone encoding a spermidine transporter, subunit PotC, was isolated from our cDNA library. This clone is known in the lab as MvU 2596. The PotC subunit contains a spermidine-binding domain; it is responsible for transporter specificity of spermidine. The silencing of spermidine transporter showed three phenocopies. Approximately 10% of the gametophyte had few and incomplete cell divisions (Figure II-12: C). These gametophytes were excluded from the analysis. The majority of the gametophytes (70%) had fewer and larger spermatogenous cells than those observed in the controls (Figure II-12: B). The nuclei of spermatogenous cells had deformed shapes. Some spermatogenous cells contained plastids, which indicated that plastids had failed to all move to the periphery of the spore prior to jacket cell formation. Alternatively, in these gametophytes, the sites of the division planes were anomalous. In this group, the nuclei of the spermatogenous cells started to elongate, but the chromatin was not condensed. Finally, 20% of the gametophytes resembled the controls at 8 h (Figure II-12: D). The number

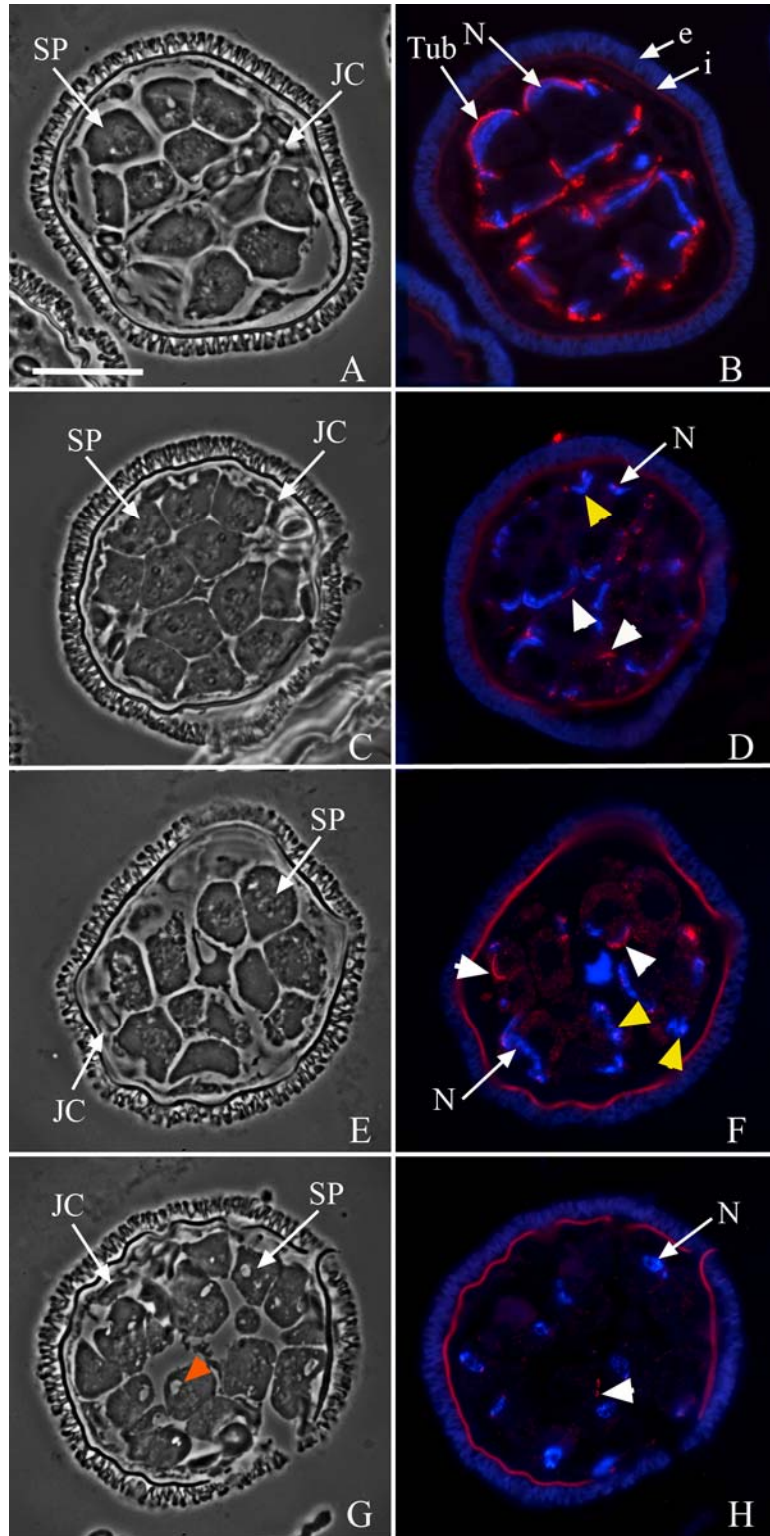


Figure II - 10: Treatment with microtubule depolymerizing drug (oryzalin) prevented the formation of microtubule ribbon but not the MLS.

Oryzalin was added to the gametophytes after 6 h of normal development and the gametophytes were then fixed after 8 h. Immunofluorescence localizations of α -tubulin after gametophytes were treated with oryzalin. (A, C, E) Phase contrast imaging showing the effects of oryzalin treatment on cell morphology (C, E) in comparison to untreated gametophytes at 8 h. (B, D, F) Images of anti- α -tubulin antibody staining (red) and DAPI nuclear staining were overlaid to show the positioning of the microtubule ribbon relative to the nucleus. (A, B) 8 h controls showed the normal formation of the microtubule ribbon. (C, D) Gametophytes treated with 1 μ M oryzalin. (E, F) Gametophytes treated with 10 μ M oryzalin. (C-F) Gametophytes treated with oryzalin showed staining of remnants of the microtubule ribbon still apparent (white arrowheads). Spermatids treated with oryzalin treated had elongated nuclei with condensed chromatin, but the nuclei failed to stretch correctly (yellow arrowhead). The spore wall autofluoresces brightly (i=intine, e=exine). **SP:** Spermatogenous cells. **JC:** Jacket cells. **N:** Nucleus. **Tub:** microtubules. Bar = 20 μ m.

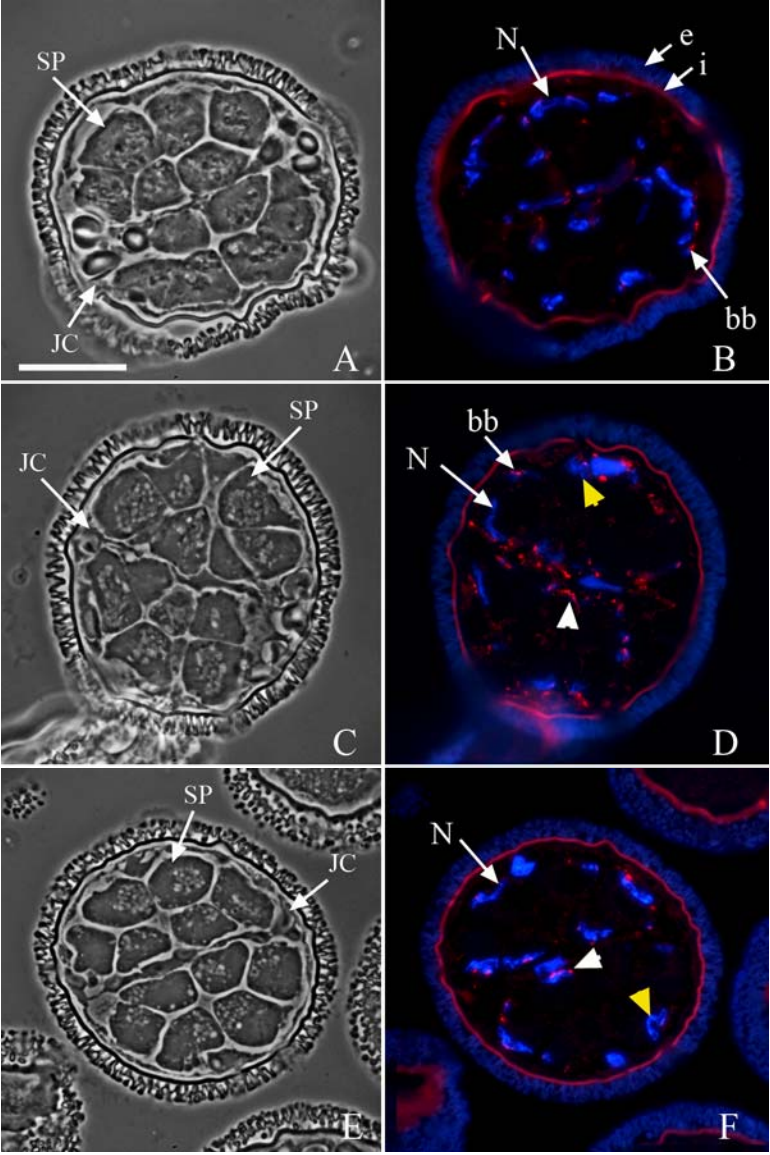


Figure II - 11: In the presence of a microtubule depolymerizing drug (oryzalin), the basal bodies failed to separate and become evenly distributed.

Oryzalin was added to the gametophytes after 6 h of normal development and the gametophytes were then fixed after 8 h. (A, B) 8 h control gametophytes are presented for comparison. (A, C, E) Phase contrast imaging showing the gametophytes' morphology in the untreated controls (A) and after the oryzalin treatments (C, E). (B, D, F) Images of anti-centrin antibody staining (red) and DAPI nuclear staining (blue) were overlaid to show the relative positioning of the basal bodies to the nuclei. (A, B) Normal basal body labeling in untreated gametophytes at 8 h. (C, D) Gametophytes treated with 1 μ M oryzalin. (E, F) Gametophytes treated with 10 μ M oryzalin. (C-F) As a result of oryzalin treatment, the basal bodies did not separate (white arrowheads) and nuclei failed to stretch properly (yellow arrowheads). The spore wall autofluoresces brightly (i=intine, e=exine). **SP**: Spermatogenous cells. **JC**: Jacket cells. **bb**: basal bodies. **N**: Nucleus. Bar = 20 μ m.

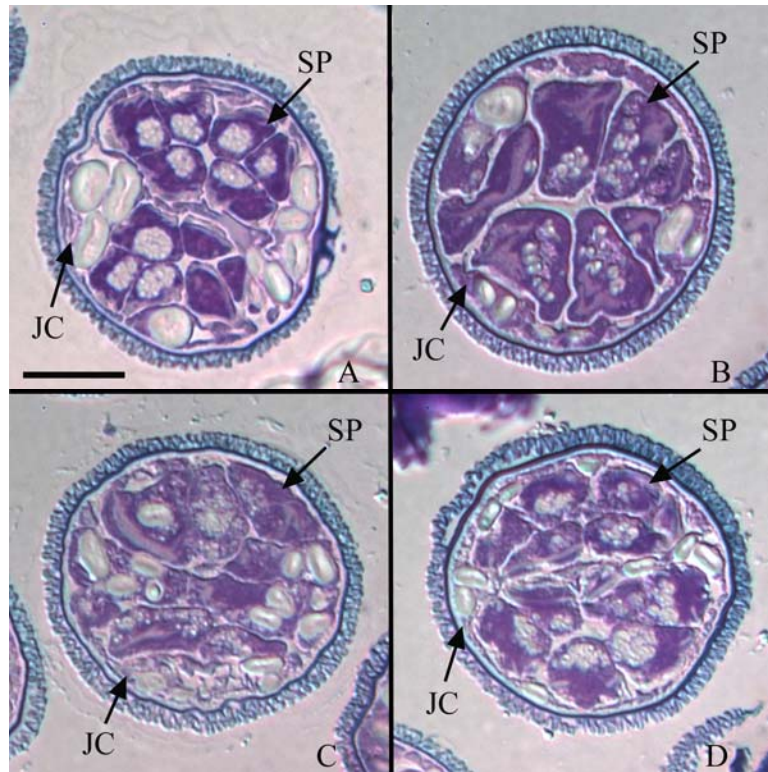


Figure II - 12: The silencing of spermidine transporter resulted in altered positioning of the division planes and reduced numbers of cell divisions.

Gametophytes were treated with spermidine transporter dsRNA, fixed after 8 h and embedded in methacrylate. Thin sections (1-2 μm) were stained with Toluidine Blue-O and observed with bright field microscopy. (A) 8 h untreated controls. (B-D) Gametophytes treated with dsRNA encoding spermidine transporter at 8 h. (B, C) Spermidine transporter RNAi treatment blocked the completion of the last division cycle. (D) Some gametophytes in the spermidine synthase RNAi treatment looked almost normal. The spermatogenous cells in these gametophytes looked bigger than those in the controls. **SP:** Spermatogenous cells. **JC:** Jacket cells. Bar = 20 μm .

and positioning of the jacket and spermatogenous cells were normal while the size and the shapes of spermatogenous cells were altered. Spermatogenous cells were bigger than those of the controls and had irregular surfaces compared to round and smooth appearance in control cells. The nuclei in the spermatogenous cells were elongated and their chromatin was condensed. *In situ* hybridization assays with spermidine transporter probe confirmed the efficiency of the spermidine transporter RNAi treatment in the affected gametophytes (Figure II-13).

In order to examine effects of SPDT silencing on SPD distribution, the treated gametophytes were labeled with anti-SPD antibody. Immunolabeling showed enhanced SPD staining outside the spermatogenous cells, and less SPD staining in the spermatogenous cells than in control gametophytes at the same developmental stage (Figure II-14: D-F). DAPI staining of the treated gametophytes showed that the nuclei of spermatogenous cells started to elongate, but the chromatin failed to condense (Figure II-14: B, C). These spermatids also failed to form a single, organized microtubule ribbon (Figure II-15: E, F, white arrowhead). While centrin was localized into discrete basal bodies in the untreated spermatids, gametophytes treated with SPDT dsRNA showed aggregation of the newly translated centrin but failed to make basal bodies (Figure II-16: E, F). SPDT RNAi phenocopies were similar to the phenocopies of spermidine synthase RNAi in terms of the effects on development and the stage at which development was arrested, but in many cases the defects of SPDT RNAi seemed to be more severe. These observations indicate that functional spermidine transporter proteins are required during at least the later parts of the division phase of gametophyte development.

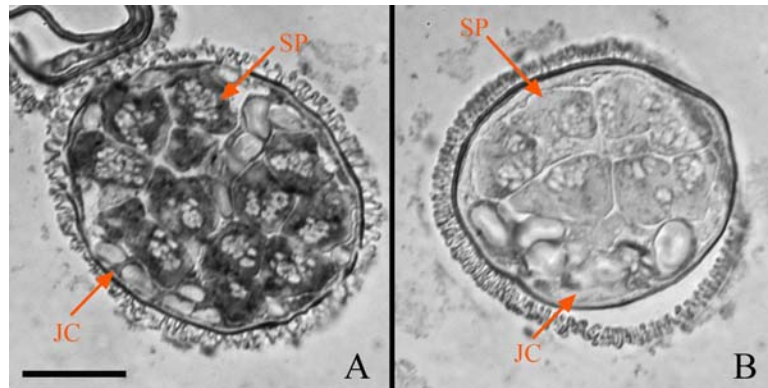


Figure II - 13: Spermidine synthase RNAi treatment resulted in reduced levels of spermidine transporter mRNA in the affected gametophytes.

Gametophytes were treated with dsRNA probes encoding spermidine transporter, fixed after 8 h of development and embedded in methacrylate. *In situ* hybridization for spermidine transporter were performed on semi-thin sections (1-2 μm). (A) Control gametophyte at 8 h showing normal dark staining for spermidine transporter transcripts. (B) Affected gametophytes in the treated sample showed significant reduction in the staining for spermidine transporter mRNA. **SP:** Spermatogenous cells. **JC:** Jacket cells. Bar = 20 μm .

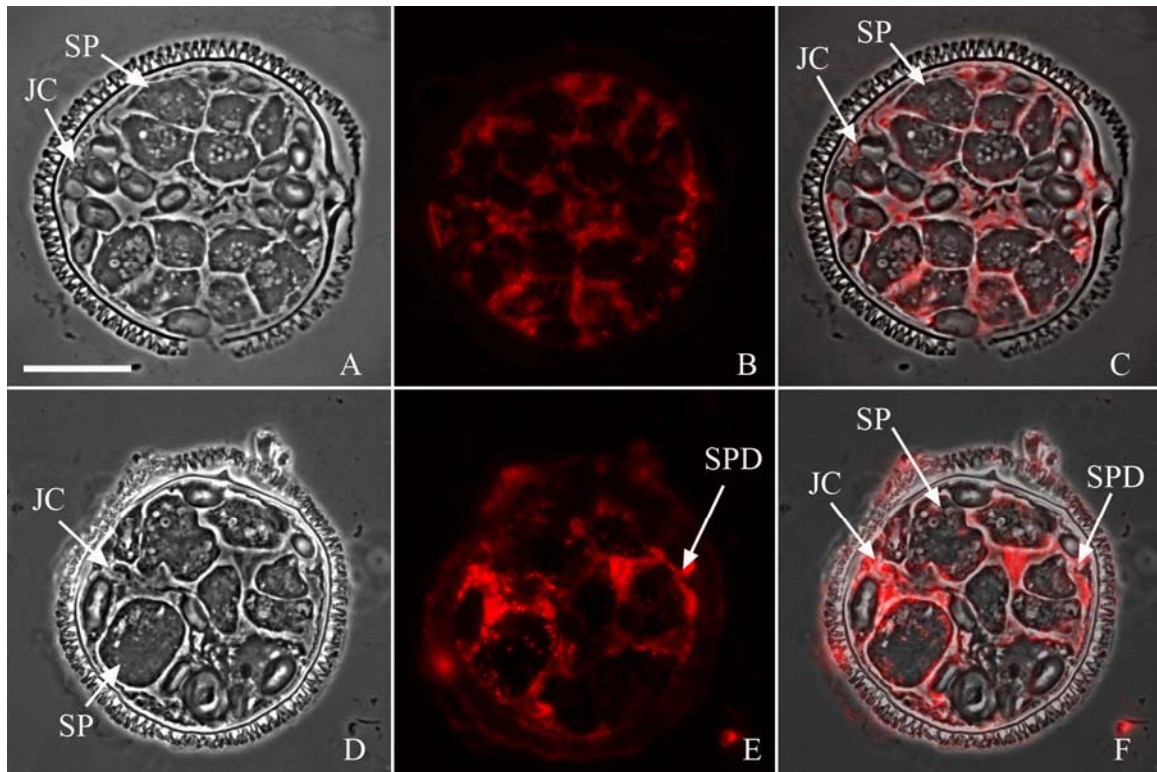


Figure II - 14: The silencing of spermidine transporter prevented the increase in SPD levels in the spermatogenous cells.

Gametophytes were treated with dsRNA encoding a spermidine transporter. The gametophytes were fixed after 8 h of development and then embedded in methacrylate and sectioned. (A, D) Images were acquired with a phase contrast microscope to compare the morphology of the treated gametophytes (D-F) to the untreated controls (A-C) at 8 h. (B, E) Immunofluorescence localization of SPD with anti-SPD primary antibody and Alexa fluor-594 conjugated secondary antibody (red). (C, F) Images of phase contrast and SPD immunolabeling were overlaid to establish the relative localization of SPD in the gametophytes. (A-C) In 8 h controls, spermidine was localized to both spermatogenous and jacket cells. (D-F) Gametophytes treated with spermidine transporter dsRNA show developmental arrest between 4-6 h of development. Anti-SPD antibody staining (red) showed increased SPD staining outside the spermatogenous cells and decreased levels of SPD staining in the spermatogenous cells. **SP**: Spermatogenous cells. **JC**: Jacket cells. **SPD**: Spermidine. Bar =20 μ m.

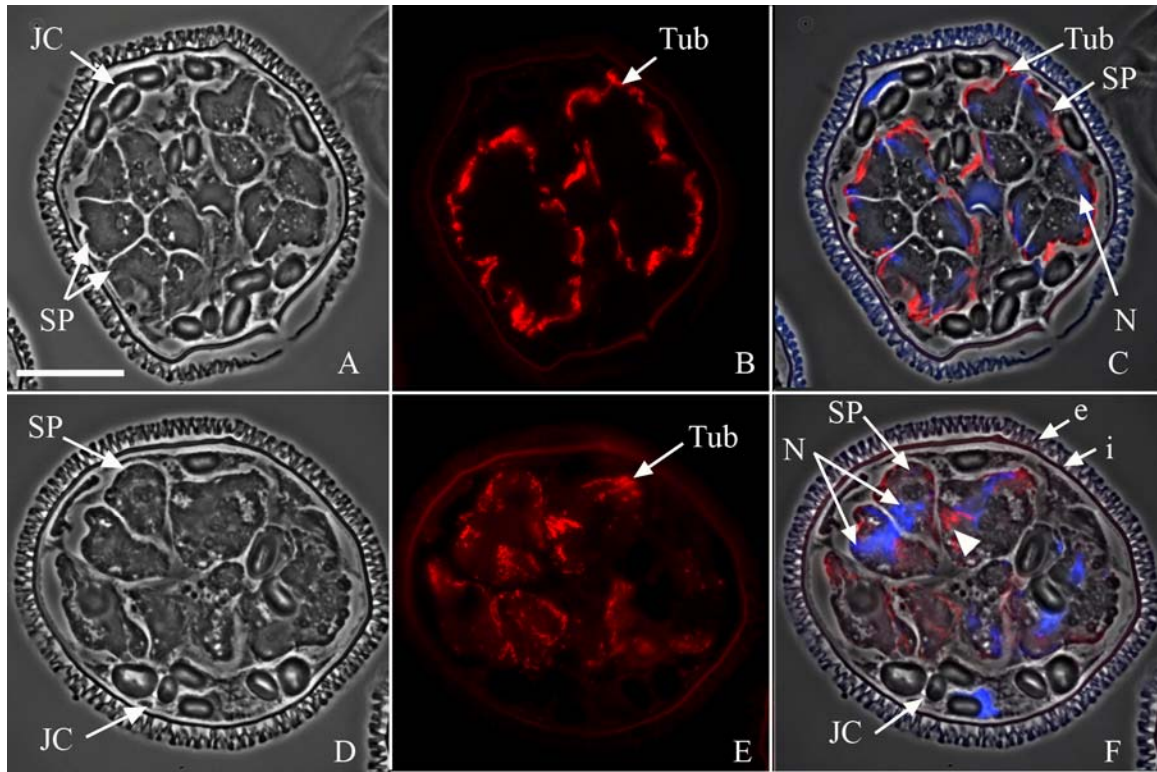


Figure II - 15: The silencing of spermidine transporter disrupted cell divisions and the formation of the microtubule ribbons.

Gametophytes were treated with dsRNA encoding a spermidine transporter. The gametophytes were fixed after 8 h of development and then embedded in methacrylate and sectioned. (A, D) Images were acquired with a phase contrast microscope to compare the morphology of the treated gametophytes (D-F) to the untreated controls (A-C) at 8 h. (B, E) The microtubule ribbon was labeled with anti- α -tubulin primary antibody and Alexa fluor-594 conjugated secondary antibody (red). (C, F) Images of phase contrast, α -tubulin immunolabeling (red) and DAPI nuclear staining (blue) were overlaid to establish the relative positioning of the microtubule ribbon the to spermatids nuclei. (A-C) Untreated gametophytes showed normal staining of the microtubule ribbon (red). (D-F) Gametophytes treated with dsRNA encoding spermidine transporter failed to condense their nuclei (blue) and form coherent bundles of the microtubule ribbon (red, white arrowhead). The spore wall autofluoresces brightly (i=intine, e=exine). **SP:** Spermatogenous cells. **JC:** Jacket cells. **N:** Nucleus. **Tub:** microtubules. Bar = 20 μ m.

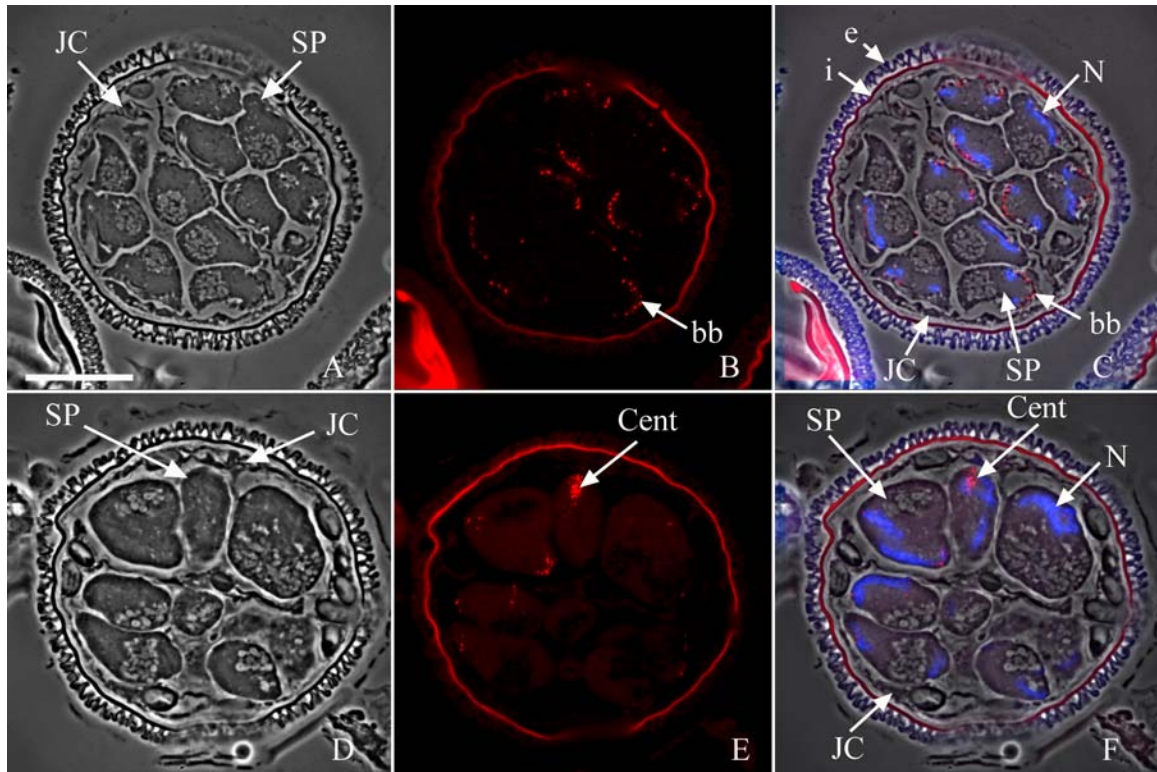


Figure II - 16: The silencing of spermidine transporter affected basal body formation.

Gametophytes were treated with dsRNA encoding a spermidine transporter. The gametophytes were fixed after 8 h of development and then embedded in methacrylate and sectioned. (A, D) Images were acquired with a phase contrast microscope to compare the morphology of the treated gametophytes (D-F) to the untreated controls (A-C) at 8 h. (B, E) The basal bodies were labeled with anti-centrin primary antibody and Alexa fluor-594 conjugated secondary antibody (red). (C, F) Images of phase contrast, centrin immunolabeling (red) and DAPI nuclear staining (blue) were overlaid to establish the relative positioning of the basal bodies in the gametophyte. (A-C) In 8 h controls, the basal bodies (red, bb) showed even distribution along the spermatids nuclei (blue). (D-F) Gametophytes treated with spermidine transporter dsRNA have fewer spermatogenous cells, as a result of arrested cell divisions (D), and fail to form basal bodies of the correct size and location (E, F, red) and remodel their nuclei (blue). The spore wall autofluoresces brightly (i=intine, e=exine). **SP:** Spermatogenous cells. **JC:** Jacket cells. **bb:** basal bodies. **N:** Nucleus. **Cent:** centrin. Bar = 20 μ m.

Discussion:

RNAi experiments, drug treatments and immunolocalization assays show that SPD is required for the normal development and differentiation of the male gametophyte of *Marsilea vestita*. The data presented here show that SPD participates in gametophyte development at two different stages, cell division and spermatid differentiation. The changes in the abundance and distribution patterns of SPD during development imply that SPD can be involved in different cellular processes in a concentration dependent manner. During early stages of development, SPD levels are low in the spermatogenous cells, and SPD is needed for the completion of cell divisions. During spermatid differentiation, SPD levels are significantly elevated, and then SPD is needed for chromatin remodeling and spermatid maturation. Reducing the levels of SPD by RNAi or pharmacological treatments alters chromatin condensation and prevents the elongation of the spermatid nuclei. It also affects the formation of basal bodies and the assembly of the microtubule ribbon. In addition, treatment with the microtubule depolymerizing drug, oryzalin, shows that the assembly of the microtubule ribbon is needed for the proper elongation of the nuclei and the correct positioning of the basal bodies. These results indicate that there is coordination between the different cellular events that take place during spermatid differentiation, and SPD can play a role in the regulation of one or more of these events.

The effects of SPD depletion on spermatid differentiation:

Changes in the abundance and localization of spermidine synthase mRNA and the SPD, made by the enzyme, show the patterns of localized synthesis in different parts of the gametophyte at different times. Collectively, these results suggest that SPD is

involved in different cellular processes at successive stages of development in the gametophyte. The silencing of spermidine synthase and the spermidine transporter led to several interpretations: First, newly translated spermidine synthase is needed for the completion of the division phase. Second, during the early division cycles, spermatogenous cells do not make the SPD; instead, they depend on the SPD provided by the jacket cells via the transmembrane protein, spermidine transporter. This shows that the sterile jacket cells support the development of the spermatogenous cells early in development. In mice, the somatic sertoli cells play a similar role to that of the jacket cells; they provide the developing spermatocytes with polyamines (Hakovirt, 1993).

The spermatogenous cells in the RNAi treated gametophytes showed few basal bodies formed in a cluster. Since the microtubule ribbons were anomalous if even present, it is likely that some of the basal body clustering is a consequence of microtubule ribbon defects. This is confirmed by the oryzalin treatments where clustered basal bodies were observed in the absence of stable microtubules. As a result of either spermidine synthase or spermidine transporter silencing, the spermatids chromatin failed to condense, so SPD made in the spermatids was clearly involved in the remodeling and condensation of the gamete nucleus. Both of these RNAi treatments suggest that both basal body positioning and microtubule ribbon growth, are closely linked to chromatin remodeling and nuclear elongation.

When SPD levels are prevented to rise in the spermatids after the completion of cell divisions, spermatid differentiation is halted. It is possible that SPD is involved in the formation of the microtubule ribbon and the basal bodies in two ways. First, SPD is essential for chromatin remodeling, which could be coordinated with the cytoplasmic

events of basal body formation and microtubule ribbon assembly. Higher order folding of chromatin requires cation dependent charge neutralization (Pollard, 1999). As a small trivalent molecule, SPD can act as a cation to neutralize the negative charge of condensed DNA. Therefore, SPD depletion would prevent the stabilization of the condensed chromatin. The initiation of chromatin remodeling results in physical changes in the size and shape of the chromatin mass. These changes could be communicated to the MLS and the microtubule ribbon through the dense nuclear material connecting the MLS to the nucleus. Therefore, SPD depletion blocks chromatin remodeling and disrupts the formation of the microtubule ribbon and basal body assembly.

Second, SPD levels could directly affect the formation and elongation of the microtubule ribbon. The polyamine may alter microtubule dynamics by affecting the tubulins directly, or by interacting with microtubule associated proteins. Previous studies showed dependence of microtubule assembly on the presence of polyamines (Pohjanpelto *et al*, 1981; Banan *et al*, 1998). A recent study by Needleman *et al*. (2004) showed that microtubules can form bundles in the presence of SPD *in vitro*. SPD is clearly involved in the formation of the microtubule ribbon, which comprises a spirally-wound linear array of crosslinked microtubules. The results in this study show that centriole aggregation for blepharoplast and later basal body formation fail to occur in the absence of SPD. It is reasonable to suspect that SPD, as a charged molecule, could act directly as a crosslinking agent for proteins involved in blepharoplast aggregation and indirectly by displacing masking components from blepharoplast proteins so that these proteins could participate in the aggregation process. In addition, SPD could be involved in the unmasking of stored transcripts encoding proteins essential for blepharoplast or basal

body formation. Some of these possibilities will be explored in the next chapter of this document.

Regulation and control of SPD levels in the microspore:

In untreated gametophytes, SPD levels increase gradually in the spermatogenous cells after the division cycles have reached completion. Similarly, spermidine synthase transcripts become available in the spermatids during a specific time interval as particular developmental events are occurring. The gametophyte is transcriptionally quiescent (Hart and Wolniak, 1999, Klink and Wolniak 2003, Tsai *et al.*, 2003), so the newly available spermidine synthase transcripts in the spermatids are not the products of new transcriptional activity. It is reasonable to suggest that they are masked messages. Transcript unmasking then presents an additional level of regulation in the male gametophyte. Similar mechanisms are present in embryos of other organisms, and are a standard feature of rapid development. While the next chapter will discuss in more details the different possible factors that control transcript masking and unmasking, this chapter is focused on some of the factors involved in the regulation of SPD levels in the gametophyte.

When gametophytes were treated with spermidine transporter dsRNA, SPD was mainly detected outside the spermatogenous cells. Although these gametophytes were fixed after 8 h and had started to differentiate, higher levels of SPD were not detected in the spermatogenous cells. This was at odds with data showing that spermidine synthase is translated in the spermatogenous cells after 6 h of development. Therefore, it is suggested that SPD provided by the jacket cells might act as a signal to enhance the translation of

spermidine synthase in the spermatogenous cells. In other systems, there is evidence that polyamines are implicated in the control of their biosynthesis pathway (Hoyt, 2000). In mammalian cells, for example, low concentrations of SPD were shown to act on the 5'-UTR of ODC transcripts and stimulate its synthesis. Similarly, it is possible that SPD acts as a signal to unmask transcripts of spermidine synthase in the spermatids, thereby making them available for translation. This hypothesis will be investigated further in the next chapter along with the mechanism by which SPD might act to unmask transcripts.

Conclusion:

This study shows that SPD levels change in different cells of the gametophyte in precise ways, and at particular times during development. This is established through the post transcriptional regulation of spermidine synthase and a spermidine transporter, *potC*. First, soon after hydration of the spore, spermidine synthase mRNA is localized in the microspore in the peripheral cytoplasm, where the jacket cells will later reside. Spermidine synthase is translated in the jacket cells and SPD is made by the enzyme in the jacket cells. Next, SPD is transported into the spermatids, presumably because *potC* and other spermidine transport proteins are translated and activated for SPD translocation. As SPD levels rise in the spermatids, spermidine synthase transcripts become available. These transcripts are translated and the functional enzymes elevate SPD concentrations in these cells. A late morphological manifestation of SPD synthesis is the effect on the shape and staining intensity of the spermatid nuclei. SPD can be involved in different cellular processes at different concentrations (Igarashi and Kashiwagi, 2000). It is evident that SPD plays different roles in gametophyte

development in a concentration dependent manner. At early stages, SPD, made in the jacket cells, becomes available in the spermatogenous cells at low concentration. At these low concentrations SPD is needed for the completion of cell divisions. Later, as SPD levels rise, division cycles cease in the spermatids and spermidine synthase transcripts are unmasked. The unmasking of spermidine synthase transcripts is followed by translation of the enzyme, and a considerable rise in SPD levels. This change coincides with the specific events in the gamete differentiation process, and includes cytoskeletal formation nuclear remodeling and the assembly of several complex structures.

Chapter III: The Regulation of Transcript Unmasking: The Likely Involvement of Spermidine and Other Cytoplasmic Factors

Introduction:

Rapid development in many living systems depends on the regulated translation of stored transcripts in the absence of new transcription. During amphibian oogenesis, high levels of transcription take place during the first meiotic prophase and end at oocyte maturation and chromatin condensation (reviewed in Sommerville, 1981; Scheer and Dabauvalle, 1985; Callan, 1986). During the completion of meiosis, egg laying, fertilization, and the rapid cell cycles of early embryonic development, transcription is silent. Development from the mature oocyte stage to the mid-blastula is driven by the translation of stored mRNAs (Sommerville and Ladomery, 1995). Similarly, during mammalian spermatogenesis, transcription is suspended during chromatin condensation at the completion of meiosis, and in the elongated spermatid. Most of the mRNA produced in the round spermatid stage is not associated with polysomes; instead these transcripts are stored as mRNP particles until they are needed at a later stage for the formation of the elongated spermatid. Y-box proteins are involved in the masking of mRNA in male germ cells (Tafari *et al.*, 1993).

Early embryonic development in plants is also driven by the regulated translation of stored mRNA. Plant seeds contain a significant amount of stored mRNA. In pine seeds, the stored mRNA molecules are synthesized during the development of the seeds and stabilized before the seeds become dormant (Davies *et al.*, 1972; Dure and Waters, 1965).

Stored mRNA in seeds is also thought to be present in a complex of ribonucleo proteins (Masumori *et al.*, 1992), but our understanding of these events in plants is not well developed. Recently, rapid development leading to spermatozoid formation in the male gametophyte of the water fern *Marsilea vestita* was shown to be controlled at a post transcriptional level (Hart and Wolniak, 1998, 1999, Klink and Wolniak, 2001, Tsai and Wolniak, 2001, Tsai *et al.*, 2004, Van der Weele *et al.*, 2007). Spermiogenesis in *M. vestita* provides an opportunity to study mRNA unmasking in a rapidly developing plant gametophyte.

Development in the endosporous male gametophyte of *M. vestita* is rapid, and synchronous in a population of spores immersed in water at the same time. The dry microspore contains significant amounts of stored proteins and stored mRNA (Hart and Wolniak, 1998). Inhibitor studies, methionine-labeling experiments, *in vitro* translation assays and northern blot analyses showed collectively that spermiogenesis was dependent on newly translated proteins from stored mRNA in the absence of transcription (Hart and Wolniak, 1998, 1999). The immunolabeling of gametophytes fixed at different time points with antibodies raised against axonemal or cytoskeletal proteins showed that these proteins were mainly localized into the spermatogenous cells (Klink and Wolniak, 2001, 2003). Some of these polypeptides, such as γ -tubulin, were detected in constant levels throughout development while others, such as centrin, became detectable and abundant at a specific time points during development (Hart and Wolniak, 1998, Klink and Wolniak, 2003). The levels of these proteins were then maintained through the remainder of development. Centrin protein provides a clear sense of how protein levels are controlled in the gametophyte: centrin is translated after 4 h of development (Hart and Wolniak,

1998), but only in the spermatogenous cells of the gametophyte (Klink and Wolniak, 2003). Centrin remains abundant in these cells as they mature into motile gametes (Hart and Wolniak, 1998, Klink and Wolniak, 2003). Gametophyte development depends on stored proteins and is driven by the special and temporal regulation of translation of the stored mRNA.

The proper segregation of proteins and specific mRNAs into the spermatogenous initials is obviously essential for the normal development of the gametophyte. This segregation is established early in development during the stage of asymmetric divisions that give rise to the sterile jacket cells and spermatogenous initials (Van der Weele *et al.*, 2007). While newly made proteins are mainly localized into the spermatogenous cells, most mRNAs (*e.g.*, transcripts encoding cytoskeletal or axonemal proteins, such as α - β - γ -tubulin and centrin and other cell maintenance proteins) are detectable throughout the gametophyte during development (Tsai *et al.*, 2004). However, transcripts encoding proteins involved in pre-mRNA processing, such as RNA helicase eIF4AIII and PRP19, are mainly localized in the spermatogenous cells (Tsai *et al.*, 2004). Clearly, the localization of RNA processing and translational machinery in the spermatogenous cells ensures the localization of these newly translated proteins in these cells. In a recent study, Van der Weele *et al.* (2007) showed that the silencing of any of the exon-exon junction complex (EJC) core components, Mv-Mago, Mv-Y14, or Mv-eIF4AIII, disrupts early cytoplasmic rearrangements and asymmetric divisions and results in uniformed distributions of transcripts and proteins that are otherwise restricted to the spermatogenous cells, such as PRP19 mRNA and centrin protein. These treatments cause the disruption of gametophyte development and the anomalous formation of

blepharoplast-like structures in sterile and spermatogenous cells of the gametophyte. Normally, centrin and blepharoplasts are found only in the spermatogenous cells of gametophytes (Van der Weele *et al.*, 2007).

SPD is a trivalent cation, a polyamine. It is ubiquitous in a many organisms (Tabor and Tabor, 1984). SPD is required for cell growth, division and differentiation (Yatin, 2002; Kaur-Sawhney *et al.*, 2002). The cellular levels of SPD are determined by the rate of its synthesis, transport and catabolism. Spermidine synthase is the enzyme responsible for the generation of SPD from a precursor polyamine, putrescine (The biosynthesis pathway was described in chapter II of this document). In *M. vestita*, SPD was shown to be essential for spermatid development and differentiation (chapter II of this dissertation). The cellular levels of SPD are tightly regulated in the gametophyte, and they show a gradual increase in the spermatids during development.

In this chapter, the distribution patterns of spermidine synthase mRNA are determined during gametophyte development. These patterns reveal that mRNA (un)masking may be an additional mechanism of translational regulation in the gametophyte. The roles of spermidine (SPD) and other cytoplasmic factors in the control of spermidine synthase mRNA masking and unmasking during development are investigated. In addition, a possible mechanism of action for SPD in the unmasking of transcripts is presented.

Materials and Methods:

Microspore culture and fixation

Microspores were cultured and fixed as described in detail in the previous chapter. In summary, microspores were obtained from *M. vestita* sporocarps as described in the previous chapter. In a 2 ml microcentrifuge tube, 4 mg of microspores were combined with 1 ml of commercial spring water (Dannon). The tubes were placed on an Orbitron Rotator with aeration at 20 °C. After 1 h, the gametophytes were transferred to 50 ml flasks; the volume was brought to 8 ml with Dannon commercial spring water in each flask. The flasks were placed in a temperature-controlled water bath shaker at 20 °C (Hepler, 1976; Klink and Wolniak, 2001; Tsai and Wolniak, 2001). Microspores were allowed to develop for the desired time interval and then fixed with paraformaldehyde using protocols modified from Klink and Wolniak (2001) and Tsai and Wolniak (2001) (Van der Weele *et al.* 2007). At time of fixation, gametophytes were first collected onto a polyester filter and transferred to a metal mortar where the gametophytes were cracked by a mechanical force. The gametophytes were washed from the filter into a 50 ml conical centrifuge tube with fixative and then placed at 4 °C for 2 h. The gametophytes were then transferred into 2 ml tubes and rinsed 3x 15 min in 1 X PBS (phosphate buffered saline, pH 7.4). Next, the gametophytes were dehydrated with a graded ethanol series and infiltrated with methacrylate mixture. The gametophytes were transferred into BEEM capsules, and the samples were polymerized in ultraviolet light at 4 °C. Semi-thin (1-2 µm) sections were made using a glass knife on an ultra-microtome, and the sections were transferred onto a microscope slide. Sections were relaxed by holding a chloroform-saturated swab in close proximity to the sections. The slides were placed on 40 °C heating block, to allow the sections to adhere to the glass.

RNAi experiments

dsRNA probes were made as described by Van der Weele *et al.* (2007). Single stranded RNAs were transcribed *in vitro* with T3 and T7 polymerase. dsRNA was generated by adding equal amounts of the sense and the antisense RNA together in a microcentrifuge tube. The RNA mixture is heated for a brief period of time and then cooled slowly to room temperature. The quality of dsRNA was checked by gel electrophoresis prior to each experiment. For each RNAi treatment, 4 mg of microspores were added to 200 µg/ml dsRNA in a total volume of 1 ml in a 2 ml microcentrifuge tube. For control samples, 4 mg of microspores were placed in Dannon water. The tubes were placed on orbiting shaker at 20 °C (Klink and Wolniak, 2001 and Tsai and Wolniak, 2001). After 5-10 min, the spores were released from the sporangia. After 1 hour, the gametophytes were transferred to 50 ml sterile flasks, and the total volume was brought up to 10 ml with commercial spring water (Dannon). The flasks were placed in a shaking water bath at 20 °C. The gametophytes were allowed to develop for the desired length of time and then fixed and embedded in methacrylate for microscopic observations as described above. Semi-thin sections (1-2 µm) of the fixed samples were obtained, and the gametophytes were examined with a light microscope. A detailed procedure is described in the second chapter of this document.

In situ hybridization

The probes used for *in situ* hybridization assays were made from cDNA clones encoding centrin (MvU184), γ -tubulin (MvU111), spermidine synthase I (MvU185), PRP19 (MvU98), and RNA binding protein (MvU620). *In situ* hybridization assays were

performed according to protocols described by Tsai and Wolniak (2001) and modified by Van der Weele *et al.* (2007). To label the RNA probes with digoxigenin, half of the dUTP was substituted with digoxigenin-11-dUTP. Thin sections were placed on silanated glass slides and relaxed holding a chloroform saturated cotton swab in close proximity to the sections; slides were dried on a heat block at 40 °C. Slides were treated with acetone, proteinase K, glycine, paraformaldehyde and triethanolamine according to procedures by Steel and coworkers (1998). Probes were hybridized and visualized with Nitro-blue tetrazolium (NBT) and 5 bromo-4 chloro-3 indolyl-phosphate (BCIP) according to procedures described by Tsai and Wolniak (2001).

Cytology and immunocytochemistry

Sections were stained with Toluidine Blue-O and viewed with bright field microscopy (O'Brien and McCully, 1981). Immunofluorescence cytochemistry was employed to localize proteins in the gametophytes. Immunocytochemistry was performed as described in details in the previous chapter. In brief, sections were etched with acetone and blocked with blocking solution. Polyclonal primary antibody anti-spermidine (1:100) (Abcam) was added to the slides. The sections were incubated with these antibodies for 1 h at room temperature. The secondary antibody used was an Alexa Fluor 594-conjugated goat-anti-mouse (Molecular Probes, Invitrogen Detection Technologies). Rinse series with 1X PBS were performed between the mentioned staining steps. Fluorescence microscopy was performed with a Zeiss Axioskop with a standard Texas Red filter set. Paired fluorescence and phase contrast images were made of at least 30 gametophytes for

each sample while hundreds of gametophytes were observed to ensure the accuracy of assessments of the treatments' effects.

Addition of polyamines

Polyamine solutions of 10 μM , 100 μM , 1 mM, 10 mM and 100 mM were prepared in 1 ml total volumes in commercial water (Dannon). Each 1 ml polyamine solution was added to 4 mg of microspores, placed in 2 ml microcentrifuge tubes. The tubes were placed on orbiting shaker at 20 °C (Klink and Wolniak, 2001 and Tsai and Wolniak, 2001). After 5-10 min, the spores were released from the sporangia by pipetting against the tube wall using 1 ml pipette tips. The gametophytes were allowed to develop for 4 h on the orbitron at 20 °C. The gametophytes were fixed, dehydrated and embedded in methacrylate mixture as described above. Thin sections (1-2 μm) of the fixed gametophytes were obtained and examined with a light microscope.

Results:

Spermidine Synthase transcripts have a distinct localization pattern in the developing gametophyte

Spermidine synthase is the protein responsible for the synthesis of SPD (Pegg *et al.*, 1995). Spermidine synthase transcripts showed a localization pattern that differed from those of other mRNAs. During early stages of development up to 4 h after dry spores are placed into water, spermidine synthase transcripts were detected in the cortical cytoplasm of the one-celled gametophyte. This labeling pattern persisted so that the transcripts were present almost exclusively in the jacket cells that formed in this region of the

gametophyte. There was no staining in the spermatogenous cells up to 4 h of development (Figure III-1: A). Between 4- 6 h, spermidine synthase mRNA was apparent in the jacket cells and became detectable as distinct, localized dots at the anterior ends of the spermatids (Figure III-1: B, yellow arrowhead). By 8 h, spermidine synthase mRNA staining was observed throughout the gametophyte (Figure III-1: C) and was most intense in the developing spermatids.

Spermiogenesis in *M. vestita* takes place in the absence of transcription (Hart and Wolniak, 1998, 1999). To confirm that spermidine synthase transcripts that appeared in the spermatogenous cells were not the products of new transcription, *in situ* hybridization assays for spermidine synthase mRNA were repeated on gametophytes treated with a transcriptional inhibitor, α -amanitin, at the time of hydration and fixed at different time points (some of these samples were generated by Vincent Klink). Gametophytes treated with α -amanitin showed the same localization patterns for spermidine synthase transcripts as in the untreated controls (Figure III-1: D-F).

Spermidine controls the availability of spermidine synthase transcripts during development

At 8 h of development, both spermidine synthase transcripts and SPD were abundant in the spermatogenous cells. When a spermidine transporter component was silenced, SPD was mainly localized outside the spermatogenous cells, being detectable both in the jacket cells and in the intercellular spaces at 8 h (Chapter II of this document). In addition, spermidine synthase transcripts were detected only in the jacket cells (Figure III-2). Based on these data, it is reasonable to suspect that SPD might play a role in the

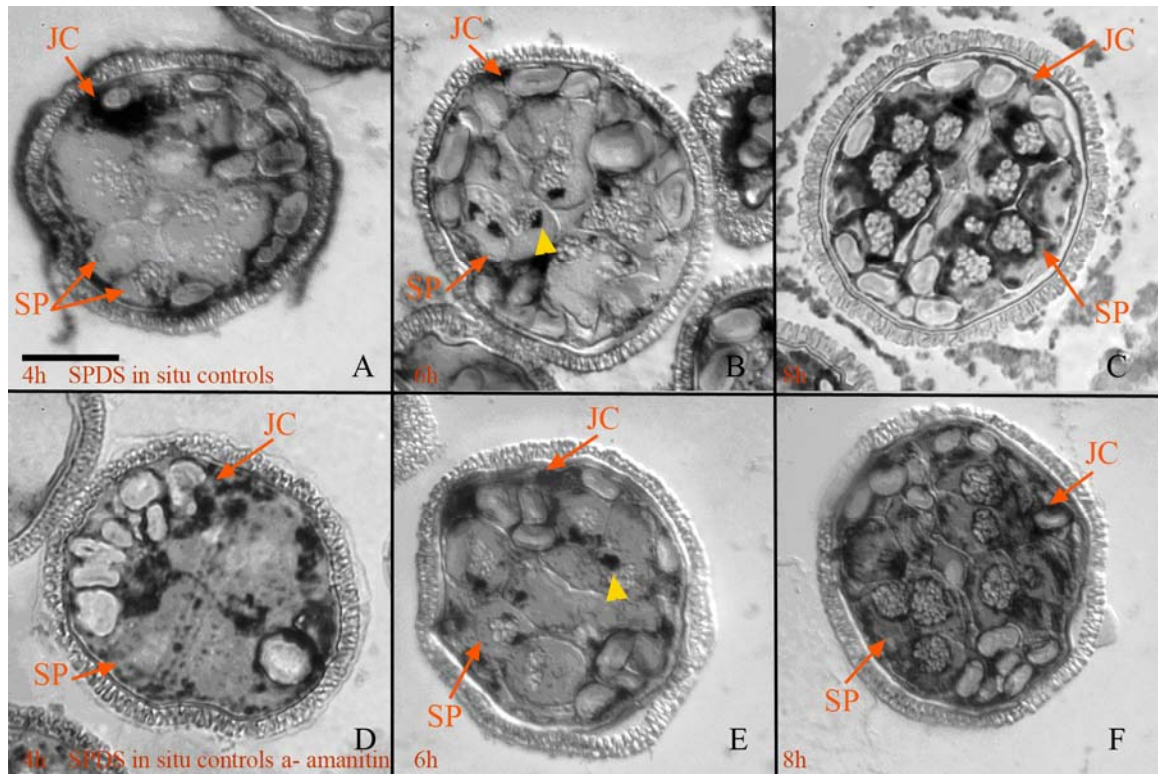


Figure III - 1: The localization patterns of spermidine synthase transcripts in the developing gametophyte.

In situ hybridization assays for spermidine synthase were performed on sections of gametophytes, fixed at 8 h and embedded in methacrylate. The sections were examined with a bright field microscope. (A-C) Normally developing gametophytes fixed at different time intervals. (A) At 4 h, spermidine synthase transcripts were detected in the jacket cells only. (B) At 6 h spermidine synthase mRNA was detected in a localized dot in the spermatogenous cells (yellow arrowhead). (C) At 8 h, spermidine synthase mRNA became abundant in the spermatogenous cells. (D-F) Gametophytes treated with transcriptional inhibitor, α -amanitin, and fixed at different times of development. Spermidine synthase transcripts showed the same localization patterns observed in the controls (A-C). **SP:** Spermatogenous cells. **JC:** Jacket cells. Bar =20 μ m.

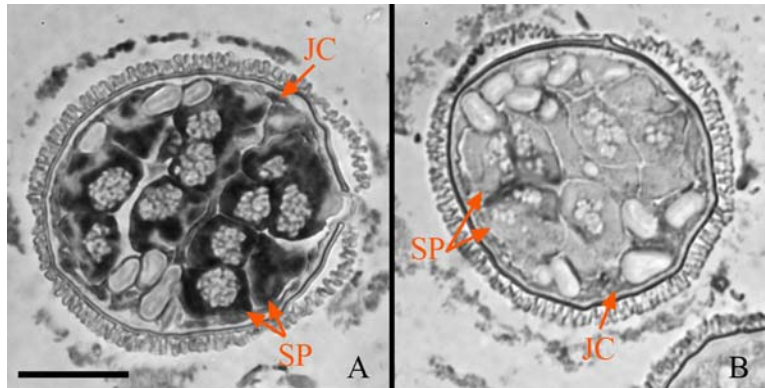


Figure III - 2: Spermidine synthase transcripts are detected only in the jacket cells of gametophytes treated with spermidine transporter dsRNA.

Spermidine synthase *in situ* hybridization assays on untreated gametophytes (A) and spermidine transporter RNAi treatments (B) fixed after 8 h of development. (A) Spermidine synthase mRNA was abundant in both the spermatogenous and jacket cells after 8 h of normal development. (B) The transcripts of spermidine synthase were not detected in the spermatogenous cells of gametophytes treated with dsRNA encoding spermidine transporter. **SP:** Spermatogenous cell. **JC:** Jacket cell. Bar =20 μ m.

unmasking of spermidine synthase transcripts in the spermatogenous cells, thereby making these transcripts available for translation. To test whether the early rise in SPD would result in premature unmasking of spermidine synthase transcripts in the spermatogenous cells, the gametophytes were allowed to develop in the presence of different SPD concentrations. The gametophytes were fixed after 4 h, a time point at which spermidine mRNAs were normally detectable only in the jacket cells.

At SPD concentrations of 10 μ M and 100 μ M, development proceeded normally in the majority of the gametophytes (>90%); the treated gametophytes resembled 4 h untreated controls. At SPD concentration of 1 mM, the majority of the gametophytes (>70%) showed slowed development; they resembled 2 h untreated controls on the bases of normal division plane, the positioning and the number of the jacket cells produced (Figure III-3: B). The remaining 30% of the gametophytes at this concentration developed normally. At 10 mM SPD, approximately 90% of the gametophytes failed to develop. Although, the plastids were localized in the peripheral cytoplasm of the gametophyte, the successive cell division cycles did not occur. For the most part, these gametophytes resembled 0 h untreated controls (Figure III-3: C). When stained with Toluidine Blue-O (TBO), the nucleus in each of these gametophyte stained dark blue unlike the light pink nuclei in 4 h controls. At 100 mM SPD, the majority of the gametophytes (>90%) completely failed to develop (data not presented). This indicated that this concentration was toxic; therefore, subsequent analyses were focused on samples treated with 1 mM, and 10 mM SPD since the later samples showed treatment effects that appeared to be related directly to the concentration of the drug.

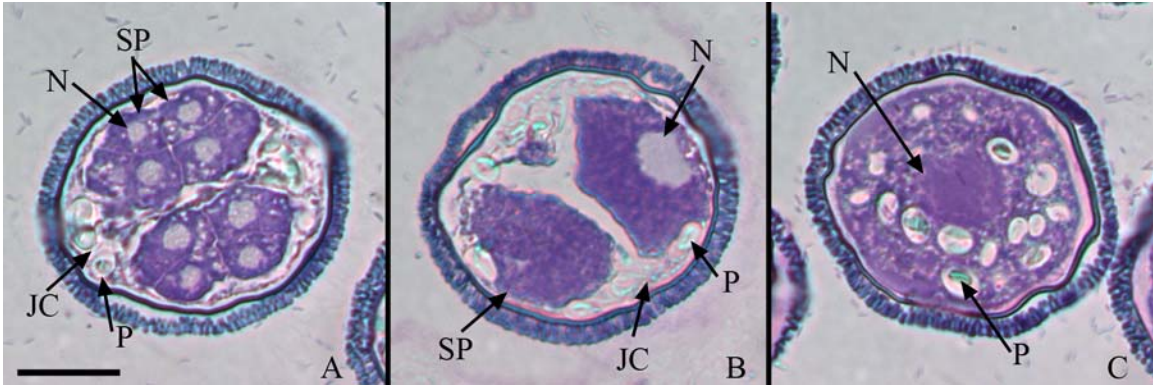


Figure III - 3: Toluidine Blue-O staining for gametophytes developed in the presence of SPD and fixed at 4 h.

Gametophytes were treated with different concentration of SPD, fixed after 4 h and embedded in methacrylate. Thin sections (1-2 μm) were stained with Toluidine Blue-O and observed with bright field microscopy. (A) Untreated controls at 4 h. (B) Gametophytes were developed in 1 mM SPD solution. Development progressed at a slow rate; gametophytes resembled those of 2 h controls. (C) Gametophytes were developed in 10 mM SPD solution; they failed to divide and develop. Gametophytes resembled 0 h controls. **SP:** Spermatogenous cell. **JC:** Jacket cell. **N:** Nucleus. **P:** Plastids. Bar =20 μm .

In situ hybridization assays for spermidine synthase transcripts were performed on SPD treated gametophytes (Figure II-4). At 1 mM SPD, spermidine synthase transcripts appeared in the cytoplasm of both the spermatogenous and jacket cells; whereas in controls, these transcripts were detected only in the jacket cells (Figure III-4: B). In samples treated with 10 mM SPD almost 80% of the gametophytes showed moderate to intense staining for spermidine synthase transcripts in the nucleus and very light staining in the cytoplasm (Figure III-4: C). Only 10% of the gametophytes in this sample showed darker staining in the cytoplasm than in the nucleus. The cytoplasmic staining was mainly localized the periphery of the gametophytes, in the sites that would normally be partitioned to give rise to jacket cells.

Added SPD affects the release of several transcripts during development

To investigate whether SPD could affect the release of transcripts other than those encoding spermidine synthase, a series of *in situ* hybridization assays was performed using probes made from different mRNAs with gametophytes treated with 10 mM SPD. The mRNAs used for these assays shared similar distribution patterns before the 2 h time point (Figure III-5), but they exhibited a variety of localization patterns in normal gametophytes beyond that 2 h period. Mv-Centrin and Mv- γ -tubulin mRNAs were detected in both the spermatogenous and jacket cells of normal gametophytes throughout development (Tsai *et al.*, 2001). In contrast, MvPRP19 mRNA was detected mainly in the spermatogenous cells of normal gametophytes (Tsai *et al.*, 2001). MvU620 mRNA exhibited the same localization pattern as spermidine synthase (Van der Weele and Wolniak, unpublished results). None of these transcripts was detected in normal

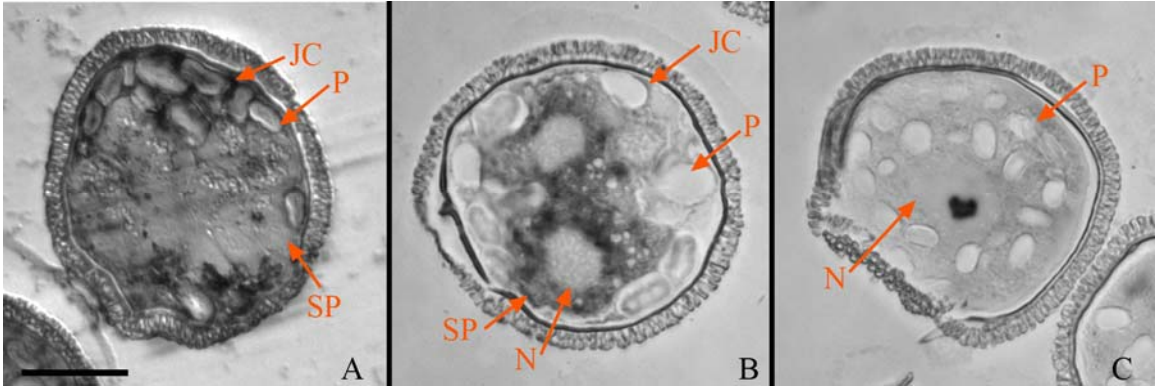


Figure III - 4: The addition of spermidine at the time of hydration affects the distribution patterns of spermidine synthase mRNA.

In situ hybridization assays for spermidine synthase mRNA were performed on gametophytes treated with different SPD concentrations and fixed after 4 h of development. The gametophytes were examined with a bright field microscope. (A) In 4 h untreated controls, spermidine synthase mRNA was detected in the jacket cells. (B) At 1 mM SPD, spermidine synthase mRNA was detected throughout the gametophyte. (B) At 10 mM SPD, spermidine synthase transcripts were detected in the nucleus. **SP:** Spermatogenous cell. **JC:** Jacket cell. **N:** Nucleus. **P:** Plastids. Bar = 20 μ m.

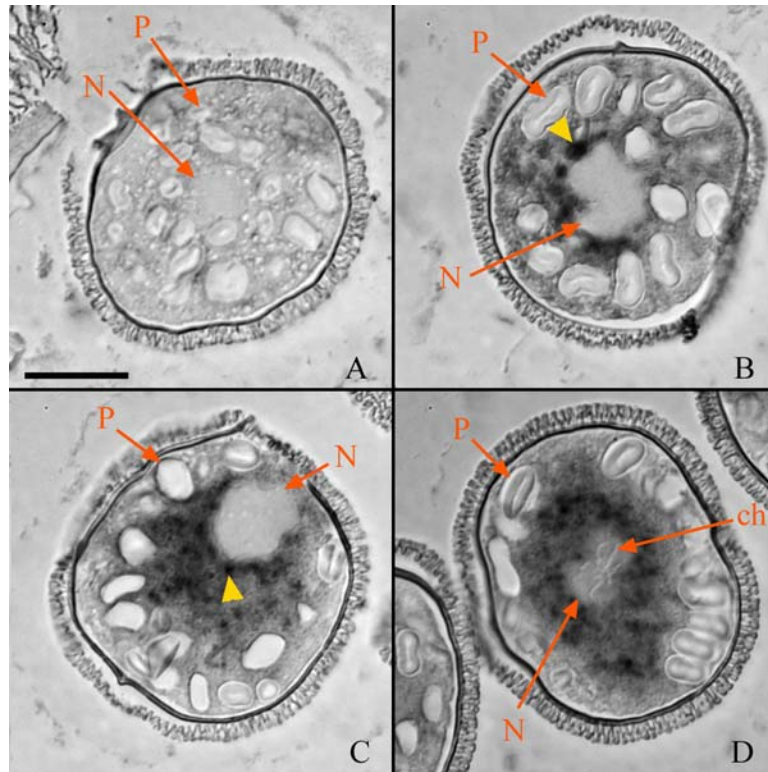


Figure III - 5: The normal localization patterns of spermidine synthase mRNA shortly after the activation of development.

Gametophytes were developed normally for short time increments, fixed and embedded in methacrylate. *In situ* hybridization assays for spermidine synthase mRNA were performed on thin sections of gametophytes fixed at different time points. The gametophytes were examined with a bright field microscope. (A) Dry microspores. (B) Untreated gametophytes fixed at 0.5 h. (C) 1 h controls. (D) 1.5 h controls. (A) Spermidine synthase transcripts were not detected in the dry microspores. (B-D) Spermidine synthase mRNA became detected in the cytoplasm after hydration. Cytoplasmic mRNA aggregates were detected at the nuclear envelope (B, C, yellow arrowheads). **N:** Nucleus. **Ch:** Condensed chromatin. **P:** Plastids. Bar =20 μ m.

gametophytes at or shortly after the time of spore hydration (Figure III-5: A). Just 30 min after the microspores are activated by hydration, cytoplasmic movements and rearrangements start to take place. The transcripts listed above showed cytoplasmic staining at this time point, with some aggregations next to the nucleus (Figure III-5: B, yellow arrowhead). No transcripts were detected in the nucleus. After 1-1.5 h of hydration, these transcripts were detected in the cytoplasm with fewer and smaller aggregates next to the nucleus (Figure III-5: C, D, yellow arrowhead).

In the gametophytes treated with 1 mM SPD, the transcripts showed cytoplasmic localization patterns similar to those of untreated gametophytes developing for 4 h. In samples treated with 10 mM SPD, the transcripts were detected in both the cytoplasm and the nucleus (Figure III-6). Spermidine synthase transcripts were mainly detected in the nucleus with light cytoplasmic staining (Figure III-6: A). Centrin, γ -tubulin and MvU620 mRNAs were detected in both the cytoplasm and the nucleus (Figure III-6: B). Finally, PRP19 transcripts were also detected in both the cytoplasm and the nucleus with significantly dark staining in the nucleus (Figure III-6: C).

With the elevation in transcripts it was reasonable to suspect a corresponding rise in the abundance of proteins encoded by these mRNAs. Immunofluorescence staining for centrin was performed on gametophytes treated with 10 mM SPD. Centrin protein was detected in the spermatogenous cells of 4 h control gametophytes (Figure III-7: B). Some centrin staining was observed in the treated gametophytes (Figure III-7: E). These staining levels were low and did not reflect a premature translation of centrin.

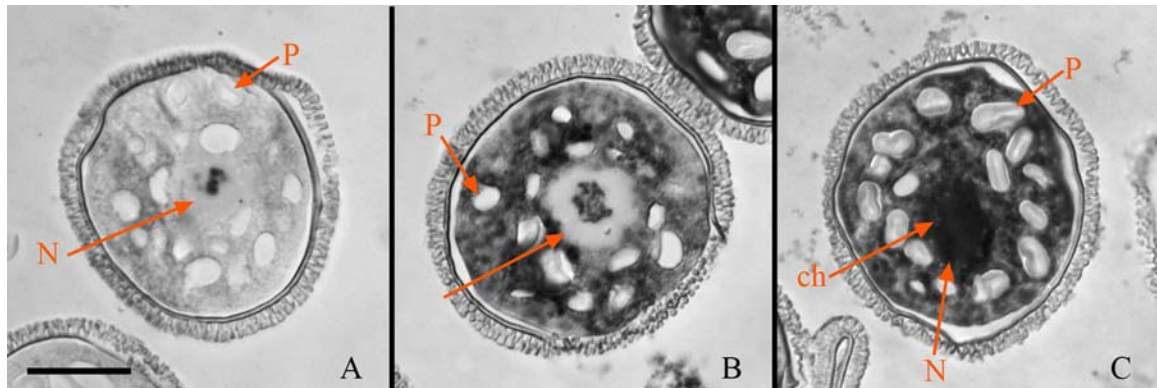


Figure III - 6: The addition of spermidine at the time of hydration affects the distribution patterns of several mRNAs.

Gametophytes were developed in a solution of 10 mM SPD, fixed after 4 h, and embedded in methacrylate. *In situ* hybridization assays were performed on the treated gametophytes with RNA probes encoding different mRNAs. The gametophytes were examined with a bright field microscope. (A) Probes encoded spermidine synthase mRNA. The transcripts were detected in a localized punctate in the nucleus. (B) Localization patterns of centrin, γ -tubulin and MvU620 mRNAs. These transcripts showed nuclear and cytoplasmic staining. (C) PRP19 mRNA showed a distinctly dark staining in the nucleus in addition to the cytoplasm. **N:** Nucleus. **Ch:** Condensed chromatin. **P:** Plastids. Bar =20 μ m.

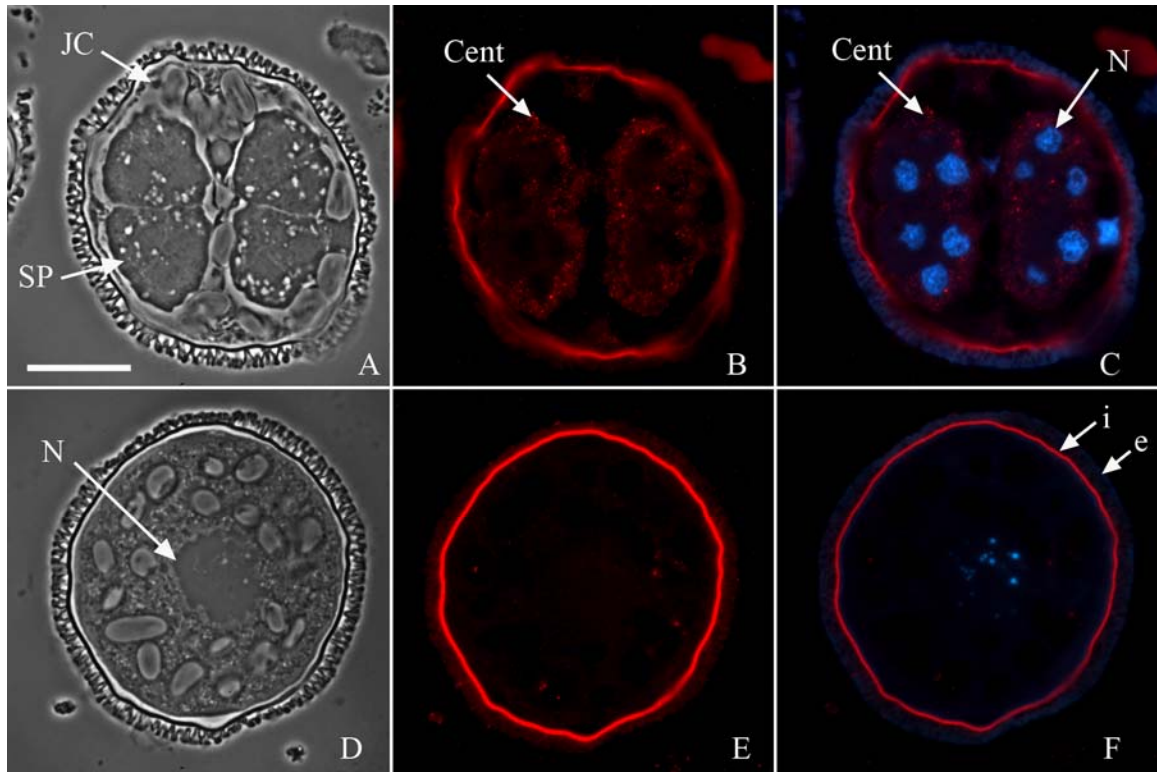


Figure III - 7: The premature release of centrin mRNA does not result in elevated levels of centrin translation.

Gametophytes were developed in the presence of 10 mM SPD, fixed after 4 h and embedded in methacrylate. (A, D) Phase contrast images showing gametophyte morphology. (B, E) Centrin was localized with anti-centrin primary antibody and Alexa Fluor-594 conjugated secondary antibody (red). (C, F) Images of centrin immunolabeling (red) and DAPI nuclear staining (blue) were overlaid to establish the relative localization of centrin in the gametophyte. (A-C) 4 h untreated controls showed centrin staining (red) in the periphery of the spermatogenous cells (B, C). (D-F) Gametophytes treated with 10 mM SPD and fixed at 4 h resembled dry microspores (D); Centrin protein was not abundant in gametophytes treated with 10 mM SPD. The spore wall autofluoresces brightly (i=intine, e=exine). **SP**: Spermatogenous cell. **JC**: Jacket cell. **Cent**: Centrin. **N**: Nucleus. Bar =20 μ m.

Transcript abundance is affected differently with different polyamines

SPD is a triamine; many of SPD cellular functions are related to its structure and charge (Clement, *et al.*, 1995, Geall, 1999). To examine whether polyamines other than SPD can also affect transcript release, putrescine, spermine or norspermidine were added to microspores at the time of hydration in concentrations similar to those used for SPD, 10 μ M, 100 μ M, 1 mM, and 10 mM. The gametophytes were fixed after 4 h of development. The majority (>90%) of the gametophytes treated with 10 μ M, 100 μ M or 1 mM of any polyamine showed normal development (data not presented). On the other hand, most of the gametophytes (>90%) treated with 10 mM of any polyamine resembled 0 h untreated controls, and appeared the same as gametophytes treated with 10 mM SPD.

In situ hybridization assays for spermidine synthase and PRP19 mRNAs were performed on gametophytes treated with the different polyamines. At the lower polyamine concentrations, up to 1 mM, the localization patterns for spermidine synthase and PRP19 mRNAs were similar to those of the untreated controls (data not presented). At 10 mM SPD or putrescine, spermidine synthase transcripts showed nuclear and light cytoplasmic staining (Figure III-8: A, B) while at 10 mM spermine or norspermidine they showed cytoplasmic staining only (Figure III-8: C, D). Few gametophytes (15%) in the spermine and norspermidine treatments showed light staining in the nucleus. On the other hand, PRP19 mRNA showed dark nuclear and cytoplasmic staining in gametophytes treated with 10 mM SPD or putrescine (Figure III-9: A, B) and only cytoplasmic staining in gametophytes treated with 10 mM spermine (Figure III-9: C). Almost 60% of the gametophytes treated with 10 mM norspermidine showed cytoplasmic staining for PRP19 mRNA, and <50% had light staining in the nuclei (Figure III-9: D).

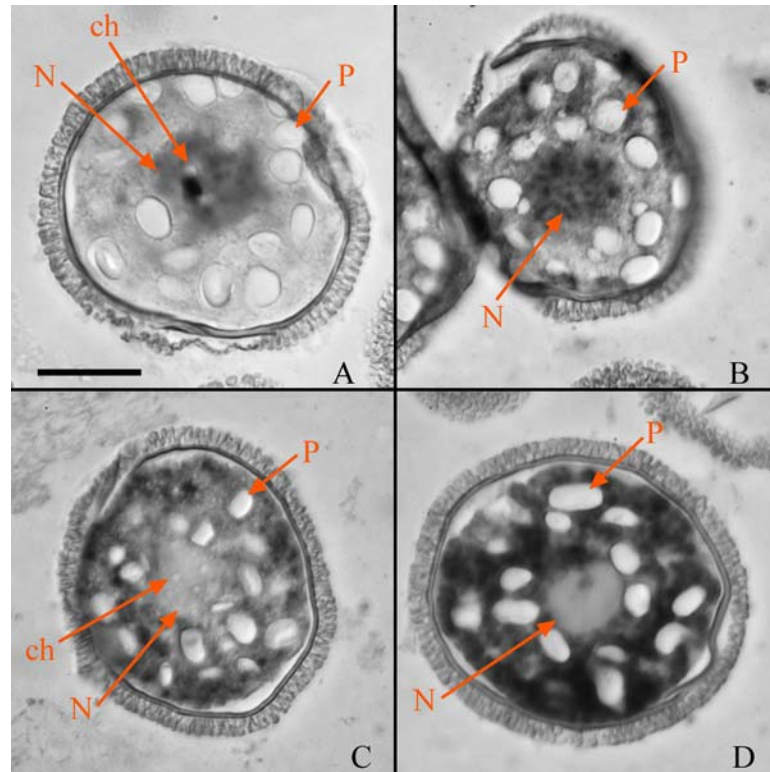


Figure III - 8: Spermidine synthase transcripts show different localization patterns in gametophytes treated with different polyamines.

Gametophytes were treated with different polyamines (10 mM each), fixed after 4 h of development, embedded in methacrylate and sectioned. *In situ* hybridization assays for spermidine synthase were performed on the treated gametophytes. The stained sections were examined with a bright field microscope. Gametophytes were treated with SPD (A), putrescine (B), spermine (C), or norspermidine (D). (A, B) Spermidine synthase mRNA was detected in the nucleus in gametophytes treated with SPD (A) or putrescine (B). (C, D) Spermidine synthase mRNA was detected mainly in the cytoplasm of gametophytes developed in the presence of spermine (C) or norspermidine (D). **N:** Nucleus. **Ch:** Condensed chromatin. **P:** Plastids. Bar = 20 μ m.

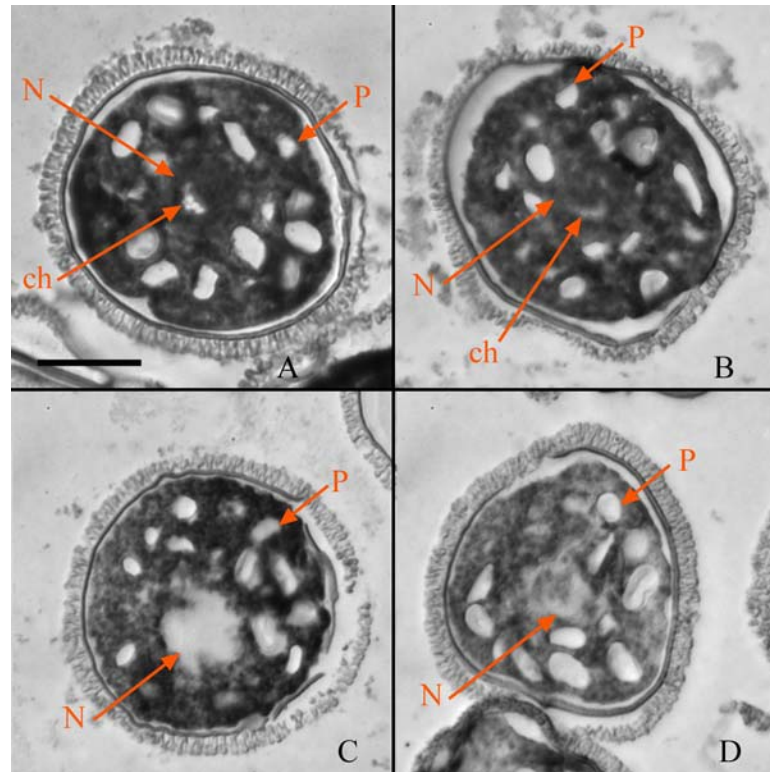


Figure III - 9: Different polyamines have different effects on the distribution patterns of PRP19 mRNA.

Gametophytes were treated with different polyamines (10 mM each), fixed after 4 h of development, embedded in methacrylate and sectioned. *In situ* hybridization assays for PRP19 were performed on the treated gametophytes. The stained sections were examined with a bright field microscope. Gametophytes were treated with SPD (A), putrescine (B), spermine (C), or norspermidine (D). (A, B) PRP19 mRNA was abundant in the cytoplasm and the nucleus of gametophytes treated with SPD (A) or putrescine. (C, D) PRP19 mRNA was detected mainly in the cytoplasm of gametophytes treated with spermine (C), or norspermidine (D). Some of later gametophytes showed light nuclear staining. **N:** Nucleus. **Ch:** Condensed chromatin. **P:** Plastids. Bar = 20 μ m.

Completed cell divisions are needed for the release of SPDS transcripts

During normal development, spermidine synthase transcripts are released in the spermatogenous cells at the start of the differentiation phase (*i.e.*, after the cell division cycles have ceased in the gametophyte). Therefore, it is reasonable to ask whether the completion of the cell divisions is a prerequisite for the release of spermidine synthase transcripts in the spermatids. Cell divisions can be arrested in the gametophyte at different stages by silencing Mv-Cyclin B or Mv-Centrin (Tsai and Wolniak, 2001; Klink and Wolniak, 2001). The silencing of Mv-Cyclin B results in arrested cell cycle after only few divisions taking place (Figure III-10: G) while the silencing of Mv-Centrin blocks the last mitotic division cycle (Figure III-10: D) (Tsai and Wolniak, 2001; Klink and Wolniak, 2001). Centrin translation takes place in both spermatogenous and jacket cells in the absence of completed cell cycles (Tsai and Wolniak, 2001). SPD immunolabeling of gametophytes treated with cyclin B dsRNA and fixed after 8 h showed low levels of SPD in the spermatogenous cells (Figure III-10). In these gametophytes, SPD was detected in the cytoplasmic domains that were to give rise to the jacket cells (Figure III-10: H, I). In gametophytes with silenced Mv-centrin and fixed at 8 h, SPD was localized mainly in the jacket cells. Staining was also observed in the peripheral cytoplasm of the spermatogenous cells (Figure III-10: E, F). Spermidine synthase mRNA was detected in the peripheral cytoplasm or in the jacket cells in centrin and cyclin B silenced gametophytes, but no staining was detected in the central cytoplasm of the one-celled gametophytes or in the centrally positioned spermatogenous cells (Figure III-11: B, C). This result suggests that the rounds of cell divisions are necessary prerequisites for the release of masked spermidine synthase transcripts in the spermatogenous cells.

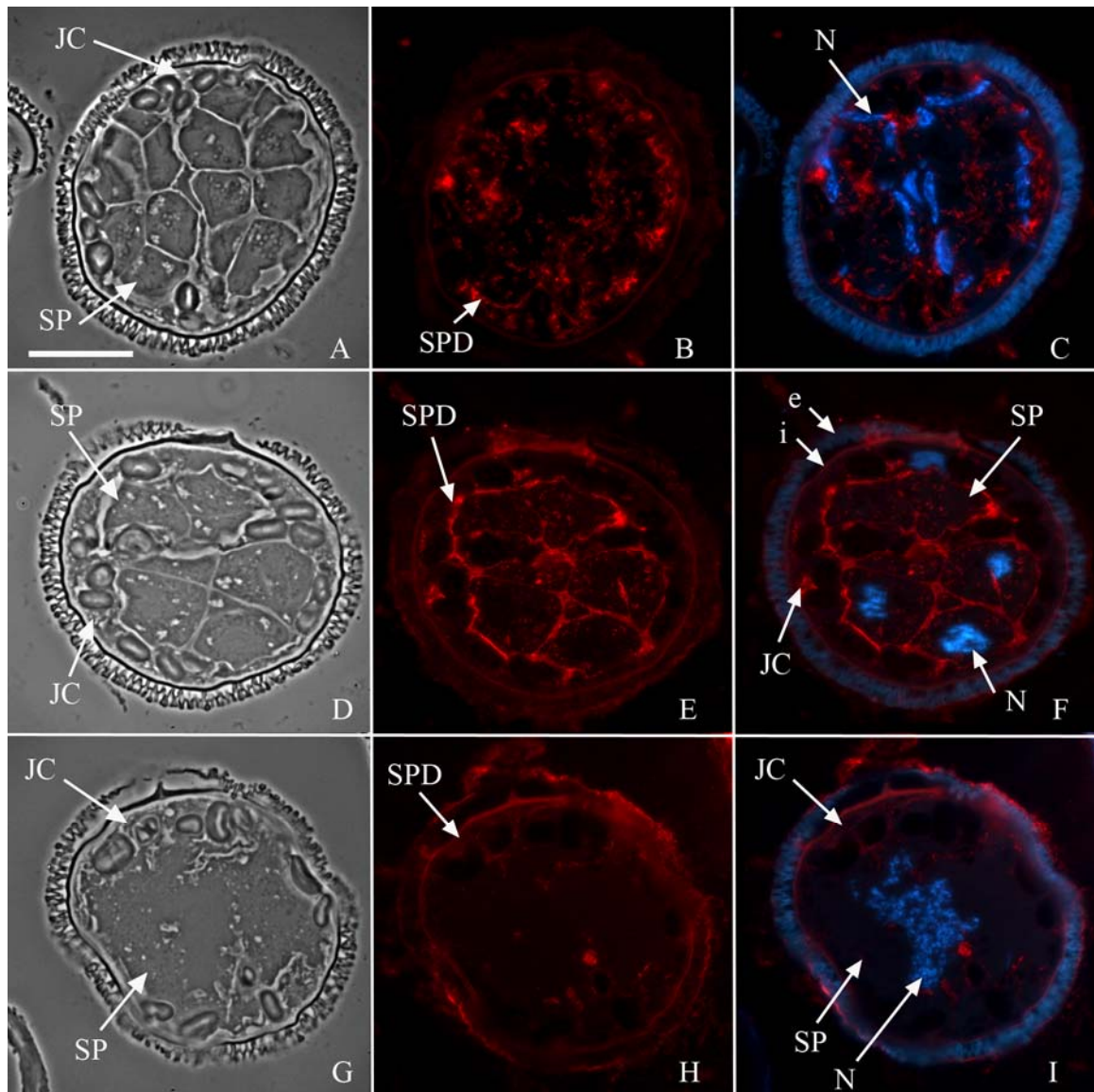


Figure III - 10: Immunolocalization of SPD on RNAi treatments for centrin and cyclin B.

Gametophytes were treated with dsRNA probes encoding either centrin or cyclin B. The gametophytes were developed for 8 h, fixed, embedded in methacrylate and sectioned. (A, D, G) Phase contrast imaging was used to examine the morphology of the gametophytes. (B, E, H) Spermidine was labeled with anti-spermidine primary antibody and Alexa fluor-594 conjugated secondary antibody (red). (C, F, I) Images of SPD labeling (red) and DAPI nuclear staining (blue) are overlaid to establish the relative localization of SPD in the gametophytes. (A-C) 8 h controls. SPD was detected in the

jacket and spermatogenous cells (red). SPD was localized next to the condensed chromatin of the spermatogenous cells. (D-F) Centrin RNAi at 8 h. SPD staining appeared to remain localized outside of the spermatogenous cells and in the jacket cells. (G-I) Cyclin B RNAi treatment at 8 h. SPD was localized to the jacket cells (red). The spore wall autofluoresces brightly (i=intine, e=exine). **SP**: Spermatogenous cells. **JC**: Jacket cells. **N**: Nucleus. **SPD**: Spermidine. **N**: Nucleus. Bar = 20 μ m.

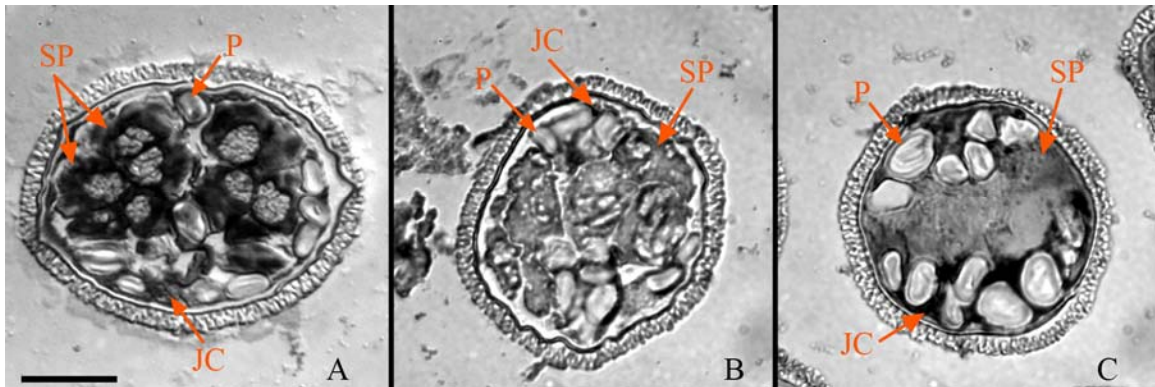


Figure III - 11: Spermidine synthase mRNA is restricted to the jacket cells in gametophytes with arrested cell cycles.

Gametophytes were treated with dsRNA probes encoding either centrin or cyclin B. The gametophytes were developed for 8 h, fixed, embedded in methacrylate and sectioned. *In situ* hybridization assays for spermidine synthase were performed on the treated gametophytes. The stained sections were examined with a bright field microscope. (A) In 8 h controls, spermidine synthase transcripts were abundant in the spermatogenous and jacket cells. (B) Cyclin B RNAi. (C) Centrin RNAi. (B, C) Spermidine synthase mRNA was detected in the jacket cells only. **SP**: Spermatogenous cell. **JC**: Jacket cell. **P**: Plastids. Bar =20 μ m.

The EJC complex is involved in the regulation of transcript masking

Different transcripts are released into different cells at different stages of development, which suggests that multiple factors control the masking and unmasking of transcripts during development. The exon-exon junction complex (EJC) is involved in the transport, processing and controlled translation of mRNA in the microspores of *M. vestita* (Van der Weele, *et al.*, 2007). Therefore, it is possible that the EJC is also involved in the masking and unmasking of spermidine synthase mRNA. *In situ* hybridization assays for spermidine synthase were performed on gametophytes treated with dsRNA encoding one of the EJC core components, Mv-Mago, Mv-Y14, or Mv-eIF4AIII RNA helicase, and fixed at 4 h (Figure III-12). SPDS mRNA was detected in both the spermatogenous and the jacket cells in the treated gametophytes (Figure III-12: B-D), unlike the control gametophytes where staining was limited to the jacket cells (Figure III-12: A). These results show that the destabilization of any of the EJC core components, mago nashi, Y14 or eIF4AIII, results in the premature release of SPDS transcripts in the spermatogenous cells. The EJC appears to play a role in maintaining these transcripts in a masked state.

Discussion:

In this study, mRNA masking is revealed as an additional mechanism of controlling the spatial and temporal patterns of mRNA translation during the male gametophyte development. The possible cytoplasmic factors involved in the regulation of mRNA masking are investigated. SPD is apparently involved in the unmasking of mRNA in a concentration dependent manner. The effectiveness of SPD in the release of transcripts is compared to that of other polyamines, and a possible mechanism of action is provided.

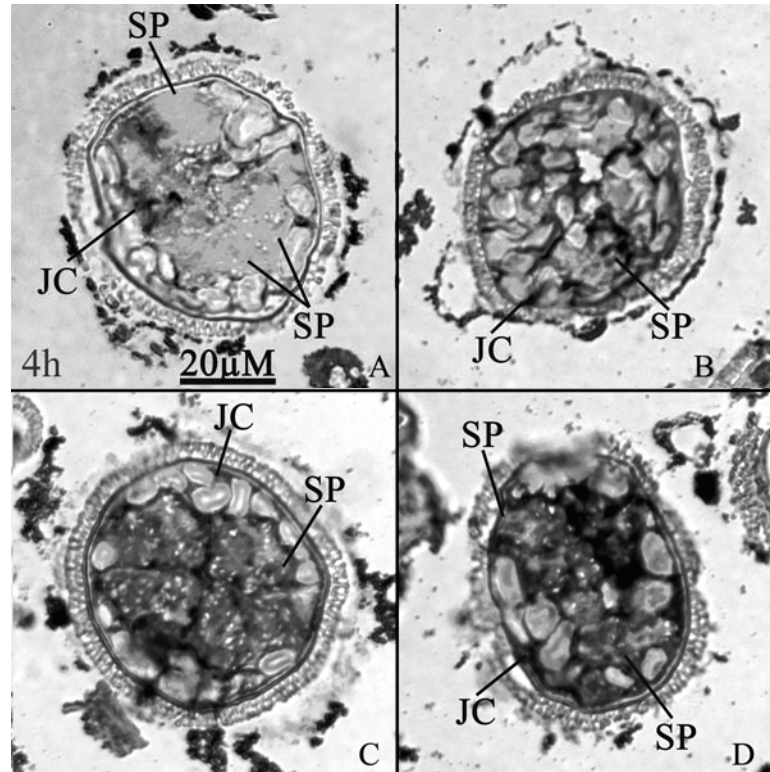


Figure III - 12: Silencing of any of the core components of the exon-exon junction complex (EJC) alters the distribution patterns of spermidine synthase mRNA.

Gametophytes were treated with dsRNA probes encoding EJC core components. The gametophytes were developed for 4 h, fixed, embedded in methacrylate and sectioned. *In situ* hybridization assays for spermidine synthase were performed on the treated gametophytes. The stained sections were examined with a bright field microscope. (A) After 4 h of normal development, spermidine synthase mRNA staining was limited to the jacket cells. (B-D) Gametophytes were treated with dsRNA encoding Mago (B), Y14 (C) or eIFIII4 (D) and fixed after 4 h of development. RNAi treated gametophytes had altered division planes. Spermidine synthase transcripts were abundant the spermatogenous cells of the treated gametophytes. **SP**: Spermatogenous cells. **JC**: Jacket cells. Bar = 20 μ m.

The regulation of mRNA masking is also linked to the cell cycle and functional exon-exon junction complex (EJC).

mRNA masking controls translational patterns the male gametophyte of M. vestita.

Spermiogenesis in *M. vestita* is similar to the early embryonic development of many organisms in that it depends on the translation of stored mRNA in the absence of transcription (Hart and Wolniak, 1998, 1999). The majority of stored transcripts are detected in both spermatogenous and jacket cells with an exception to few transcripts that are detected mainly in the spermatogenous cells (Tsai *et al.*, 2001). These latter transcripts encode proteins involved in the processing and translation of mRNA, which consequently drive the localized translation of transcripts in the spermatogenous cells (Tsai *et al.*, 2001). Spermidine synthase transcripts have a distinct localization pattern in the developing gametophyte (Figure III-1). During the early stages of development, spermidine synthase mRNA is detected in the jacket cells only. Strikingly, the transcript becomes detectable in the spermatogenous cells at the start of the spermatid differentiation. Since transcription is quiescent during the spermiogenesis of *M. vestita*, (Fig. III-1; Hart and Wolniak, 1998, Klink and Wolniak 2001, 2003; Tsai *et al.*, 2004) spermidine synthase mRNA localization patterns suggest that we are looking at unmasking of preexisting transcripts. RNA masking is an established mechanism by which mRNA can be stored in the cytoplasm in an inactive and stable state (Spirin, 1994). The storage of mRNA by RNA masking is prominent in eukaryotes with the classical examples presented in the oocytes and spermatocytes (Spirin, 1994; Davison, 1986).

Spermidine synthase mRNA was the first transcript detected in the gametophytes that exhibited this localization pattern. Since then, lab members have found other transcripts with similar localization and emergence patterns (Van der Weele, unpublished results). Transcripts that exhibit this distinct localization pattern encode proteins that seem to play important roles in spermatid differentiation, for example spermidine synthase (Chapter II of this document) and MvU620 (Van der Weele, unpublished results). These results suggest that in the microspore of *M. vestita*, mRNA masking provides an additional mechanism for the spatial and temporal control of translation of stored mRNA during the gametophyte development.

SPD plays a role in transcript unmasking

The data presented in the previous chapter indicate a possible link between the elevation of SPD levels and the unmasking of spermidine synthase transcripts in the spermatogenous cells. The silencing of a spermidine transporter shows that in the absence of the appropriate levels of SPD in the spermatogenous cells, the transcripts of spermidine synthase are not released (Figure III-2). It is been shown that SPD can control the expression levels of the enzymes involved in the polyamine pathway by binding to 5'-UTR of these transcripts (Hoyt *et al.*, 2000). Therefore, it is reasonable to suspect that SPD controls the translation levels of spermidine synthase transcripts first by unmasking these transcripts and later by enhancing their translation. The addition of SPD to the gametophytes results in unmasking and release of spermidine synthase transcripts from either cytoplasmic or nuclear pools of stored mRNAs. Elevated SPD levels also release several different transcripts in the nucleus and the cytoplasm. In other organisms, it has

been shown that mRNA can be stored in the nucleus. For example, mRNA is stored in the nucleus in cotton seeds, and it is translocated to the cytoplasm when the seeds are hydrated (Hammett and Katterman, 1975). Similarly, in *M. vestita*, *in situ* hybridization assays, performed on dry and newly hydrated spores, show that a variety of transcripts are stored in the nucleus of the dry spore; mRNA starts to exit the nucleus and become detectable by RNA probes within the first 30 min of development (Figure III-5). It is possible that most of the mRNA remains in the nucleus until the first mitotic division where the break down of the nuclear envelope results in the release of the remaining transcripts into the cytoplasm. These transcripts could remain undetectable by *in situ* hybridization until the division cycles are completed because they remain complexed with the storage proteins.

The arrested development observed in gametophytes treated with SPD is most likely the effect of premature mRNA abundance in the gametophytes. Previously, Klink and Wolniak showed that the premature abundance of mRNA, as a result of transcriptional activation, led to suppression of divisions and development (Klink and Wolniak unpublished results). This emphasizes the importance of mRNA masking as a posttranscriptional mechanism to control transcript abundance in the gametophyte. It is likely that the gradual elevation in SPD levels during the differentiation phase results in the unmasking of transcripts needed for spermatid differentiation and morphogenesis, such as spermidine synthase mRNA. SPD can be directly involved in the release of transcripts from masking proteins. The polyvalent SPD can bind to proteins and change their net charge altering their secondary structure (Beauchemin *et al.*, 2007). The high levels of SPD would allow it to function in this charge-based manner to alter the

confirmation of masking proteins and result in the release of stored transcripts. At higher concentrations, SPD can also selectively enhance the translation of some mRNAs (Chroboczek, 1985).

Different polyamines exert different effects on transcript unmasking

In vivo and *in vitro* functions of SPD are mainly charge based. This would imply that the excess of other polyamines of similar charges could also result in the release of transcripts. The addition of different polyamines (SPD, putrescine, spermine and norspermidine) to the gametophytes resulted in a premature release of mRNA in the gametophyte and, therefore, to arrested development. SPD and putrescine had similar effects on transcript release; spermidine synthase and PRP19 transcripts were detected in both the nucleus and the cytoplasm. On the other hand, spermine and norspermidine showed mostly cytoplasmic release of transcripts. Putrescine, SPD and spermine are all naturally occurring polyamines in the gametophyte. However, norspermidine is known to be absent in ferns (Slocum and Flores, 1991). Although norspermidine was a foreign molecule to the *Marsilea* spores, it induced the release of transcripts. This confirms that the action of polyamines on mRNA unmasking is mostly charge based. However, the different mRNA localization patterns in the different polyamine treatments suggest that the mere presence of the positive charge is not sufficient to induce the same effects.

The different polyamines have different structures and charge distribution (Figure III-13). Putrescine and SPD are the smallest of the polyamines and, therefore, the charges are positioned most closely to each other. These polyamines induced the strongest release

of transcripts, nuclear and cytoplasmic release. Like spermidine, norspermidine is a trivalent molecule but is larger than SPD and the charges are therefore further apart than

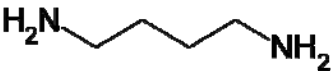
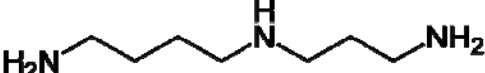
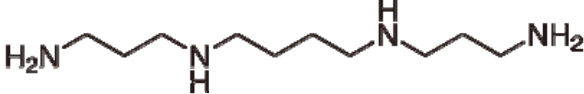
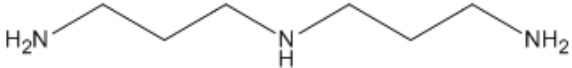
		Methyl spacing
A- Putrescine		4
B- Spermidine		4-3
C- Spermine		3- 4- 3
D- Norspermidine		4- 4

Figure III - 13: The structures of polyamines.

(A) Putrescine is the first polyamine synthesized. It has two positive charges. (B) Spermidine is a tivalent molecule. (C) Spermine is a tetravalent molecule. It is the biggest polyamine presented here. (D) Norspermidine had three charges, like spermidine but bigger structure. The charges are therefore further apart.

those of SPD. Norspermidine showed a weaker effect on transcript release than SPD at the same concentration; less than half of the treated gametophytes showed nuclear staining. Finally, spermine is a tetravalent molecule. It is the largest of all the tested polyamines. Although it has the biggest net positive charge, the charges are the most spread apart and therefore it had the weakest effect on transcript release; transcripts were not detected in the nuclei of the treated gametophytes. In conclusion, elevated levels of putrescine and SPD can induce the release of masked mRNA in the gametophyte. Putrescine and SPD have the highest density of positive charge among the polyamines tested; it is not surprising that they have lower effective concentrations for transcript release than spermine and norspermidine.

Several cytoplasmic factors are involved in the control of transcript masking and unmasking in the developing gametophyte

The results presented in this chapter indicate that mRNA masking is a prominent mechanism for the regulation of translation during gametophyte development. It is reasonable to suggest that there are several cytoplasmic factors involved in the regulation of transcript masking and unmasking. Spermidine synthase transcripts become available for translation in the spermatogenous cells after the completion of the cell division cycles. Blocking of the cell divisions, early with cyclin B silencing or late with centrin silencing, prevents the release of spermidine synthase mRNA the spermatogenous cells. This confirms that completed rounds of cell division are needed for the activation of the unmasking of spermidine synthase transcripts and consequently its translation.

SPD can play a role in linking the cell cycle to transcript unmasking during differentiation. Different SPD concentrations enhance the translation of different mRNAs (Chroboczek, 1985). In the spermatogenous cells, different SPD levels could enhance the translation of selective pools of stored mRNAs at different time points of development. It appears that the elevated levels of SPD towards the end of the division cycles enhance the translation of proteins involved in ceasing the cell cycle and initiating the differentiation phase. In this way, SPD facilitates the transition from the division stage to the differentiation phase. Future studies are needed to provide evidence of such mechanism of action in the gametophyte.

The exon-exon junction complex (EJC) has three core components, Mago, Y14 and eIF4AIII; the EJC associates with other components transiently (Palacios *et al.*, 2004; Shibuya *et al.*, 2004; Tange *et al.*, 2005). Depending on the factors associated with the core, the EJC can play multiple roles in different processes such as mRNA nuclear export, cytoplasmic localization, translation, and quality control (Tange *et al.*, 2004). In *M. vestita*, the EJC is involved in mRNA processing and in restricting the translation of certain transcripts, such as centrin, to the spermatogenous cells (Van der Weele *et al.*, 2007). It is likely that the EJC also plays a role in the maintenance of mRNA masking to restrict translation. The silencing of any of the EJC core components shows premature staining of spermidine synthase mRNA in the spermatogenous cell. This indicates that a functional EJC is needed to sustain the masking of spermidine synthase transcripts. The EJC is known to localize to the nucleus in regions enriched in pre-mRNA and splicing proteins machinery (Lamond and Spector; 2003). In addition, it can play a role in the export of mRNA from the nucleus (Luo and Reed, 1999; Zhou *et al.*, 2000; Le Hir *et al.*,

2001b). Therefore, the EJC could be involved in mRNA masking at early stage of development. Since the EJC is also involved in mRNA processing, it is reasonable to suspect that the EJC is responsible for splicing transcripts that encode masking proteins.

Chapter IV: The Role of Kinesin Motors in the Gametophyte Development

Introduction:

Motor proteins are abundant in all eukaryotic cells. Motors bind with their heads to microtubules or microfilaments and with their tails to ligands and cargos (Kreirs and Vale, 1993, Reddy, 2001). The heads bind and hydrolyze ATP and thereby generate energy to drive movement along cytoskeletal filaments. Motors provide a transport system for macromolecules and organelles within the cytoplasm. Heads and motor domains show high degrees of conservation within a particular super-family of proteins, while tails vary in structure both among super-families and within single families. These traits reflect the diversity and specificity of motors interactions with the potential cargo molecules (Kreirs and Vale, 1993).

Through their interactions with the cytoskeleton, motors localize vesicles, proteins and mRNAs into specific sites in the cell. Therefore, they establish cell polarity by creating asymmetrical distributions of cytoplasmic factors, organelles or components. This asymmetry is crucial for cell development, differentiation and cell fate determination (Lopez de Heredia and Jansen, 2004). Motors also mediate cell division and morphogenesis (Mayer and Jurgens, 2002). In the past two decades, extensive studies have been carried out with the aim of understanding the roles that motor proteins play in variety of cellular processes. Motors are involved in chromosome movement during mitosis, cytokinesis, spindle assembly and maintenance, pollen tube growth and neuron

cell function. During *Drosophila* oogenesis, the microtubule associated motors, kinesins and dyneins, are involved in establishing cell asymmetry through the localization of anterior and posterior determinants such as *oskar* and *bicoid* mRNAs, respectively. In addition, *mago nashi*, a germ cell determinant factor, is localized to the oocyte posterior by a kinesin motor (Hachet and Ephrussi, 2001). Our laboratory (van der Weele *et al.*, 2007) has shown that *mago nashi* plays a critical role in cell fate determination in the male gametophyte of *Marsilea*. In yeast, actin microfilaments and myosin motors are involved in establishing cell polarity. The localization of certain proteins and mRNAs at a specified location give rise to the budding daughter cell. Moreover, actinomyosin-based transport system is responsible for movement of molecules, such as *Ash1* mRNA, from the mother to the daughter cell in budding yeast (Bertrand *et al.*, 1998). *ASH1* is crucial for the switching of mating type. Finally, in *Chlamydomonas*, kinesin and kinesin-like proteins are important for the formation and function of flagella. During flagellar regeneration protein particles are moved bidirectionally along the axoneme. Kinesin proteins facilitate the anterograde movement, from the cell body to flagellar tip while dyneins facilitate the retrograde movement, from the flagellar tip to the cell body (Cole, 2003).

In *M. vestita*, the cytoskeleton plays an essential role in the development of the male gametophyte. Its involvement starts from the onset of development. As soon as the dry spores are immersed in water, plastids are moved to one side of the cell and the nucleus to the opposite side, prior to any divisions. After the first asymmetric division, the prothallial cell is formed, the nucleus is moved back to the center of the spore and the plastids become positioned at the periphery of the spore. Following the first symmetric

division, specific proteins and mRNAs become localized to the center of the daughter cells, into zones that later become spermatogenous initials. Asymmetric divisions produce jacket (sterile) cells at the periphery of the spore and spermatogenous cells at the center of the spore. All of these cytoplasmic movements are carried out by the different components of the cytoskeleton, microfilaments and their motors, myosin proteins, and microtubules and their motors, kinesin proteins.

Studies in our laboratory show that microfilaments are involved at early stages of development and at the end, after 8 hr, during nuclear and cell body elongation. (Molk and Wolniak, 2001; Swamy and Wolniak, 2004). These studies showed that both actin disrupting drugs and actin knockdowns cause early arrest in gametophyte development. Myosin silencing experiments show that different myosin isoforms play distinct roles at different developmental stages. Most newly translated myosin isoforms appear to be involved after 8 hr of development (Swamy and Wolniak, 2004). Early on, preexisting myosins may be involved in several processes.

The working hypothesis presented here is that while actin plays roles at early stages of development to establish division planes, microtubules and their motors are involved in establishing spermatogenous domains. It is suspected that the asymmetric distributions of proteins and certain mRNAs into cytoplasmic domains that will later become the spermatogenous cells are driven by microtubule-based motility systems. Since dyneins appear to be absent from the gametophyte, it is likely that kinesin-driven movements control the movements along microtubules. The purpose of this project is to provide a better understanding of how different kinesins are involved in the segregation and localization of transcripts and proteins into spermatogenous domains of the male

gametophyte of *M. vestita*. This study is focused on the effects of the different kinesin proteins on the formation of the motile apparatus, basal bodies and the microtubule ribbon in the spermatids. These structures are linked to spermatid cell identity and they are the hallmarks for gamete differentiation. The *de novo* formation of the basal bodies requires the timely translation and localization of the necessary proteins, such as centrin (Hart and Wolniak, 1998, Klink and Wolniak, 2001). In addition, the formation of functional cilia in the developing gamete is dependent on the proper formation of the basal bodies and perhaps on the proper assembly of the microtubule ribbon.

Materials and Methods:

Microspore culture and fixation

Microspores were cultured and fixed as described in details in chapter II. In summary, microspores were obtained from *M. vestita* sporocarps as described in the previous chapter. In a 2 ml microcentrifuge tube, 4 mg of microspores were combined with 1 ml of commercial spring water (Dannon). The tubes were placed on an Orbitron Rotator with aeration at 20 °C. After 1 h, the gametophytes were transferred to 50 ml flasks; the volume was brought to 8 ml with Dannon commercial spring water in each flask. The flasks were placed in a temperature-controlled water bath shaker at 20 °C (Hepler, 1976; Klink and Wolniak, 2001; Tsai and Wolniak, 2001). Microspores were allowed to develop for the desired time interval and then fixed with paraformaldehyde using protocols modified from Klink and Wolniak (2001) and Tsai and Wolniak (2001) (Van der Weele *et al.* 2007). At time of fixation, gametophytes were first collected onto a polyester filter and transferred to a metal mortar where the gametophytes were cracked

by a mechanical force (Hepler, 1976). The gametophytes were washed from the filter into a 50 ml conical centrifuge tube with fixative and then placed at 4 °C for 2 h. The gametophytes were then transferred into 2 ml tubes and rinsed 3x 15 min in 1 X PBS (phosphate buffered saline, pH 7.4). Next, the gametophytes were dehydrated with a graded ethanol series and infiltrated with methacrylate mixture. The gametophytes were transferred into BEEM capsules, and the samples were polymerized in ultraviolet light at 4 °C. Semi-thin (1-2 µm) sections were made using a glass knife on an ultra-microtome, and the sections were transferred onto a microscope slide. Sections were relaxed by holding a chloroform-saturated swab in close proximity to the sections. The slides were placed on 40 °C heating block, to allow the sections to adhere to the glass.

RNAi experiments

dsRNA was made as described by Van der Weele *et al* (2007). Single stranded RNAs were transcribed *in vitro* with T3 and T7 polymerase. dsRNA was generated by adding equal amounts of the sense and the antisense RNA together in a microcentrifuge tube. The RNA mixture is heated for a brief period of time and then cooled slowly to room temperature. The quality of dsRNA was checked by gel electrophoresis prior to each experiment. For each RNAi treatment, 4 mg of microspores were added to 200 µg/ml dsRNA in a total volume of 1 ml in a 2 ml microcentrifuge tube. For control samples, 4 mg of microspores were placed in Dannon water. The tubes were placed on orbiting shaker at 20 °C (Klink and Wolniak, 2001 and Tsai and Wolniak, 2001). After 5-10 min, the spores were released from the sporangia. After 1 hour, the gametophytes were transferred to 50 ml sterile flasks, and the total volume was brought up to 10 ml with

commercial spring water (Dannon). The flasks were placed in a shaking water bath at 20 °C. The gametophytes were allowed to develop for the desired length of time and then fixed and embedded in methacrylate for microscopic observations as described above. Thin sections (1-2 µm) of the fixed samples were obtained, and the gametophytes were examined with a light microscope. While hundreds of gametophytes were examined to establish an accurate assessment of the phenocopies, images of at least 30 gametophytes were acquired for each RNAi or pharmacological treatment and assay performed on the gametophytes. The images presented in this document were most representative of the effects of the different treatments and assays performed on the gametophytes. A detailed procedure is described in the second chapter of this document.

Cytology and immunocytochemistry

Immunofluorescence cytochemistry was employed to localize proteins in the gametophytes. Immunocytochemistry was performed as described in details in chapter II. In brief, sections were etched with acetone and incubated with blocking solution. Monoclonal primary antibodies anti-centrin (1:100), anti-β-tubulin (1:100) and anti-α-tubulin (1:100) were added to the slides. The sections were incubated with these antibodies for 1 h at room temperature. The secondary antibody used was an Alexa Fluor 594-conjugated goat-anti-mouse (1:1000) (Molecular Probes, Invitrogen Detection Technologies). Series of rinses with 1X PBS (phosphate buffered saline) were performed between the previous steps. Fluorescence microscopy was performed with a Zeiss Axioskop with a standard Texas Red filter set. Hundreds of gametophytes were examined with the microscope to ensure the accuracy of the phenocopy assessment. Paired

fluorescence and phase contrast images were made of at least 30 gametophytes from each sample.

Results:

Isolation of kinesin isoforms from M. vestita cDNA library

MvU#	Identity as determined by BLAST search	Accession #
99	Kinesin 5 [<i>Arabidopsis thaliana</i>]	NM-116758.3
130	POK1 (Phragmoplast orienting Kinesin 1) [<i>Arabidopsis thaliana</i>]	NM-112614.3
629	Kinesin II/ KIF3B	DQ680042
951	Kinesin 1	AB290928.1
1647	Kinesin 13A [<i>Arabidopsis thaliana</i>]	NM_180267.1
2336	POK2 (Phragmoplast orienting Kinesin 1) [<i>Arabidopsis thaliana</i>]	NM-112791.4
2357	Kinesin-like protein [<i>Arabidopsis thaliana</i>]	AF159052.1

Table IV-1: List of the different kinesin clones that were isolated from our cDNA library as identified by searching against sequence database through tBlastx. These clones were used in this study to generate dsRNA constructs and induce RNAi effects.

The effects of different kinesin proteins on development and differentiation

RNAi treatments were performed for the kinesin proteins listed above. Control and dsRNA treated gametophytes were fixed after 8 h of development, a time point at which the cell divisions were completed and spermatid differentiation had been initiated (Klink and Wolniak, 2001). Fixing after 8 h of development allows for the examination of the effects of kinesin knockdowns on both cell division and spermatid differentiation. The silencing of different kinesins affected development differently (Figure IV-1). Divisions were arrested at different stages and protein translation and localization patterns were altered as examined by anti-centrin and anti- β -tubulin antibody staining. Some kinesin

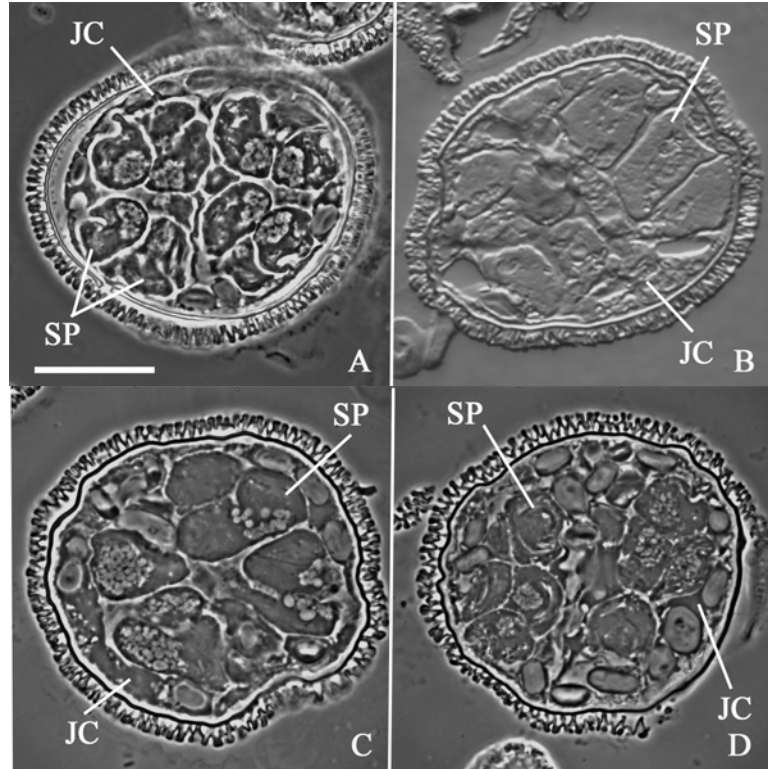


Figure IV - 1: Different kinesin proteins are apparently required at different developmental stages.

Gametophytes were treated with dsRNA probes encoding different kinesin proteins. The samples were fixed at 8 h and embedded in methacrylate. Thin sections (1- 2 μm) were examined with a phase contrast microscope. (A) 8 h untreated controls showed normal development. (B) MvU629 silencing arrested development before the divisions had reached completion. The gametophytes resembled untreated ones fixed at 4 h. (C) MvU2357 silencing arrested development at a stage comparable to controls fixed between 4- 6 h. (D) MvU951 RNAi. Divisions proceeded normally and differentiation was initiated with subtle anomalies in the spermatids. **SP**: Spermatogenous cells. **JC**: Jacket cells. Bar = 20 μm .

RNAi treatments arrested divisions between 3-4 h of development (Figure IV-1: B). Other kinesin RNAi treatments resulted in arrested divisions between 4-6 h of development (Figure IV-1: C). Finally, some kinesin RNAi treatments showed no phenocopies or very subtle effects on the differentiating spermatids (Figure IV-1: D).

RNAi treatments for kinesin 5 (MvU99) and POK1 (phragmoplast orienting kinesin 1) (MvU130) showed no defects in development or differentiation when observed with light microscopy. When these treated gametophytes were stained with anti-centrin or anti- β -tubulin antibodies, they showed normal labeling and distribution of the basal bodies and microtubule ribbon, respectively (Figures IV-2, IV-3).

The some kinesin motors are required for early stages of development

Two different kinesin isoforms, encoded by MvU2357 (Kinesin-like protein) and MvU1647 (Kinesin 13A), shared similar phenocopies (Figure IV-4: D-F, Figure IV-5: D-F). Most of the treated gametophytes (70%) showed disrupted cell divisions. The spermatogenous cells did not divide past the 3-4 h stage. This resulted in the formation of bigger and fewer spermatogenous cells. About 50% of the treated gametophytes showed anomalously enlarged jacket cells, which was mostly a sign of improper placement of the cell plate. To examine whether the spermatogenous cells in the silenced gametophytes were able to undergo any differentiation, sections of the treated gametophytes were labeled with antibodies against centrin and β -tubulin proteins. Centrin was translated and aggregated in the spermatogenous cells only (Figure IV-4: E, F), which matched the condition observed in normal development (Figure IV-4: B, C) (Klink and Wolniak, 2001, 2003). However, centrin aggregates resembled the centrin staining of centrosomes

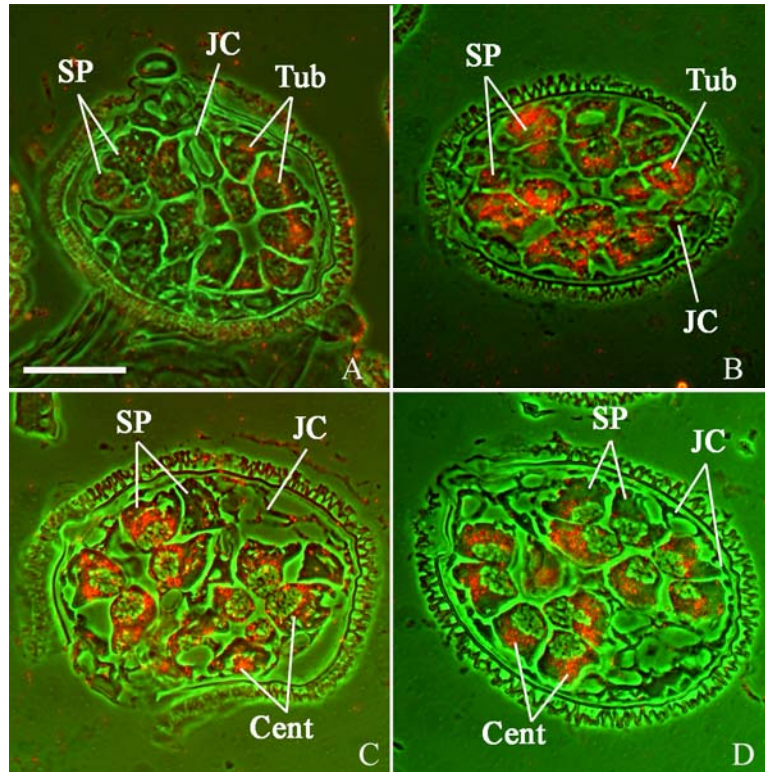


Figure IV - 2: The silencing of kinesin 5 (Kin5) homolog, (MvU99) does not show detectable effects on cell divisions and differentiation.

Fixed, methacrylate embedded and sectioned gametophytes were stained with antigen specific primary antibodies and gold-conjugated secondary antibodies. The immunolabeling was detected with reflected light (orange). Images of phase contrast (green) and antibody labeling were overlaid. (A) Untreated gametophytes fixed at 8 h and stained with anti- β -tubulin antibody showed the normal distribution of the microtubule ribbon. (B) MvU99 RNAi stained with anti- β -tubulin antibody showed similar localization patterns of microtubules to that observed in the controls. (C) Centrin immunolabeling in normally developing gametophytes fixed at 8 h. (D) MvU99 RNAi showed normal distribution patterns of basal bodies. **SP:** Spermatogenous cells. **JC:** Jacket cells. **Tub:** Tubulin. **Cent:** centrin. Bar = 20 μ m.

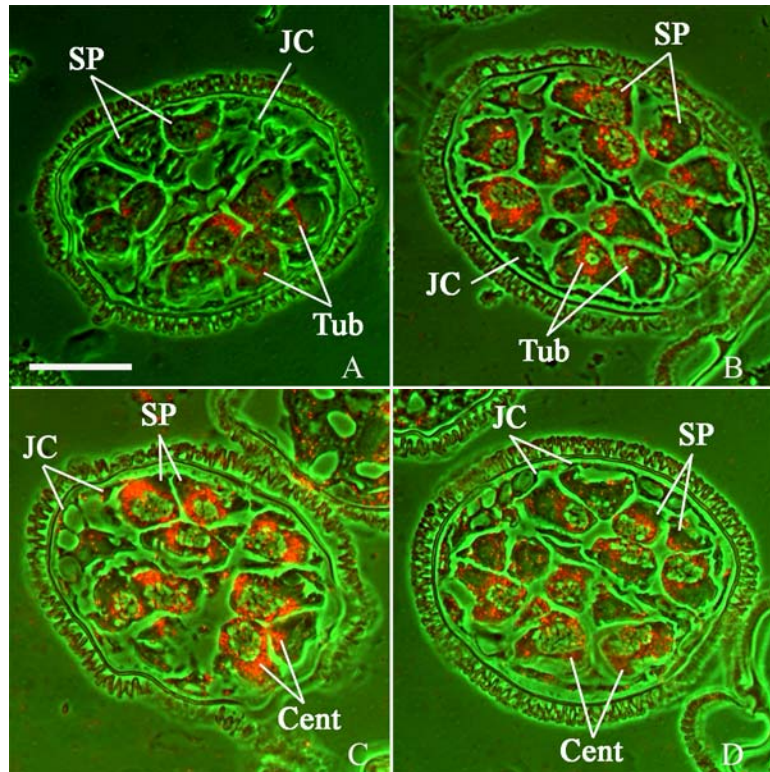


Figure IV - 3: Gametophytes treated with POK1 kinesin protein (MvU130) dsRNA show no detectable defects after 8 h of development.

Control (A, C) and RNAi treated gametophytes (B, C) were fixed at 8 h, embedded in methacrylate, sectioned and stained with antigen specific primary antibodies and gold-conjugated secondary antibodies. The immunolabeling was detected with reflected light (orange). Images of phase contrast (green) and antibody labeling were overlaid. (A) Anti- β -tubulin antibody labeling in 8 h untreated gametophytes. (B) The arrangement of the microtubule ribbons in MvU130 RNAi treatments exhibited normal patterns. (D) MvU130 silencing did not affect the localization and distribution of basal bodies in the spermatogenous cells. **SP:** Spermatogenous cells. **JC:** Jacket cells. **bb:** basal bodies. **Tub:** Tubulin. **Cent:** centrin. Bar =20 μ m.

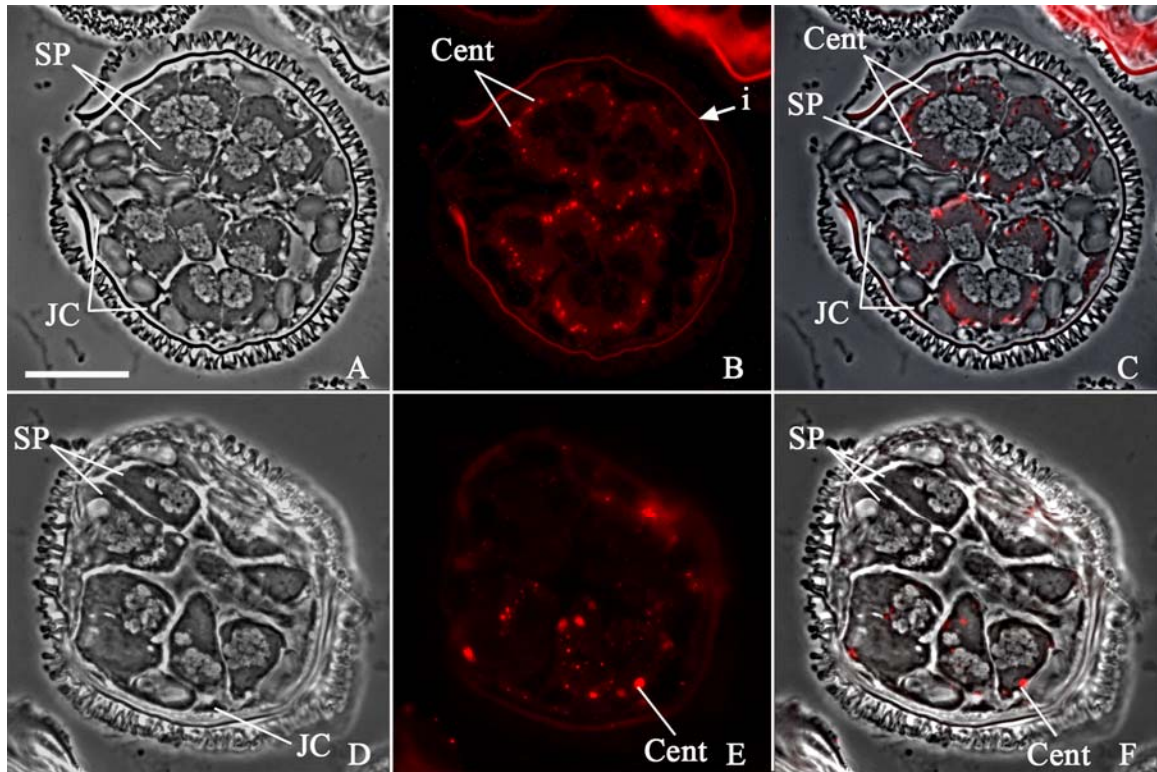


Figure IV - 4: Several different kinesin knockdowns show similar defects in basal body formation.

The effects MvU2357 (Kinesin-like protein) and MvU1647 (Kinesin 13A) silencing on basal body formation. Phase contrast imaging was utilized to examine the effects of kinesin silencing (D) and compare it to the patterns of normal development (A). (B, E) Centrin was localized with anti-centrin primary antibody and Alexa fluor-594 conjugated secondary antibody (red). (C, F) Images of phase contrast and centrin labeling were overlaid to establish the relative cellular localization of centrin in the gametophytes. (A-C) At 8 h, normally developing gametophytes had basal bodies positioned in even intervals (red, cent). (C-E) RNAi treatments for MvU2357 and MvU1647: the cell division planes were disrupted, and some of the later divisions failed to occur. Centrin was translated and aggregated exclusively in the spermatogenous cells of the gametophyte.

The spore wall autofluoresces brightly (i=intine). **SP:** Spermatogenous cell. **JC:** Jacket cell. **Cent:** Centrin. Bar = 20 μ m.

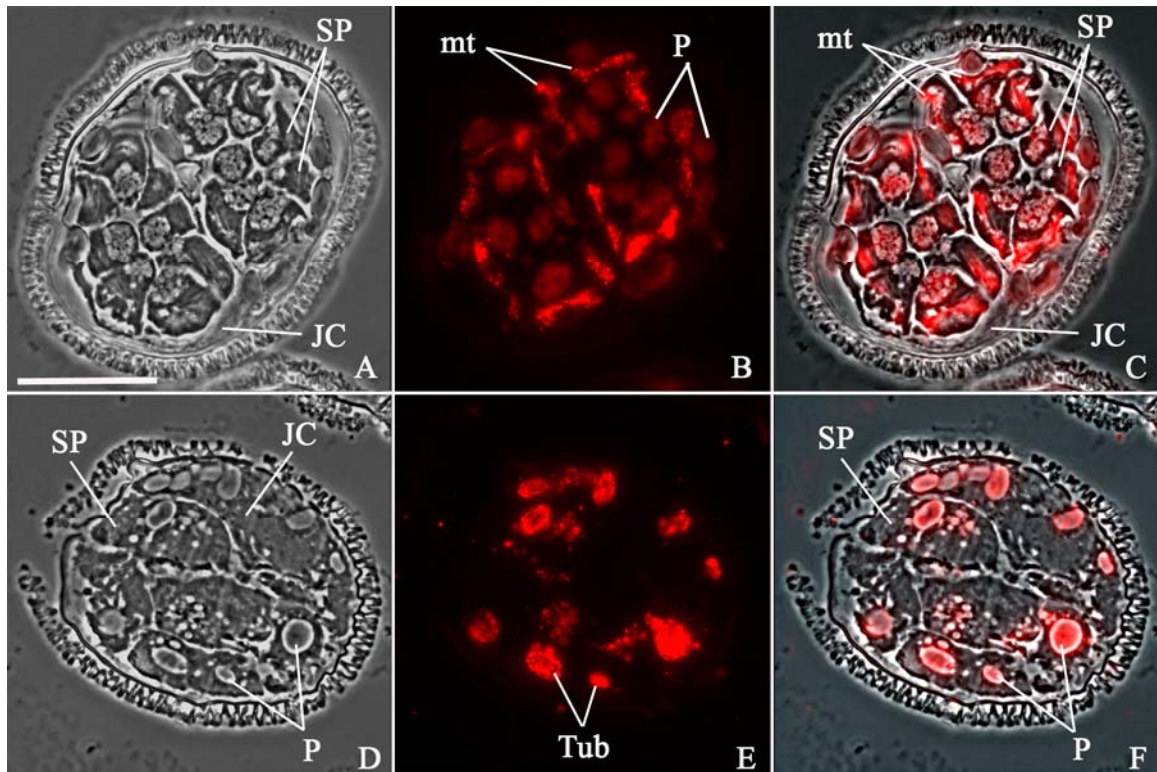


Figure IV - 5: Several different kinesin knockdowns inhibit the formation of the microtubule ribbon.

Images were acquired with a phase contrast microscope (A, D) to compare the defects of kinesin RNAi treatments (D-F) to normal development (A-C) at 8 h. (B, E) Immunofluorescence labeling with anti- β -tubulin primary antibodies and Alexa fluor-594 conjugated secondary antibodies (red). (C, F) The phase contrast images are overlaid with the antibody staining to show the positioning of the microtubule ribbons in the gametophytes. (A-C) At 8 h, the untreated gametophytes exhibited bright labeling of the microtubule ribbon (red, mt). (D-F) After the silencing of MvU2357 and MvU1647, the microtubule ribbon was not observed. The microtubules associated with the plastids were stained when this particular anti- β -tubulin antibody was used for immunofluorescence (red, P). **SP:** Spermatogenous cell. **JC:** Jacket cell. **Tub:** tubulin. **mt:** microtubule ribbon. **P:** Plastids. Bar = 20 μ m.

at 4 h of development rather than the evenly spaced punctae of basal body staining at 8 h of normal gametophyte. No tubulin staining was detected in the spermatogenous cells (Figure IV-5: E, F). This indicated that the MLS and microtubule ribbon failed to form as a result of these RNAi treatments. With this particular anti- β -tubulin antibody, the plastids were stained. It is possible that this antibody labeled microtubules associated with the plastids.

Kinesin II knockdown alters divisions and centrin translational patterns

The silencing of Kinesin II (MvU629) produced two main phenocopies. First, approximately 40% of the gametophytes showed developmental effects at an early stage (Figure IV-6: D-F). The early division planes were altered. The jacket cells failed to partition properly from the spermatogenous domains, which produced jacket cells of different sizes and some spermatogenous cells with plastids. The spermatogenous cells were of unequal sizes, and they were fewer and larger than their counterparts in untreated controls. Centrin protein was abundant in both the spermatogenous and the jacket cells (it is normally only present in spermatogenous cells), and centrin aggregates, resembling blepharoplasts, formed in both cell types. Anti- α -tubulin immunolabeling showed scattered microtubules in the spermatogenous cells (Figure IV-7: E, F).

Second, approximately 40% of the affected gametophytes showed subtle developmental defects (Figure IV-6: G-I). The gametophytes had the correct number and positioning of jacket and spermatogenous cells at 8 h. However, spermatogenous cells were of unequal sizes. Some spermatogenous cells were larger than those observed in the

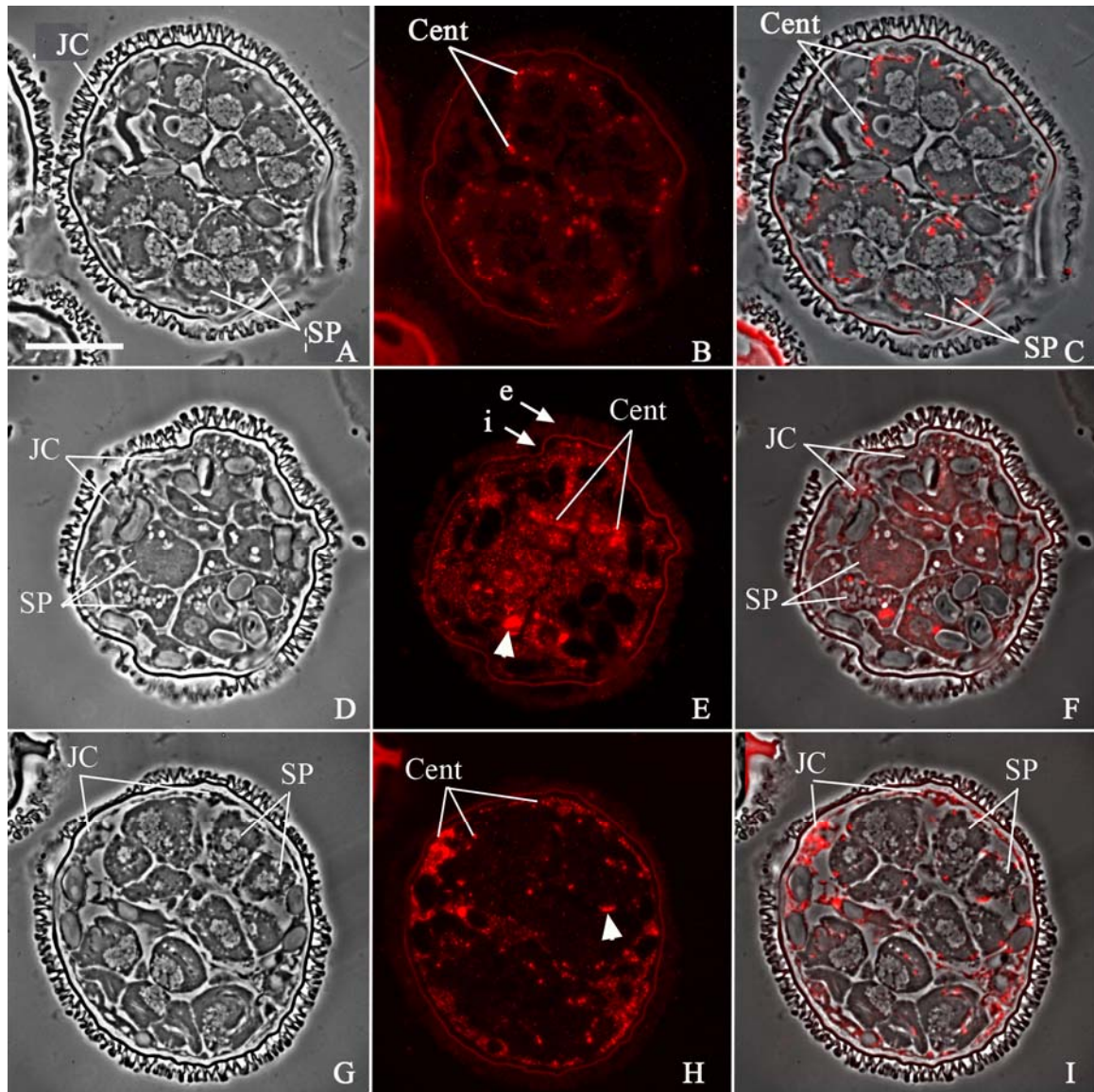


Figure IV - 6: The effects of MvU629 (Kinesin II) silencing on cell divisions and centrin translational patterns.

Phase contrast imaging was used to examine the morphology of the RNAi treated gametophytes (D, G) and compare it to normal development (A). (B, E, H) Centrin was localized with anti-centrin primary antibody and Alexa fluor-594 conjugated secondary antibody (red). (C, F, I) Images of phase contrast and centrin labeling were overlaid to establish the relative cellular localization of centrin in the gametophytes. (A-C) Control gametophytes fixed at 8 h showed the normal localization and distribution of the basal bodies (B, cent). (D-F) Early effects of MvU629 RNAi treatment: centrin was translated

throughout the microspore and formed big aggregates (E, arrow head). (G-I) Late effects of MvU629 silencing: the spermatids showed fewer basal bodies. Centrin was translated and aggregated in the jacket cells in addition to the spermatids.

The spore wall autofluoresces brightly (i=intine, e=exine). **SP:** Spermatogenous cell. **JC:** Jacket cell. **Cent:** Centrin. Bar = 20 μm .

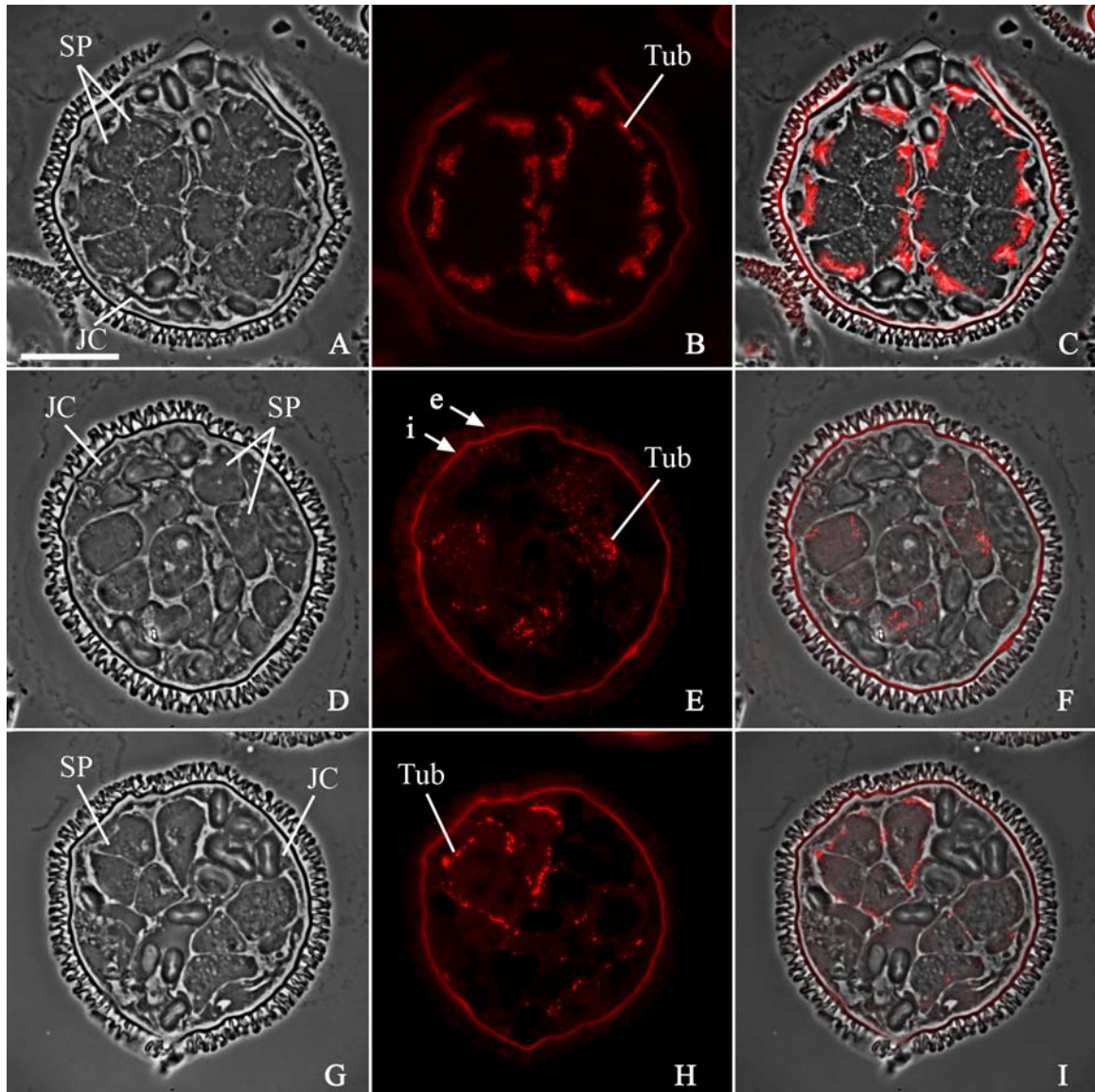


Figure IV - 7: The effects of MvU629 (Kinesin II) silencing on the formation of the microtubule ribbon.

Phase contrast imaging was used to compare the effects of MvU629 silencing (D, G) to normal development (A). (B, E, H) The microtubule ribbon was labeled with anti- β -tubulin primary antibody and Alexa fluor-594 conjugated secondary antibody (red). (C, F, I) Images of phase contrast and antibody staining were overlaid to establish the relative positioning of tubulin staining the gametophytes. (A-C) Control gametophytes fixed at 8 h showed the normal formation of the microtubule ribbon (red). (D-F) Early effects of MvU629 RNAi treatment: some microtubules were formed, but they were not assembled

into an organized structure, no microtubule ribbon was observed. (G-I) Late effects of MvU629 RNAi treatment: light staining of the microtubule ribbon was observed.

The spore wall autofluoresces brightly (i=intine, e=exine). **SP:** Spermatogenous cell. **JC:** Jacket cell. **Tub:** Tubulin. Bar = 20 μm .

untreated controls. The spermatogenous cells appeared to have initiated gamete differentiation; the chromatin was condensed and the nuclei became elongated. Unlike normal gametophytes where centrin was only translated in spermatogenous cells, after this kinesin II was silenced, centrin protein was detected in all cells of the gametophytes. In the spermatogenous cells, centrin was localized into fewer and bigger basal bodies-like structures than those observed in untreated controls. In the jacket cells, centrin was also localized into aggregates that resembled blepharoplasts (Figure IV-6: H, I). The microtubule ribbon was not formed properly. The MLS showed thin staining with anti- α -tubulin antibody (Figure IV-7: H, I).

Kinesin encoded by MvU2336 affects cell divisions and basal body positioning.

Gametophytes treated with dsRNA encoding a centromeric kinesin-like protein (MvU2336) showed two main phenocopies with equal percentages. Nearly half of the affected gametophytes showed developmental defects at an early stage (Figure IV-8: D-F). The number of spermatogenous cells observed in these gametophytes suggests that the last two rounds of divisions were blocked. The jacket cells occupied the correct positions in the microspore; however, their size was altered. Some jacket cells appeared larger than those in the controls, a sign of improper cell plate placement during cytokinesis. Again, centrin protein was detected in all cells of the gametophytes (Figure IV-8: E, F), and it was aggregated into blepharoplast or basal body-like structures both in the spermatogenous cells and in the jacket cells. Anti- α -tubulin immunolabeling showed high background staining in these gametophytes. Microtubules were not detected for the most part, but when observed, they had very light staining (Figure IV-9: E).

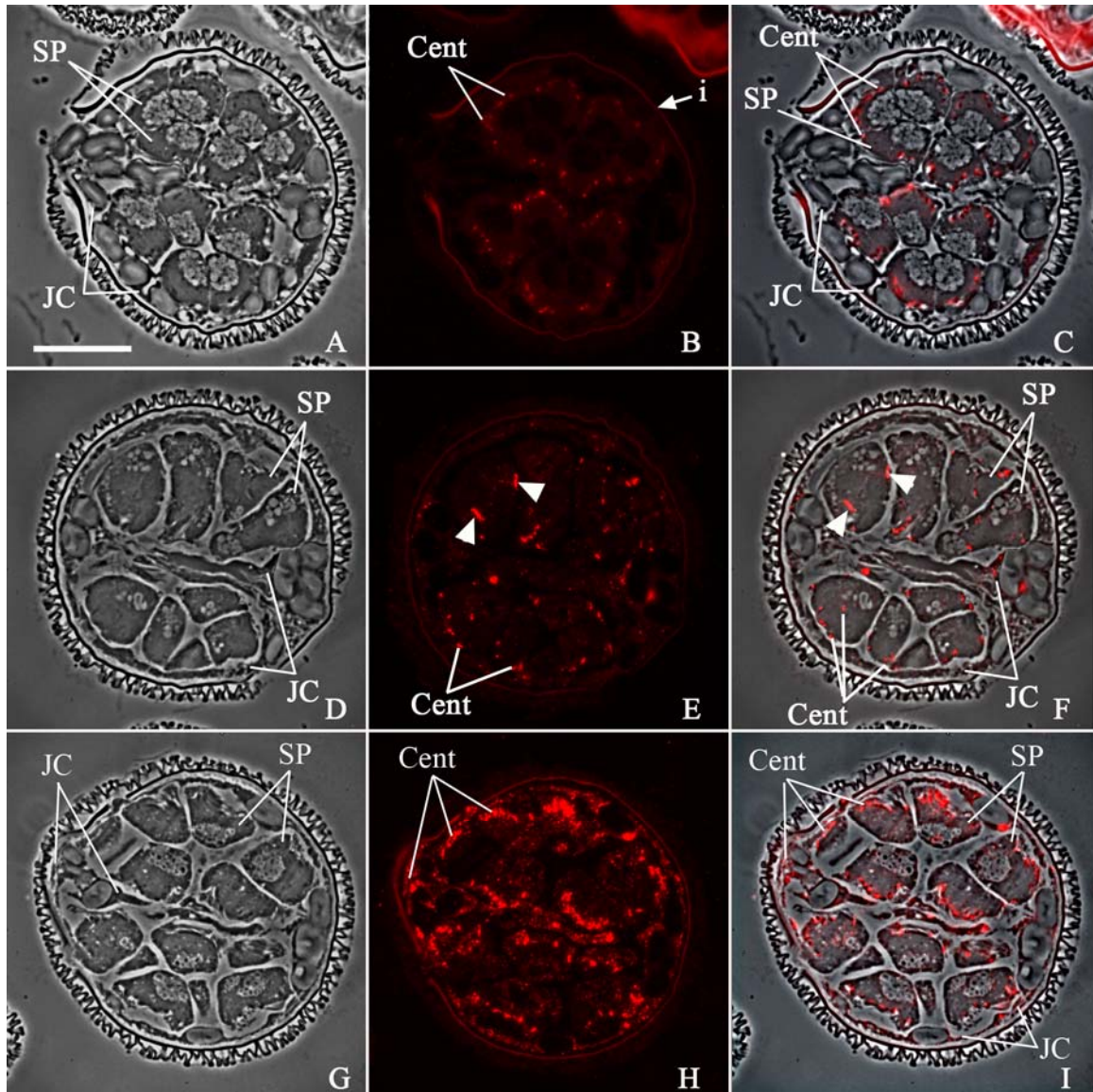


Figure IV - 8: The effects centromeric kinesin-like protein (MvU2336) silencing on cell division and centrin translational patterns.

Phase contrast imaging was used to compare the effects of MvU2336 silencing (D, G) to normal development (A). (B, E, H) Centrin was localized with anti-centrin primary antibody and Alexa fluor-594 conjugated secondary antibody (red). (C, F, I) Images of phase contrast and centrin labeling were overlaid to establish the relative positioning of the basal bodies in the gametophytes. (A-C) Control gametophytes fixed at 8 h showed the normal localization and distribution of the basal bodies (B, cent). (D-F) Early effects of MvU2336 silencing: cell divisions were arrested early. Centrin was translated and

localized into basal body-like structures in the jacket cells in addition to the spermatogenous cells. The positioning of the basal bodies was altered. (G-I) Late effects of MvU2336 silencing: the treated gametophytes looked almost normal. Centrin was translated and localized in both the spermatogenous and jacket cells. The basal bodies formed were much bigger than those in the controls.

The spore wall autofluoresces brightly (i=intine). **SP:** Spermatogenous cell. **JC:** Jacket cell. **Cent:** Centrin. Bar = 20 μ m.

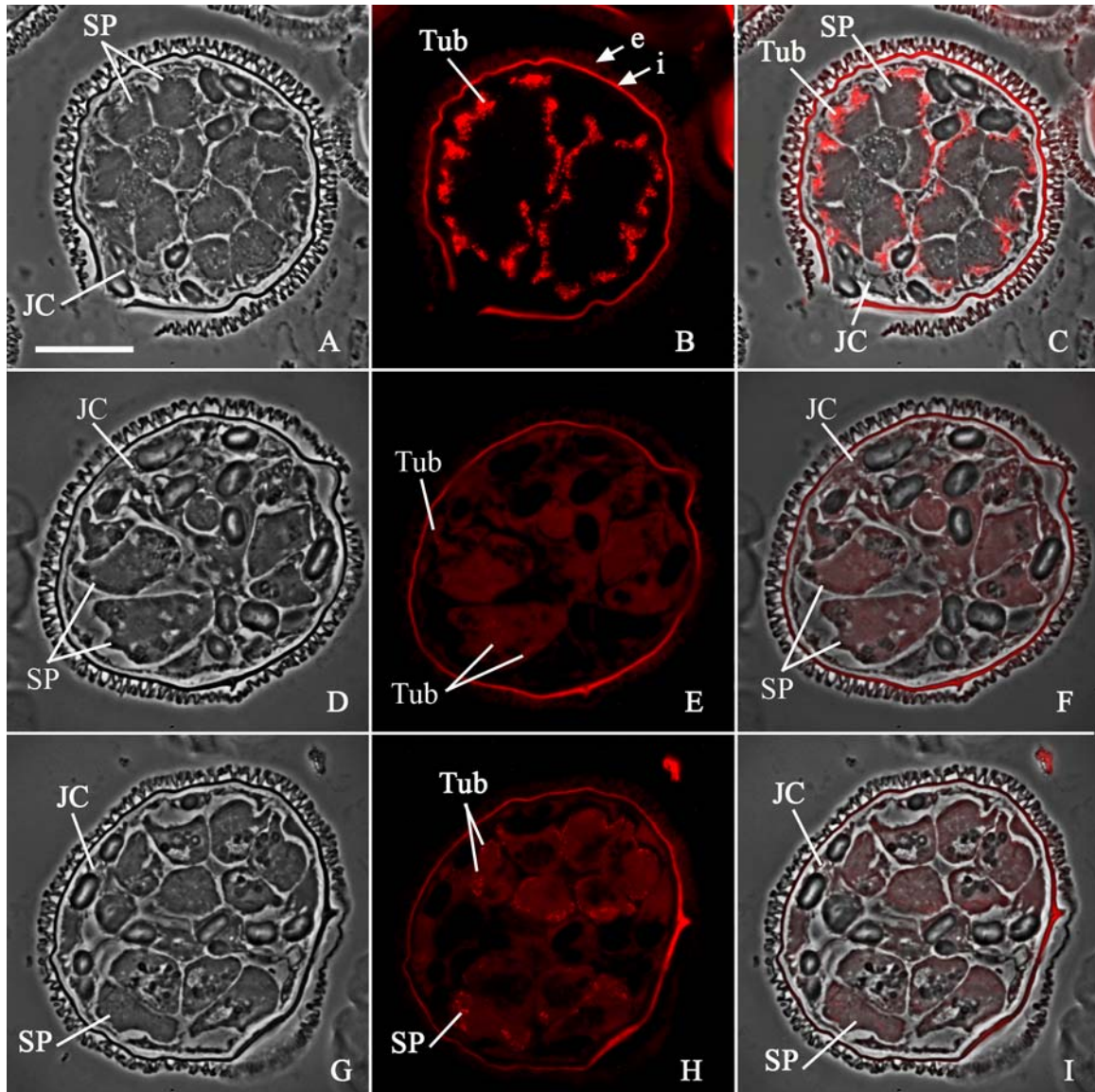


Figure IV - 9: The effects centromeric kinesin-like protein (MvU2336) silencing on the formation of the microtubule ribbon.

Phase contrast imaging was used to compare the effects of MvU2336 silencing (D, G) to normal development (A). (B, E, H) The microtubule ribbon was labeled with anti- β -tubulin primary antibody and Alexa fluor-594 conjugated secondary antibody (red). (C, F, I) Images of phase contrast and antibody staining were overlaid to establish the relative positioning of tubulin staining the gametophytes. (A-C) Control gametophytes fixed at 8 h showed the normal formation of the microtubule ribbon (red). (D-F) MvU2336 silencing showed early developmental arrest in some gametophytes. Very few microtubules were detected in the spermatogenous cells. (G-I) MvU2336 silencing

showed some gametophytes with late developmental defects. The developing spermatids looked mostly normal with phase contrast (G) but they showed light staining of the microtubule ribbon (H, I).

The spore wall autofluoresces brightly (i=intine, e=exine). **SP:** Spermatogenous cell. **JC:** Jacket cell. **Tub:** Tubulin. Bar = 20 μm .

The other half of the affected gametophytes showed anomalies that were manifested as subtle defects in the differentiating spermatids (Figure IV-8: G-I). Morphologically, the treated gametophytes resembled the untreated controls in terms of cell numbers, positions and sizes. The jacket cells were indistinguishable from those in normal gametophytes, but the spermatogenous cells, though normal in number, appeared to be slightly larger than normal in size. The spermatids started to differentiate; their nuclei were elongated and the chromatin was condensed. In terms of protein composition and distribution, the treated gametophytes were distinctly different from the untreated controls. Centrin was detected in both the jacket and spermatogenous cells (Figure IV-8: E, F). In the spermatogenous cells, it appeared as if excess centrin was localized into the basal bodies; making the basal bodies appear larger than normal. The basal bodies were arranged linearly along the anterior side of the spermatids; the increased localization of centrin into the basal bodies made them appear connected to each other in some of the spermatids. Some centrin staining was also detected in the cytoplasm of the spermatogenous cells, apart from the staining observed in the basal bodies. In the jacket cells, centrin was abundant, and some basal body-like structures were formed. These gametophytes had abnormally high background staining for tubulin in all cells of the gametophyte and a slightly brighter staining of the microtubule ribbon in the spermatids (Figure IV-9: H, I).

Discussion:

Proper development within the microspores of *M. vestita* relies on precise positioning of cell plates for the partitioning of the meiotic product into a total of 39 cells. Seven of

the cells are sterile and 32 are spermatids. With no movement of cells, and with development dependent on the processing and translation of stored mRNAs at particular times in specific cells of the gametophyte, it is clear that proper protein and mRNA localizations are necessary to establish cell identity, and to determine cell fate. This highlights the important role the cytoskeleton plays in development of this male gametophyte. The involvement of the cytoskeleton apparently begins at the onset of development. Substantive cytoplasmic movements are observed after the spores are immersed into water to establish two different domains that give rise to two different cell types, the spermatogenous cells and jacket cells. Wolniak and others have shown that a dynamic microtubule cytoskeleton is needed for development (Swamy and Wolniak, 2004; Molk and Wolniak, 2001). Treatment of the gametophytes with taxol, a microtubule stabilizing drug, arrests development early (Klink and Wolniak, unpublished results). The purpose of this chapter is to provide a broad understanding of when and how different kinesin motors participate in cellular processes to help regulate gamete development and differentiation.

Different kinesin motors are needed at different developmental stages

The silencing of different kinesins affects development at distinct stages. It is reasonable to suspect that specific kinesins are utilized in development at different time points. Two RNAi treatments (for clones MvU99, and MvU130) show no effects on the mature spermatids. It is likely that these kinesins are redundant in the microspores, or the affected gametophytes have defects in ciliogenesis that are not detected in these 8 h experiments. To distinguish between these possibilities, further analysis with longer

development times and perhaps ultrastructural analysis would allow for the dissection among the effects of these treatments on the structure of the ciliary axonemes.

Some kinesin knockdowns arrest cell divisions in the gametophyte early in development, but they exerted similar effects on spermatid differentiation much later (MvU951, MvU1647, and MvU2357). Although early and late effects were observed with these treatments, cell identity was not altered since centrin protein was translated and localized in the spermatogenous cells only. Centrin formed a few large aggregates in the spermatogenous cells. It is likely that centrin staining corresponds to the blepharoplast. This would indicate that the blepharoplast failed to break up into the individual basal bodies. In addition, the lack of vibrant staining along the dorsal face of the spermatid with the tubulin antibody indicates that the spermatogenous cells failed to form the microtubule ribbon. Therefore, subsequent differentiation in these cells was also blocked. It is likely that these kinesin proteins, known as MvU951, MvU1647 and MvU2357 in our naming scheme, are required to transport and localize molecules essential for the completion of cell divisions. In the absence of these kinesin motors, their cargos become misslocalized, which arrests cell division (or alters division planes) and blocks subsequent differentiation.

Kinesin II is needed for the establishment of cell identity

Kinesin II performs a variety of different functions in different cell types (Miller *et al.*, 2005). It has been implicated in several microtubule-based transport events. In *Xenopus*, it is involved in the dispersion of pigment granules (Tuma *et al.*, 1998; Deacon *et al.*, 2003), transport from endoplasmic reticulum-to-Golgi (Le Bot *et al.*, 1998), and

localization of Vg1 mRNA (Betley *et al.*, 2004). In *Drosophila*, it is involved the transport of choline acetyltransferase in neurons (Ray *et al.*, 1999) and the movement of cell fate components during oogenesis. In addition, kinesin II is known to be required for ciliogenesis in *C. elegans* (Shakir *et al.*, 1993), *Tetrahymena* (Brown *et al.*, 1999), *Drosophila* (Han *et al.*, 2003; Sarpal *et al.*, 2003), sea urchins (Morris and Scholey, 1997), and mice (Yamazaki *et al.*, 1995; Yang *et al.*, 2001).

Stored proteins and mRNAs are distributed uniformly in the dry microspore (Klink and Wolniak, 2003, Tsai *et al.*, 2004). After development is initiated, the spermatogenous domains are formed mainly as a result of protein movements. While the vast majority of mRNAs remain uniformly distributed throughout the gametophyte, some specific mRNAs and most ribosomes become localized in the domains that will later become occupied by the spermatogenous cells. Kinesin II silencing disrupts the positioning of the cell plates. Cell identity is altered as indicated by the abundance of centrin in all cells of the gametophyte (Tsai *et al.*, 2004). The effects of kinesin II knockdowns resemble those of mago nashi silencing (van der Weele *et al.*, 2007). In mago nashi knockdowns, cell identity is altered; centrin is translated in the jacket cells and is aggregated into basal body-like structures similar to those observed after the silencing of kinesin II. Based on the results presented here, it is reasonable to suggest that kinesin II plays a role in establishing cell polarity and the positioning of the division plane and thus, in establishing cell identity and cell fate. Kinesin II can also be involved in the localization of cytoplasmic factors that determine cell fate, such as the EJC (exon-exon junction complex) (van der Weele *et al.*, 2007).

Future studies would be carried out to establish the distribution patterns of other proteins that are usually restricted to the spermatogenous cells and determine how they are affected by the silencing of kinesin II. In addition, RNAi treatments would be repeated and the gametophytes fixed at earlier time points to examine the distribution patterns of transcripts that are normally localized in the spermatogenous cells (*e.g.*, PRP19 or spermidine synthase). It is possible that these transcripts would become randomly distributed in all cells of the gametophyte after the silencing of kinesin II.

MvU2336 encodes a kinesin protein required for the orientation of the division plane.

MvU2336 encodes a motor protein that is homologous to a phragmoplast orienting kinesin2 (POK2). This kinesin was originally identified in *Arabidopsis* (Muller *et al.*, 2006) and is highly expressed in tissues of dividing cells, such as root meristems (Muller *et al.*, 2006). In maize, POK2 is associated with Tan1 protein, which is known to be involved in the guidance and positioning of the phragmoplast (Cleary and Smith, 1998). Similarly, POK2 was found to be needed for the correct positioning of the phragmoplast in *Arabidopsis*.

MvU2336 silencing experiments in the male gametophytes indicate that it has similar functions in *M. vestita* to that in maize and *Arabidopsis* in positioning of the cell plate. The mis-positioning of the division plane might be responsible for the translation of centrin in the jacket cells and the formation of basal body-like structures there. Most interesting are the RNAi effects later in development where cell divisions proceed mostly normally, but spermatid differentiation is profoundly affected. Anomalously large basal bodies are formed and positioned to the anterior side of the spermatid, and large centrin

aggregates are formed in the jacket cells. In addition, tubulin is abundant (perhaps is translated for the assembly of the ciliary axonemes), but very few polymerized microtubules are formed. This indicates that MvU2336 kinesin might play a role in cytoskeletal formation in the gametophyte in addition to its role in the positioning of cell plate.

Some of the gametophytes arrested early show centrin staining in two elongated structures in a single spermatid (Figure IV-8: E, white arrowhead). These structures are different than the anomalous centrin aggregation usually observed in altered basal bodies; they resemble staining of the MLS. The MLS in bryophytes and pteridophytes has been shown to contain centrin, in the ribbed zone of the organelle, proximal to the microtubule ribbon (Vaughn *et al.*, 1993). In the liverwort *Riella Americana*, the disruption of the microtubule organizing centers with several different microtubule destabilizing drugs show that the gametophyte fails to undergo the last mitotic division to produce spermatids. These spermatid mother cells, with multiple organizing centers form paired multi-layered structures in a single spermatid (Figure IV-10) (Wolniak, unpublished results). Normal numbers of basal bodies are associated with *each* MLS, so in the cells where the last division failed to occur, four basal bodies can be observed (Wolniak, unpublished results). The early effects of MvU2336 silencing resemble those described above in *R. americana*. The silencing of MvU2336 prevents microtubule polymerization, blocks the last division cycle and exhibits an anomalously large centrin localization, some in paired elongated structures. Therefore, it is reasonable to suggest that MvU2336 kinesin is needed for the proper formation or maintenance of the microtubule organizing centers. Along with the observations discussed above, MvU2336 is most likely involved

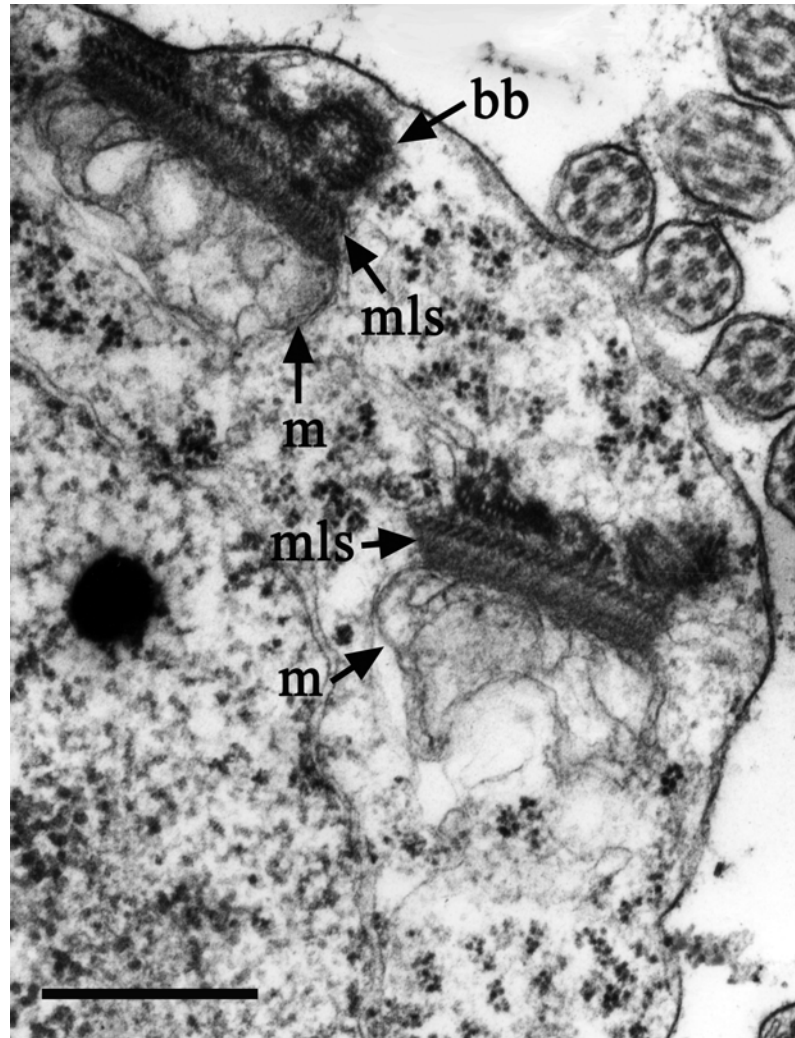


Figure IV - 10: Spermatid of *R. americana* treated with drugs that disrupt the microtubule organizing centers showing paired-MLS structures.

Gametophytes of *R. americana* were treated with 5 μm Amiprofos-methyl, an herbicide that disrupts microtubule organizing centers. Each spermatid formed two MLS structures, instead of a normal single structure (mls). Each MLS structure was associated with a mitochondrion (m) and paired basal bodies (bb). (Reprinted with permission from Wolniak, unpublished results). **bb**: basal bodies. **m**: mitochondria. **mls**: multi-layered structure. Bar = 30 μm .

in the organization of the cytoskeleton. It might also affect microtubule assembly in the growing axonemes. In future studies, electron microscopy can be utilized to examine and define the structures in which centrin is aggregated. The localization patterns of other proteins involved in basal body maturation and axonemal assembly such as γ -tubulin and x-grip can also be investigated. It is likely to find the localization of these proteins altered.

Chapter V: Conclusions and Perspectives

Conclusions:

The findings of this dissertation describe how spermiogenesis in *Marsilea vestita* is regulated by the coordinated functions of kinesin motor proteins and by levels of the polyamine, spermidine. The work on this dissertation over the past few years has been full of challenges and exciting learning opportunities. Presented here are summarized conclusions of the different studies that were addressed in each chapter of this document and suggested sets of future experiments.

The objective in the spermidine project was to investigate the role of spermidine (SPD) in the gametophyte development. More specifically, the role of SPD in chromatin remodeling was the initial focus of the study, but that expanded to how SPD is linked to other processes of spermatid differentiation, ciliogenesis and the formation of the multi-layered structure (MLS). The studies carried out in chapter II reveal that chromatin remodeling and nuclear elongation are linked to the formation of the MLS and the correct positioning of the basal bodies. SPD levels are elevated during these processes indicating its involvement in the events of spermatid differentiation. SPD is also shown to be involved in distinct cellular processes at different developmental stages in a concentration dependent manner, and, therefore, SPD levels are under tight regulation.

Chapter III shows that the spatial and temporal regulation of translation of spermidine synthase transcripts is controlled by mRNA masking. The presented data imply that mRNA masking is mostly involved in the translational regulation of proteins utilized during spermatid differentiation. The studies in chapter III are focused on cytoplasmic

factors that may be involved in the control of the masking and unmasking of spermidine synthase mRNA. The results show that elevated levels of SPD coincide with the unmasking of spermidine synthase transcripts in the gametophyte, which indicates that SPD might play a role in this process. The results also show that the masking of spermidine synthase transcripts is dependent on a functional exon-exon junction complex (EJC) while their unmasking is linked to the completed progression of the cell cycles and elevated levels of SPD. High levels of SPD can also result in the premature unmasking of transcripts other than those of spermidine synthase. The results suggest that SPD can function as a general regulator of transcript unmasking at different cellular concentration ranges.

The collective data presented in chapters II and III allows for the construction of a model representing how SPD can be involved in multiple cellular processes during the different stages of the gametophyte development and differentiation (Figure V-1). It seems clear that there are different levels of SPD in the cytoplasm of the spermatogenous and sterile cells of the gametophyte, and different developmental events take place in each cell type. Therefore, it is suggested that SPD can play a role in the regulation of development in a concentration dependent manner.

Developmental events are precisely ordered in the spermatogenous cells and are driven by the translation of specific pools of the stored mRNA at specific time points (Figure V-I: A). The events that take place during the first two hours of development set the stage for the consequent developmental events. For example, within 30 min of hydration, mRNA is processed and become polyadenylated (Figure V-I: A). Cytoplasmic movements take place to localize proteins and certain mRNAs to establish two different

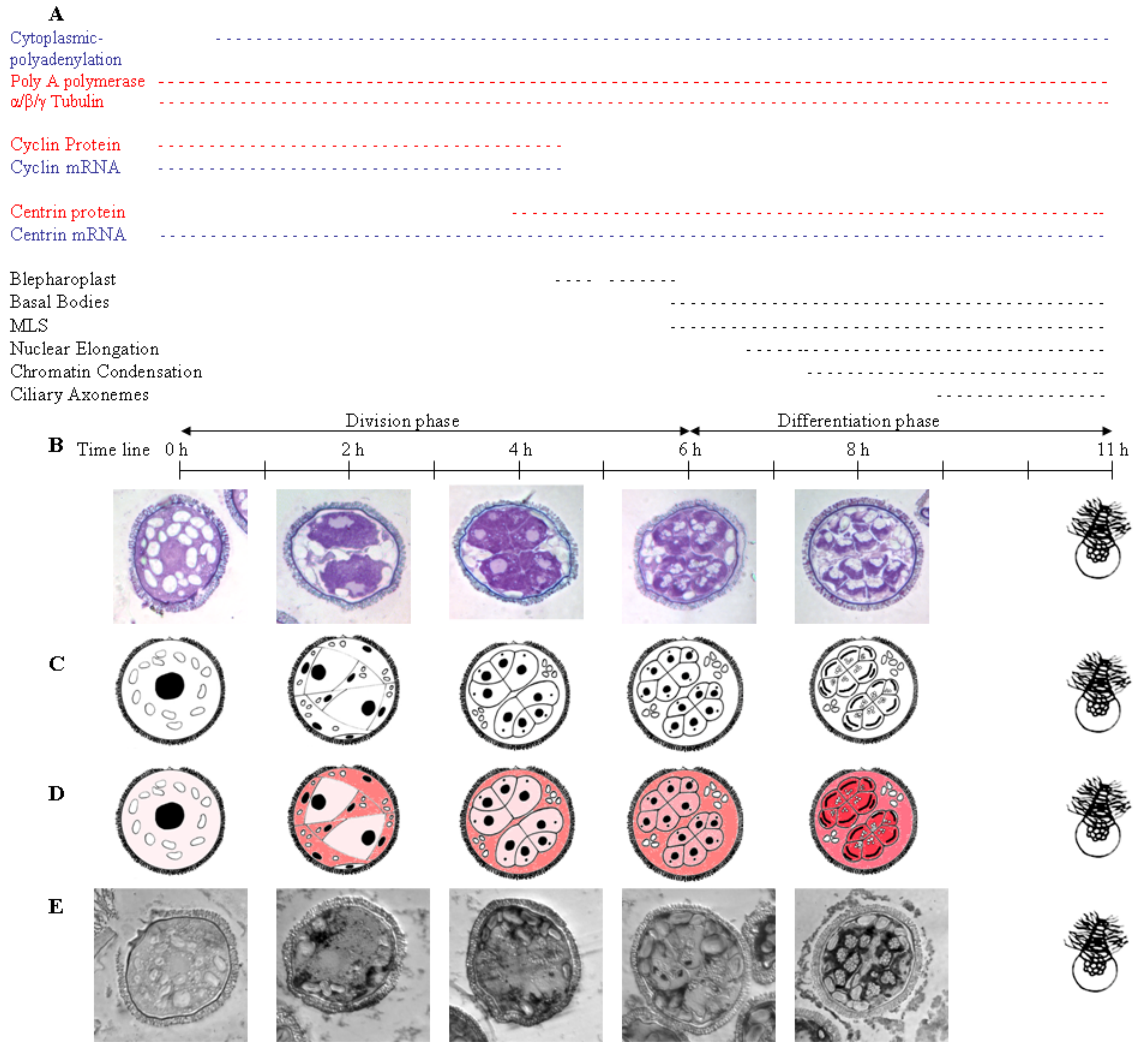


Figure V - 1: A model linking the changes in spermidine distribution patterns in the gametophytes to developmental events.

B: Developmental time line. Gametophytes fixed at different time points, embedded in methacrylate, sectioned and stained with Toluidine Blue-O. The division phase is completed by 6 h of development. Spermatid differentiation and morphogenesis takes place after 6 h of development. **C:** Cell division patterns during the gametophyte development.

B & C: 0 h shows the dry microspore, a single cell. 2 h after hydration, a series of asymmetric divisions give rise to 7 jacket cells and 2 primary spermatogenous cells. Between 2- 6 h, the spermatogenous cells undergo a series of symmetric divisions to give rise to 32 spermatids. Between 6-11 h, each spermatid undergoes a complex

differentiation process. The spermatids chromatin becomes condensed and the nucleus elongate. At 11 h, the mature motile spermatids are released into the water.

A: Several cytoplasmic events that take place during the gametophyte development. The dotted lines relate the cytoplasmic event to the developmental stage at which it takes place. Blue lines represent mRNA; red lines represent proteins, and black lines represent structures. **A:** Cytoplasmic Poly(A) RNA polymerase enzyme is present in the dry microspore, and it persists throughout development. Poly adenylated mRNA is detected after 30 min of development. Some proteins such as $\alpha/\beta/\gamma$ -tubulin are detected throughout development. Cyclin mRNA is detected during the division phase and cyclin proteins are translated at that stage. On the other hand, centrin mRNA is detected throughout development, but centrin protein is only translated after 4 h. The blepharoplast is formed shortly after 4 h, and it persists for a short time. The blepharoplast disappears and later reforms around 5 h. The blepharoplast is transformed into basal bodies during the differentiation stage.

D: Spermidine (SPD) distribution patterns based on SPD antibody staining and spermidine synthase *in situ* hybridization assays. **E:** The distribution patterns of spermidine synthase mRNA. **D:** Soon after hydration of the spore, spermidine levels are low in the gametophyte. By 2 h of development, two different domains are established in the gametophyte based on spermidine levels, a spermidine rich environment in the jacket cells and a spermidine poor environment in the spermatogenous. Cell divisions are arrested in the jacket cells where SPD levels are high. The translation of cell cycle proteins and cell divisions take place in the spermatogenous cells where SPD levels are low. Next SPD is transported into the spermatids, presumably by spermidine transport proteins. By 6 h, SPD levels are elevated in the spermatogenous cells. Cell divisions cease in these cells and differentiation is initiated. Between 6-8 h, more spermidine synthase transcripts are unmasked; therefore, more spermidine synthase is translated, and SPD is accumulated. At 8 h, spermidine synthase mRNA is abundant, and SPD levels are high in the spermatogenous cells; chromatin condensation, nuclear elongation and the formation of the ciliary axonemes take place.

domains in the gametophyte, a spermatogenous domain and a sterile domain. By 2 h, the first five mitotic divisions partition the two different domains to give rise to two cell types, 7 sterile cells (jacket cells) and 2 primary spermatogenous cells, each of which is committed to a specified fate (Figure V-I: B, C, 2 h). The spermatogenous cells undergo further divisions and differentiation to produce mature motile gametes while the jacket cells remain undifferentiated (Figure V-I: B, C, 2 h- 11 h).

SPD levels and distribution patterns are tightly regulated in the developing gametophytes through the post transcriptional regulation of a spermidine synthase and spermidine transporter. The tight control of the spatial distribution patterns of SPD in the gametophyte allows for the early establishment of two developmental domains (or environments), a spermidine rich environment in the jacket cells and a spermidine poor environment in the spermatogenous cells. Different developmental events take place in the different spermidine environments.

Once the dry microspores are hydrated, spermidine synthase mRNA becomes localized in the peripheral cytoplasmic domains that will soon partition into the jacket cells. SPD is maintained at low levels in the gametophyte to ensure the completion of the division cycles in the antheridial initials to produce the sterile jacket cells (Figure V-I: C, 0 h- 2 h). During the early rounds of cell division, spermidine synthase transcripts are detected in the jacket cells only (Figure V-1: E, 2 h, 4 h). Spermidine synthase is translated in the jacket cells and SPD is made by the enzyme in these cells (Figure V-I: D, 2 h). As SPD levels increase in the jacket cells, cell divisions cease there (Figure V-I: C, D, 2 h). SPD is then transported into the spermatogenous initials *via* spermidine transporter proteins. The involvement of these transporters is clear from RNAi

experiments, where transporter components were knocked down, and SPD remained in the jacket cells or in the intercellular spaces outside of the spermatogenous cells. Low concentrations of SPD in the spermatogenous cells are apparently needed for the translation of cell cycle control proteins, such as cyclins, and the progression of the cell divisions that produce the spermatids (Figure V-I: D, 2 h, 4 h). Centrin protein is also translated, and the blepharoplast is formed under these SPD conditions (Figure V-I: A, 4-6 h). By 6 h, SPD levels rise in the spermatids to an intermediate level through the intercellular transport from the jacket cells (Figure V-I: D, 6 h). All cell divisions cease and cell differentiation is initiated; the MLS and the basal bodies are formed and the nuclei start to elongate. Spermidine synthase transcripts become unmasked as localized punctae in the spermatids (Figure V-1: E, 6 h). This unmasking of spermidine synthase mRNA is followed by translation of the functional enzyme and production of considerably higher levels of SPD, which results in an increase in the abundance of spermidine synthase transcripts (Figure V-1: D, E, 8 h). Shortly thereafter, the SPD concentration reaches a high level in the spermatids, and later events of the spermatid differentiation take place, namely chromatin condensation and the assembly of the ciliary axonemes. It is possible that the high concentrations of SPD at this stage results in the unmasking and translation of other transcripts involved in the processes of spermatid differentiation and the formation of the motile apparatus.

Comparative studies of the different polyamines showed that SPD and putrescine are the most effective polyamines in transcript unmasking. The different patterns of charge distribution and cationic charge density of the different polyamines appear to be responsible for their differential effects on the cells. It is likely that the combination of

structure and charge distribution allow the polyamines to interact differently with different molecules, which gives them their distinctive functions.

In chapter IV, the important role the cytoskeleton plays in development is highlighted. The studies in this chapter are focused on the kinesin microtubule motors, , and are designed to address questions about their roles in the regulation of the development and differentiation of the spermatids. The silencing of different kinesin proteins shows that different kinesin isoforms function at different developmental stages. Sometimes redundant kinesin proteins are utilized to ensure the proper localization of molecules. These findings highlight the importance of the establishment of the proper localization of protein and mRNAs for cell fate determination. A key event in cell specification in the gametophyte is the translation of centrin from stored mRNAs, which, in normal gametophytes, occurs exclusively in spermatogenous cells and is an essential prerequisite for blepharoplast formation and basal body assembly. Centrin synthesis and blepharoplast formation do not occur in jacket cells, and they precede the onset of spermatid differentiation. Several kinesin motors were shown to be essential for the completion of cell division and initiation of spermatid differentiation. In the absence of newly translated kinesins encoded by MvU2357 or MvU1647, development is arrested early with altered positioning of cell plates, reduced numbers of cell divisions and halted differentiation of spermatogenous cells. Anti-centrin and anti-tubulin immunolabeling show that the gametophytes exposed to these RNAi treatments fail to form basal bodies and fail to assemble microtubule ribbons. These RNAi treatments, however, do not result in the loss of cell identity, because centrin translation is still restricted to the (presumptive) spermatogenous cells.

The most interesting kinesin silencing effects are those of MvU629 (kinesin II homologue) and MvU2336 (a phragmoplast orienting kinesin2 (POK2) homologue). The silencing of these kinesins results in altered positioning of cell plates, but the treatments do not always affect the numbers of cell division cycles. Centrin translational patterns are also altered, to the extent that some or all of the jacket cells can translate centrin protein, thereby indicating that the treatments cause modifications of cell specification in the gametophyte. Some of the silencing effects of these kinesins in *M. vestita* suggest that these proteins function in establishing cell polarity and in ciliogenesis (MvU629) and in the correct positioning of the cell plate (MvU2336). The functions of MvU629 and MvU2336 in *M. vestita* are similar to those of their homologues as described in several other systems (Tuma *et al.*, 1998; Brown *et al.*, 1999; Muller *et al.*, 2006). Interestingly, the silencing results show that MvU2336 has an additional function during the development of the male gametophyte of *M. vestita*. MvU2336 is needed for MLS formation in addition to positioning of the cell plate.

Future experiments:

The data presented in this document has broadened our understating of the function of spermidine during cellular development and differentiation of fern spermatozoids; however, several questions remain unanswered. Elevated levels of SPD result in the unmasking of spermidine synthase mRNA. Does SPD also enhance the translation of these unmasked transcripts? In addition, high levels of SPD in the spermatid coincide with the formation of the ciliary axonemes and the MLS. Remarkably, in the absence of high SPD levels in the spermatids, the microtubule structures (MLS) fail to form and

tubulin protein is not detectable. Does that mean that the translation of tubulin subunits is enhanced in the presence of high levels of SPD? Does SPD also enhance the translation of other proteins needed for the formation of the ciliary axonemes? This hypothesis could be tested with an *in vitro* translation system. The transcripts of different axonemal proteins can be translated *in vitro* in the presence of different concentrations of SPD. I suspect that at least a subset of these proteins would show an enhanced translation at a certain high concentration of SPD. Centrin translation, on the other hand, takes place at a time point when SPD concentrations are relatively low in the spermatogenous cell (at 4 h), and it is not translated in the jacket cells where SPD levels are high. Does centrin translation take place only in the presence of low levels of SPD? Is the translation of other proteins that are utilized during the early stages of cell division and development, such as cyclin proteins, also dependent on low SPD levels? If so, does the increase in SPD levels prevent the translation of these proteins (or reduce their translational efficiency) and enhance the translation of other sets of proteins that are needed in the next developmental stages, spermatid maturation? These questions could be answered by coupling *in vitro* translations studies, as described above and (Hart and Wolniak, 1999), with comparative western blot analysis (Klink and Wolniak, 2003).

The analyses of SPD levels *in vivo* were deduced by immunolabeling, so they are only qualitative assessments of the relative abundance of SPD. *In vitro* experiments would allow quantitative analyses of SPD concentrations that inhibit or promote specific effects. Those kinds of experiments are beyond the scope of this dissertation. As an initial extension of the studies presented in this thesis, SPD levels could be modulated in the developing gametophytes. They could be either increased (by adding SPD to the

hydration solution) or decreased (by adding spermidine synthase inhibitor at the time of hydration). The gametophytes would be allowed to develop for the desired time interval when protein lysates would be prepared. Western blots would be performed for different proteins, some of which are translated early in development when SPD levels are low in the spermatogenous cells and others that are translated in the spermatids when SPD levels are high. The comparative western blot analysis would help determine effects of various SPD concentrations on the relative abundance levels of the tested proteins.

Finally, a closer look is needed to examine the effects of the kinesin proteins encoded by MvU629 and MvU2336 and to specify their roles in the formation of the ciliary axonemes and the MLS. The silencing effects of these kinesins were examined with light microscopy. Although, this strategy is useful for determining the morphological defects and showing the altered patterns of protein translation and localization, it is limited to identifying structural defects in the basal bodies and MLS. Therefore, the examination of the basal bodies and MLS with electron microscopy would enhance our understanding of the specific roles of these kinesins in the construction of these complex structures. In addition, pull down assays could be performed for these kinesins to identify their binding cargos.

APPENDIX I

Programmed Cell Death in the Jacket Cells

Introduction:

In the microspore of *M. vestita*, the jacket cells are partitioned from the antheridial initial cell by a series of three early asymmetric divisions. These cells are sterile and they do not undergo any further divisions or apparent development. The jacket cells disappear late in spermatid maturation. Since the timing of jacket cell disappearance is strikingly precise in gametophyte development, it seemed reasonable to suspect that these cells undergo programmed cell death at the last stage of development, which could contribute to weakening of the spore wall (perhaps through the release of lytic enzymes from jacket cell vacuoles) and the release of mature spermatids. To investigate the role of the jacket cells could play during development, a protocol to test for cell death *in situ* was developed and RNAi studies were performed on the clone MvU271, isolated from our cDNA library. MvU271 encodes HSR203J, a gene that controls and blocks cell death in tobacco.

***In situ* cell death detection assay**

LR White embedding

Gametophytes were embedded in LR White to avoid the exposure to UV during methacrylate polymerization, which causes DNA breaks. The LR White was polymerized

chemically, at 4 °C. Microspores were isolated from sporocarps and grown as described in Chapter II. Spores were allowed to grow for 8, 9 and 10 h. At the time of fixation, the gametophytes were first collected onto a polyester filter and transferred to a metal mortar. Two 0.03 mm brass rings were placed on the filter and the spores were cracked by the mechanical force from a hammer strike to a tight-fitting pestle. Microspores were washed from the filter into a 50 ml conical centrifuge tube with fixative and held at 4 °C for 2 h. The microspores were then transferred into 2 ml tubes and rinsed 3 x 15 min in 1 X PBS (phosphate buffer, pH 7.4). Next, spores were dehydrated with a graded ethanol series of 25, 50, 75 and 90% ethanol (2 h each) followed by 6 x 100% ethanol for 30 min each. Spores were infiltrated with ethanol-LR White (medium) mixture (2:1, 1:1, 1:2) 2 h each followed by 5 washes of 100% LR white mixture 1 h each at 4 °C. For polymerization, spores were transferred to BEEM capsules, allowed to settle and excess LR White was removed. Capsules were placed on ice. 2 µl of LR White accelerator (EMS, Hatfield, PA) was placed in a 2 ml centrifuge tube on ice. 1 ml LR White was added to the accelerator. The LR White accelerator mixture was quickly transferred to the beam capsules containing the spores. A thin layer of mineral oil was placed on top of the LR White to prevent the exposure to oxygen. The samples were allowed to polymerize overnight at 4 °C. Then, the samples were placed in 55 °C incubator for 24- 48 h. The mineral oil was removed and semi-thin sections were obtained as described previously in Chapter II.

In situ cell death assay

An *in situ* cell death detection kit was obtained from Roche, Germany (Cat# 12156 792910). Semi-thin sections were placed on silanated microscope slides. Slides were

placed in 1X PBS (Phosphate buffer PH 7.4) for 5 min on a rocker shaker. 100 µl of proteinase K solution (20 µg/ml proteinase K in 10 mM Tris-HCl PH 7.5) were placed on the sections. The slides were incubated in a humid chamber at 37 °C for 15 min. Buffer-1 (enzyme solution of the kit) was diluted 1:100 in dilution buffer (Roche, Cat# 11966006001). 5 µl of the diluted Buffer-1 was added to 45 µl of Buffer-2. The buffer mixture was added to the sections. The slides were incubated in the dark at 37 °C for 1 h. The sections were then stained with DAPI solution (2.5 µg/ml) for 10 min at RT in the dark. A series of rinses was performed in 1 X PBS between each of the staining steps, 3 x 15 min each. Sections were mounted with VectaShield (Vector Laboratory) and observed with fluorescence microscopy using a Zeiss Axioskop with standard Texas Red and DAPI filter sets. When desired, RNase treatments were performed after slides were treated with proteinase K. Sections were incubated with RNase A solution (5 µg/ml RNase A and 1 mg/ml BSA in 50 mM Tris PH 7.5) at 37 °C for 30 min. For RNase H treatments, slides were incubated with RNase H solution (50 u/ml in 1 X RNase H reaction buffer) at 37 °C overnight.

Results:

In situ cell death assay on control gametophytes

Figure AI-1: Untreated gametophytes were fixed at 8, 9, and 10 h of development. Spores were embedded in LR White and stained with the *in situ* cell death detection kit. At 8 h, the gametophytes showed positive staining in the cytoplasm of the spermatogenous cells and the nuclei of the prothallial cells. This kit depends on recognizing and labeling the 3' OH in nicked DNA. However, it can also label the 3'OH

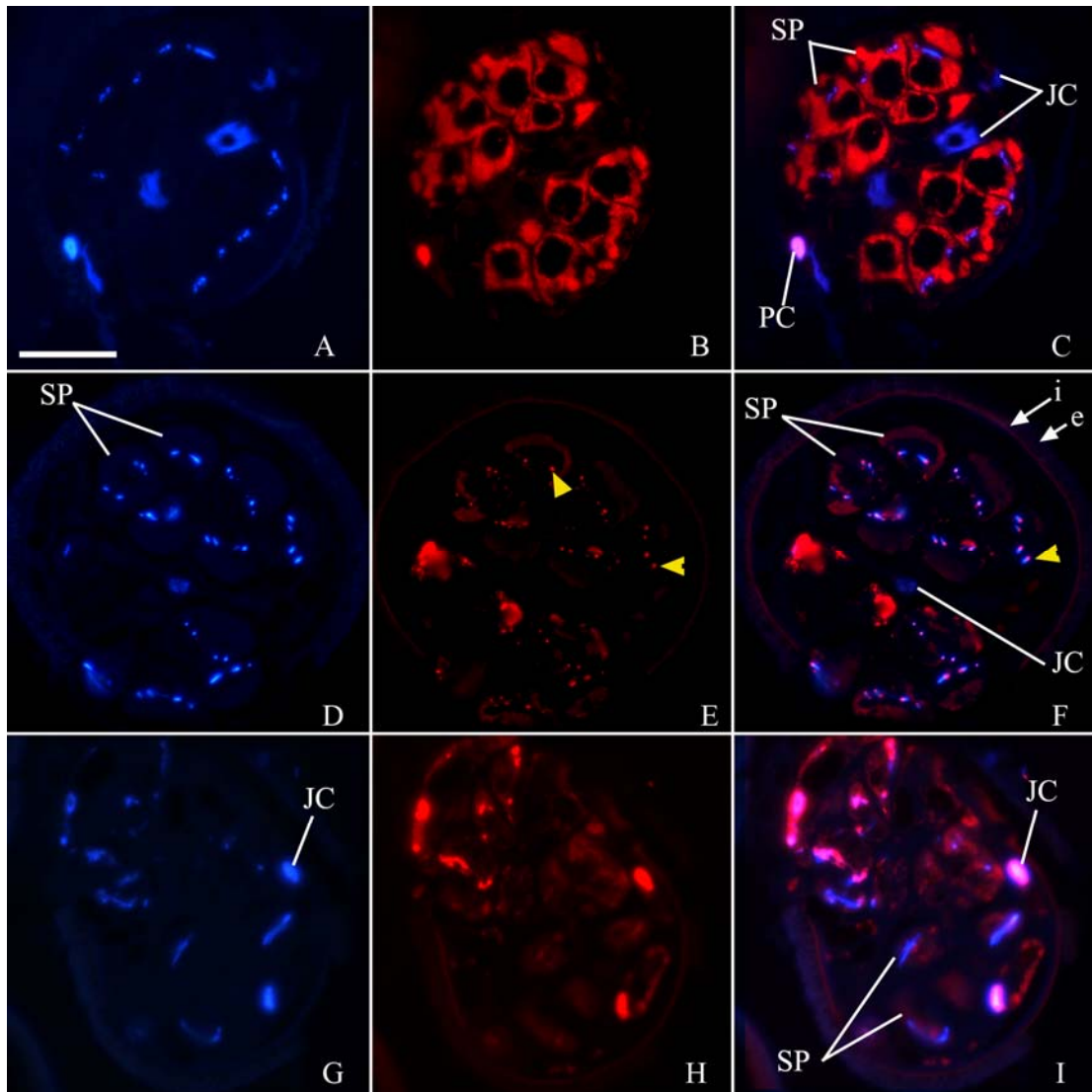


Figure AI - 1: *In situ* cell death assay on untreated gametophytes embedded in LR White.

(A, D, G) DAPI nuclear staining (blue). (B, E, H) *In situ* cell death detection assay. (C, F, I) Images of DAPI staining and cell death assay were overlaid. (A-C) In 8 h controls, the nuclei of the prothallial cell showed positive staining for cell death. The cytoplasm of the spermatogenous cells was labeled red with the *in situ* cell death kit. (D-F) In 9 h controls, some cytoplasmic staining was detected in the spermatogenous cells. Some staining was detected on the periphery of the condensed chromatin in the nuclei of the spermatogenous cells (yellow arrowheads). (G-I) In 10 h controls, the nuclei of the jacket cells showed positive staining for cell death. **SP**: Spermatogenous cells, **JC**: Jacket

cells. **PC:** Prothallial cell. The spore wall autofluoresces brightly (i=intine, e=exine). Bar = 20 μm .

group in mRNA. Therefore, when mRNA levels are high, this kit can show high background staining. At 9 h, the staining in the cytoplasm of the spermatogenous cells was reduced and some staining was observed in the nuclei of the spermatogenous cells (Figure AI-1: E, F. yellow arrowheads). The nucleus of the prothallial cell showed positive staining when observed. At 10 h, no cytoplasmic staining was observed in the spermatogenous cells. The nuclei of the jacket cells and the prothallial cells showed positive staining. Staining was detected in the nuclei of the spermatogenous cells, localized to the periphery of the condensed nuclei. The decrease in the background staining can be the result of the decrease in mRNA levels in the mature gametophytes. The staining in the nuclei of the spermatogenous cells can be explained as an artifact of sectioning. Sectioning can damage the tightly condensed chromatin, which would result in the formation of nicked DNA that can be detected by this kit. Another possibility is that RNA could be incorporated in the nuclei of the spermatids (Ostermeier *et al.*, 2004).

Figure AI-2: Sections of control spores, fixed at 8, 9 and 10 h, were treated with RNase A and RNase H and stained with *in situ* cell death detection kit. At 8 h, localized staining was detected in the nuclei of spermatogenous cells, on the periphery of the condensed chromatin. Light staining was detected in the nuclei of jacket cells. At 9 h, staining was observed in localized dots in the nuclei of the spermatogenous cells (Figure AI-2: E, F, yellow arrowheads). At 10 h, the nuclei of the jacket cells showed positive staining for cell death.

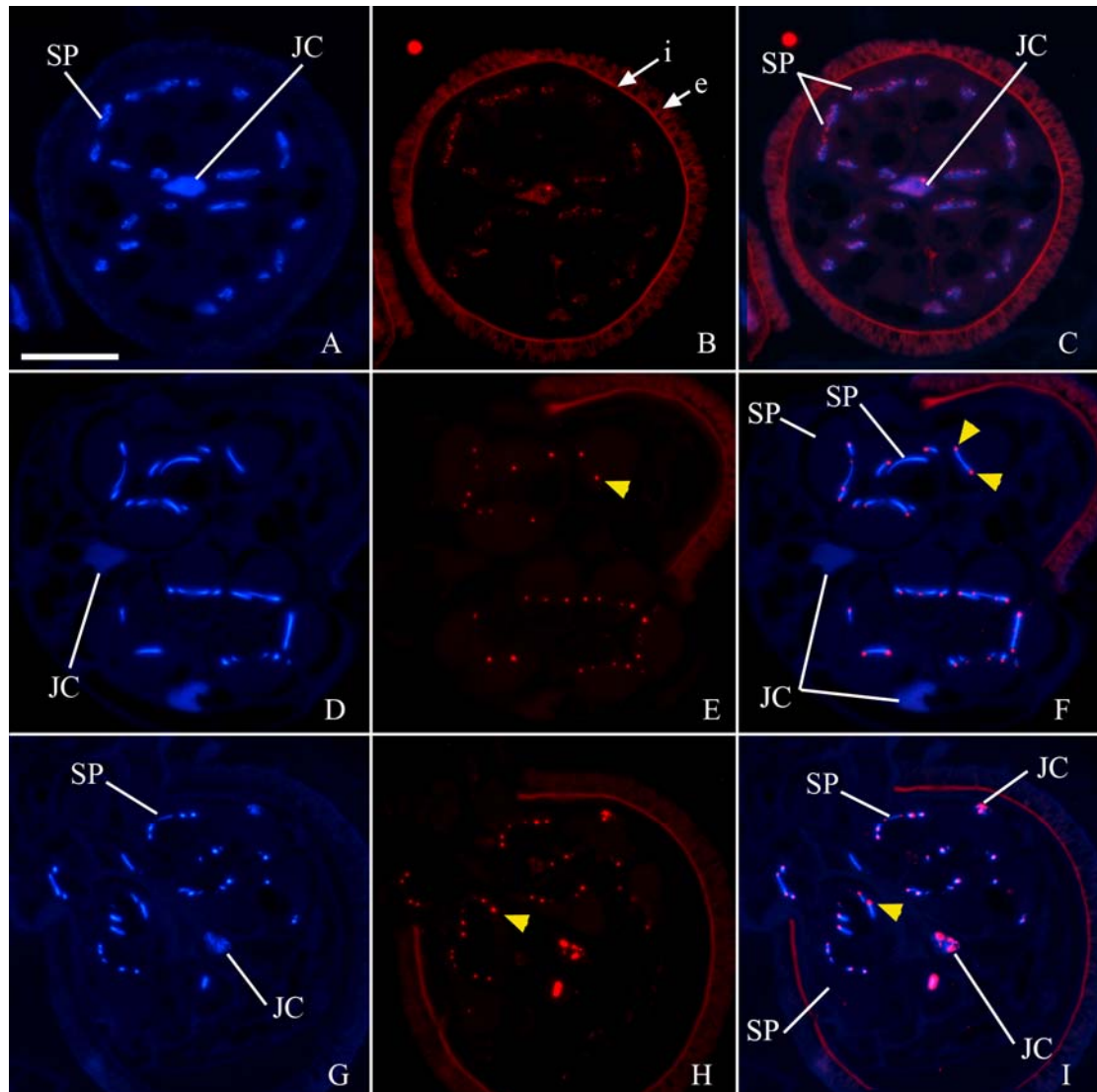


Figure AI - 2: *In situ* cell death assay on untreated gametophytes embedded in LR White and treatment with RNase.

Sections of the control samples were treated with RNase A and RNase H. No cytoplasmic staining was observed. (A, D, G) DAPI nuclear staining (blue). (B, E, H) *In situ* cell death assay (red). (C, F, I) Images of DAPI staining and cell death assay were overlaid. (A-C) In 8 h controls, the nuclei of both the spermatogenous and jacket cells showed unspecific staining with the *in situ* cell death kit (red). (D-F) 9 h controls. (E, F) The nuclei of the spermatogenous cells showed localized staining with the *in situ* cell death assay at the periphery of the condensed chromatin (red, yellow arrowhead). The nuclei of the jacket cells did not show staining with the *in situ* cell death kit. (G-I) In 10 h

controls, the nuclei of the jacket cells showed positive staining for cell death. **SP:** Spermatogenous cells, **JC:** Jacket cells. The spore wall autofluoresces brightly (i=intine, e=exine). Bar = 20 μ m.

These assays indicate that the jacket cells undergo programmed cell death after 10 h of development, shortly before the release of mature spermatids at 11 h. The prothallial cell, on the other hand, undergoes cell death early in development.

The effects of RNAi treatment for MvU271 on development

Microspores were treated with dsRNA encoding HSR203J (MvU271), a gene that controls and blocks cell death in tobacco. Spores were fixed after 8 h of development. The silenced gametophytes showed arrested development at two distinct stages. Almost 30% of the treated gametophytes showed arrested development at an early stage (Figure AI-3: B); they showed protein aggregation in the cytoplasm and incomplete nuclear division, shown by Toluidine Blue O staining. Approximately 60% of the treated gametophytes showed effects at a later stage. The later gametophytes underwent further divisions and produced fewer and bigger spermatogenous cells than observed in the untreated controls (Figure AI-3: C). In these gametophytes, it was hard to distinguish the spermatogenous cells from the jacket cells. The jacket cells appeared bigger than normal, and they had fewer plastids. Some spermatogenous cells also contained plastids. They seemed to fail to separate from the jacket cells. HSR203J might play a role at an early stage of development to establish cell fate.

Centrin translation and localization patterns in gametophytes treated with MvU271

dsRNA

In the untreated gametophytes, centrin was translated and localized into basal bodies in the spermatogenous cells (Figure AI-4: A-C). Centrin was translated throughout the

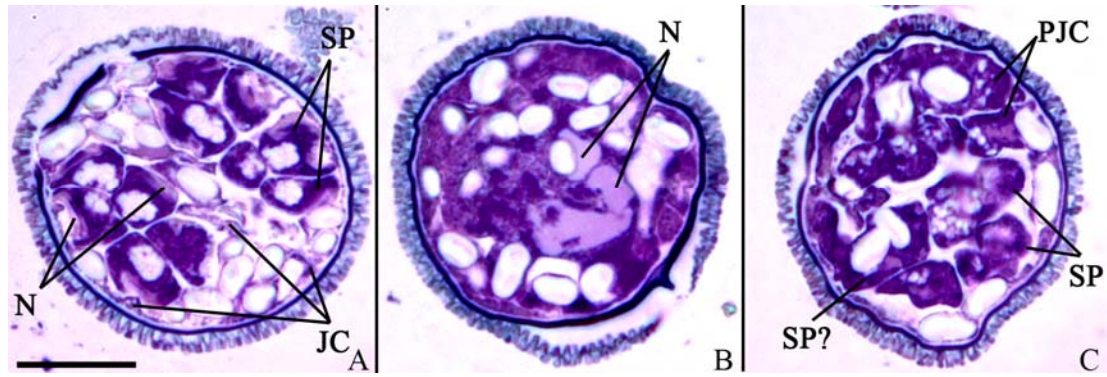


Figure AI - 3: Toluidine Blue-O staining for MvU271 RNAi treatment.

Gametophytes were treated with dsRNA encoding MvU271, fixed after 8 h of development, and embedded in Methacrylate. Thin sections (1-2 μm) were stained with TBO. (A) 8 h controls shed normal development. (B) MvU271 RNAi, severe effects. The plastids failed to localize to the periphery and divisions were incomplete. (C) MvU271 RNAi. Cell divisions were disrupted and the jacket cells failed to partition correctly.

SP: Spermatogenous cells, **JC:** Jacket cells, **P:** plastids, **N:** Nucleus. **PJC:** Presumptive jacket cells. Bar = 20 μm .

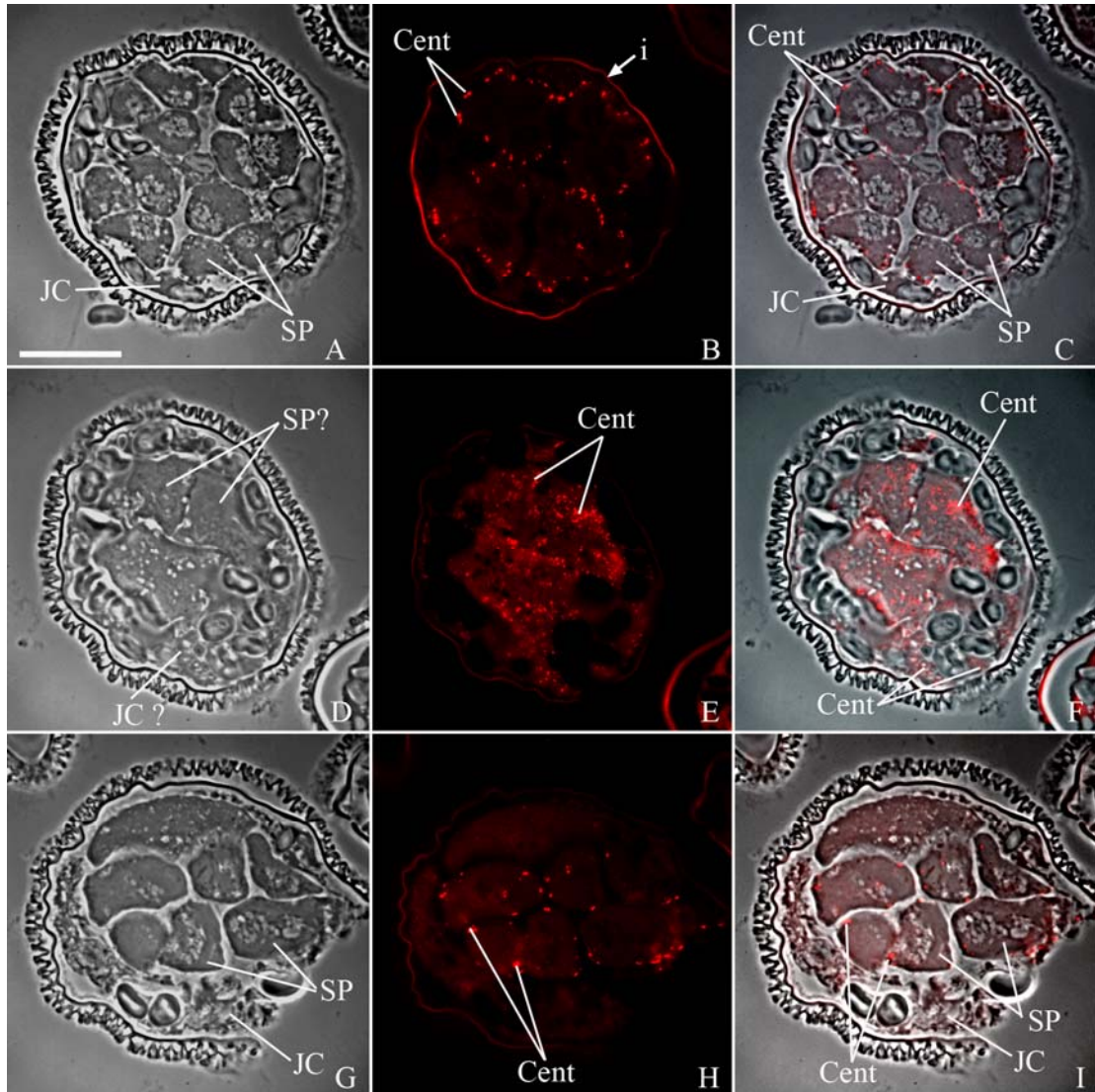


Figure AI - 4: Centrin immunofluorescence staining after MvU271 RNAi treatment.

Gametophytes were treated with dsRNA encoding MvU271, fixed after 8 h of development, and embedded in Methacrylate. (A, D, G) Phase contrast imaging. (B, E, H) Immunolabeling with anti-centrin antibody and Alexa fluor-594 conjugated secondary antibodies (red). (C, F, I) Overlay of Phase and antibody staining. (A-C) In 8 h controls, centrin was localized in distinct and evenly spaced dots (red). (D-F) MvU271 RNAi, severe effects. Development was arrested early. Centrin staining was observed in both the spermatogenous and jacket cells. (G-I) MvU271 RNAi, late effects. Few divisions took place giving rise to few and big spermatogenous cells. Centrin was localized into basal

bodies in the spermatogenous cells only (red). **SP:** Spermatogenous cell. **JC:** Jacket cells.
Cent: Centrin. The spore wall autofluoresces brightly (i=intine). Bar = 20 μm .

microspore in treated gametophytes with severe effects on development clearly present (Figure AI-4: D-F). Gametophytes arrested at a later stage showed centrin staining in the spermatogenous cells only

(Figure AI-4: G-I). Centrin was translated and localized into basal body-like structures. The basal body-like structures were fewer in numbers than observed in the untreated controls, and they were scattered throughout the spermatogenous cells. The positioning of the basal bodies was altered in the treated gametophytes.

Tubulin localization patterns in spores treated with MvU271 dsRNA

In 8 h controls, the microtubule ribbon was formed in the differentiating spermatids. This ribbon was detected with anti- β -tubulin antibody (Figure AI-5: A-C). Gametophytes with silenced MvU271 showed no β -tubulin staining in the spermatogenous cells in all affected gametophytes. The silenced gametophytes failed to form the microtubule ribbon.

Cell death in MvU271 RNAi

Microspores were treated with dsRNA made from MvU271 cDNA. dsRNA probes were introduced to the spores at the time of hydration. Spores were allowed to develop for 8 h, fixed and then embedded in LR White resin. Sections were made and stained with the *in situ* cell death detection kit. The nuclei of gametophytes treated with MvU271 dsRNA showed no staining for cell death (Figure AI-6: C-E).

Although this RNAi treatment had effects on development and differentiation, it did not result in premature activation of cell death in the gametophyte. Therefore, it is

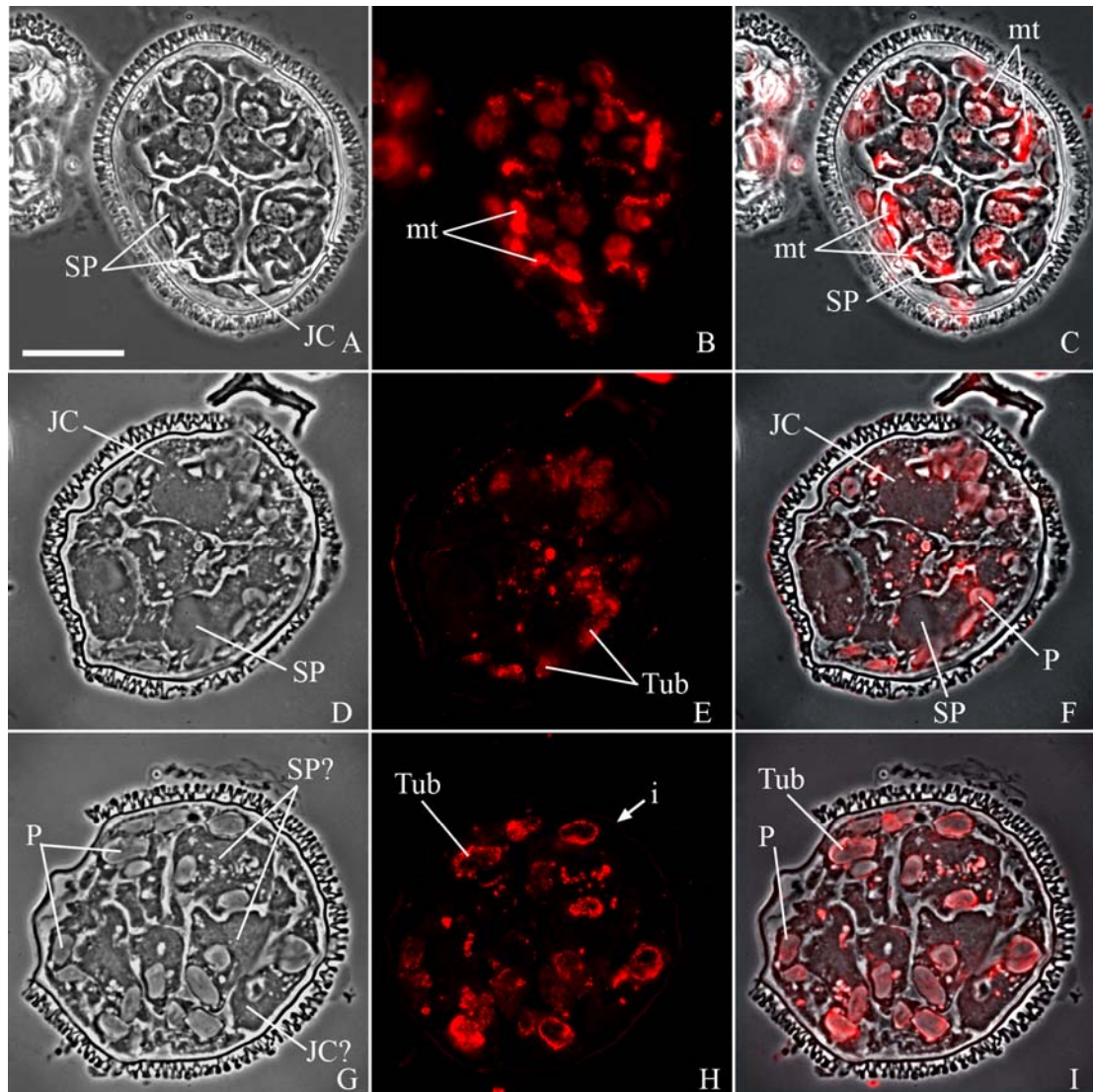


Figure AI - 5: β -tubulin immunofluorescence staining after MvU271 silencing.

Gametophytes were treated with dsRNA encoding MvU271, fixed after 8 h of development and embedded Methacrylate (A, D, G) Phase contrast imaging. (B, E, H) Immunolabeling with anti- β -tubulin antibody and Alexa fluor-594 conjugated secondary antibodies (red). (C, F, I) Phase and antibody staining images were overlaid. (A-C) 8 h controls showing normal development. The differentiating spermatids have microtubule ribbon (red, Tub). (D-F) MvU271 RNAi, severe effects. (G-I) MvU271 RNAi, late effects. (D-I) Gametophytes treated with MvU271 dsRNA failed to form the microtubule ribbon. **SP:** Spermatogenous cell. **JC:** Jacket cells. **Tub:** β -tubulin. **Mt:** Microtubule ribbon. The spore wall autofluoresces brightly (i=intine). Bar =20 μ m.

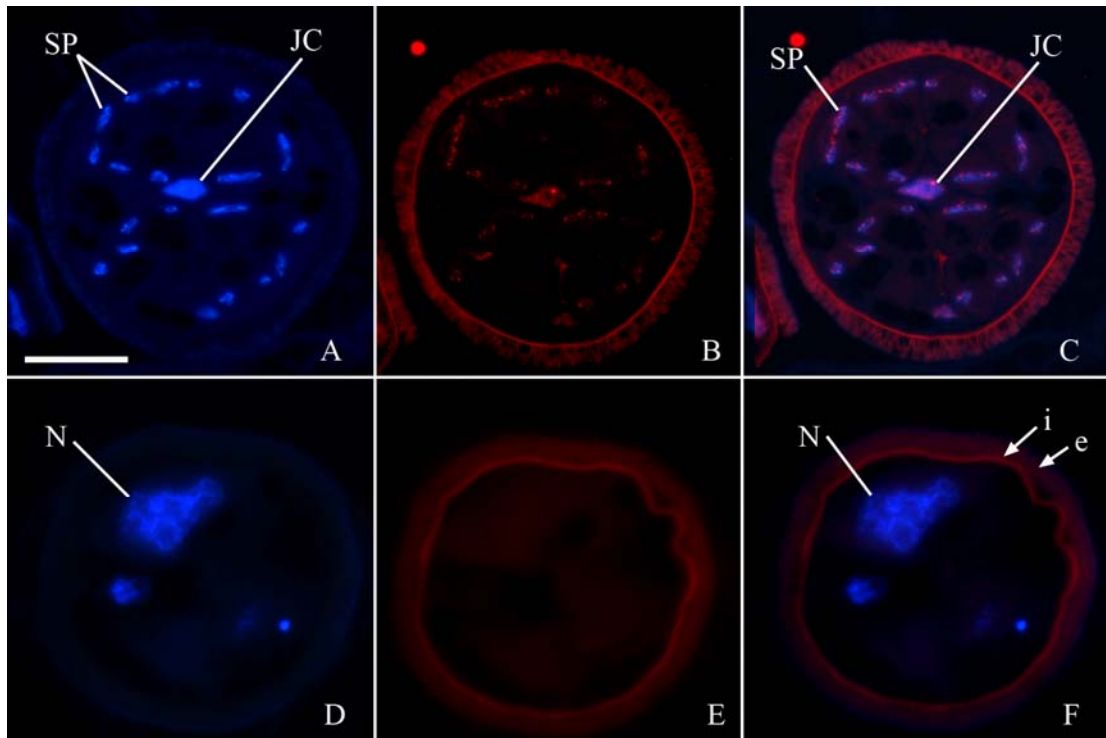


Figure AI - 6: *In situ* cell death detection assay on spores treated with MvU271 dsRNA.

Gametophytes were treated with dsRNA encoding MvU271, fixed after 8 h of development, and embedded in LR White. (A, D, G) DAPI nuclear staining (blue). (B, E, H) *In situ* cell death assay (red). (C, F, I) Overlay of DAPI staining and cell death assay images. (A-C) 8 h controls. The nuclei of both the spermatogenous and jacket cells showed unspecific staining with the *in situ* cell death assay (red). (A) DAPI nuclear staining (blue). (D-F) MvU271 RNAi fixed at 8 h. The treated gametophytes did not undergo programmed cell death. The nuclei of the treated gametophytes did not show positive staining for cell death. **N:** Nucleus. **SP:** Spermatogenous cells. **JC:** Jacket cells. The spore wall autofluoresces brightly (i=intine, e=exine). Bar = 20 μ m.

possible that the function of HSR203J gene in the microspore of *Marsilea* is different than that in tobacco.

APPENDIX II

Transient Translation in the Developing Gametophytes

Introduction:

Development in the microspore of *M. vestita* relies on stored proteins and mRNAs. The spatial and temporal regulation of translation provides the main driving force for development in the absence of transcription. Until recently, our experimental manipulations have depended mainly on RNAi strategies to reduce the levels of translation of proteins of interest and immunocytochemistry to determine their subcellular localization patterns. Transcriptional quiescence in the developing gametophyte sets limits on our ability to perform some helpful and desired genetic manipulations. In addition, we are constrained by the availability of high-quality antibodies that can bind and recognize our antigens efficiently and specifically. Therefore, the development of a protocol that would allow the induction of the translation of genes of interest in the gametophytes would expand our options of experimental designs. A protocol of transient translation would allow the manipulation of the expression levels of proteins, the induction of overexpression or premature translation of normal proteins, or alternatively, the expression of mutated proteins as a means to determine their functions in the gametophyte. In addition, this protocol would allow the translation of labeled recombinant proteins to determine their localization patterns in living, developing gametophytes. In this study, a protocol of transient translation is developed by taking advantage of the robust translational machinery in the microspores and the ability to

introduce molecules into the microspores in the hydration solution at the onset of development.

Transient Translation of β -galactosidase

Generation of LacZ RNA:

The vector pcDNA3.1/v5-His/lacZ was used to generate RNA for lacZ (Invitrogen cat# V81020, a gift from Dr. Michael Keller, NICHD, Bethesda, MD) (Figure AII-1). The vector was digested with *pme1* restriction digest enzyme. Single stranded RNA was transcribed with a T7 transcription kit (Epicentre, cat# AS3107, Madison, WI). The RNA was purified by precipitation with ammonium acetate and resuspended in RNase free water (DEPC water). The quality of ssRNA was checked by gel electrophoresis prior to each experiment.

Transient translation of lacZ-His, color development and imbedding:

RNA solutions of 1, 10, 100, 200 $\mu\text{g/ml}$ in 1 ml were made with RNase free water. Each of the RNA solutions was added to 2 mg of microspores in a 2 ml microcentrifuge tube. The spores were allowed to develop for 4 h on the Orbitron rotating shaker at 20 °C. The gametophytes were then fixed with 4% paraformaldehyde in 50 mM PIPES (pH 7.4) for 2 h at 4 °C as described in detail in Chapter II. The gametophytes were spun in a benchtop centrifuge for 1 min at 30 rpm; the entire fixative buffer was removed and the pelleted gametophytes were resuspended in 1 X PBS (phosphate buffer saline). The gametophytes were rinsed 5 x 15 min in 1 X PBS and then incubated overnight with X-Gal buffer (35 mM Potassium Ferrocyanide, 35 mM Potassium Ferricyanide, 2 mM

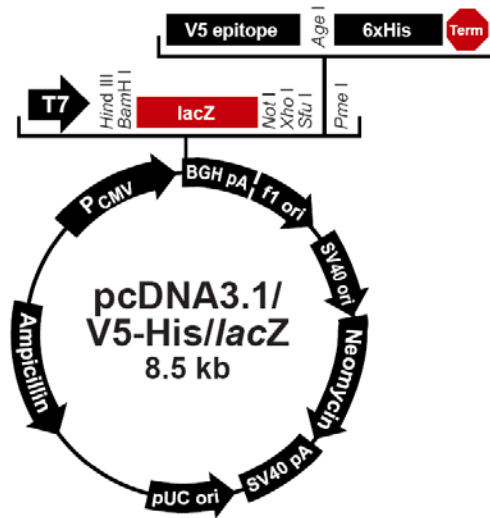


Figure AII - 1: LacZ-His vector.

The vector from Invitrogen that was used to generate RNA constructs encoding lacZ with 6x HIS tag attached at the C-terminus.

MgCl₂, 0.1% Tween, 0.01% Sodium deoxycholate, 1 mg/ml X-gal in dimethylformamide). The gametophytes were rinsed in 1 X PBS buffer until all of the buffer color was clear and then placed in fixative buffer overnight at 4 °C. Next, the gametophytes were rinsed in 1 X PBS 3 x 5 min and then dehydrated with a graded ethanol series of 10, 25, 50, 75 and 90% ethanol for 2 h each followed by 4 x 100% ethanol for 30 min each. The specimens were infiltrated with ethanol-methacrylate mixtures (3:1, 1:1, 1:3) for 2 h each followed by 5 washes of 100% methacrylate for 1 h each. Gametophytes were transferred into BEEM capsules, and the samples were polymerized for 5 h in ultraviolet light at 4 °C.

Results:

Color detection for lacZ-His:

Gametophytes were treated with ssRNA encoding lacZ-His protein. gametophytes were fixed and placed in a buffer containing X-gal. X-gal is a carbohydrate substrate for β -galactosidase enzyme. When β -galactosidase is expressed, X-gal is transformed into an insoluble blue product. Some gametophyte samples were removed after the X-gal color development, but before the ethanol dehydration steps, and observed with a light microscope. To remove the spore wall, some spores were placed on a glass slide and covered with a cover glass; fingertip pressure was applied to the cover glass with a gentle, circular motion. Treated gametophyte showed blue staining, indicating the uptake of the introduced RNA and its translation. Samples treated with 10 μ g/ml RNA solution showed the darkest blue staining throughout the gametophyte (Figure AII-2).

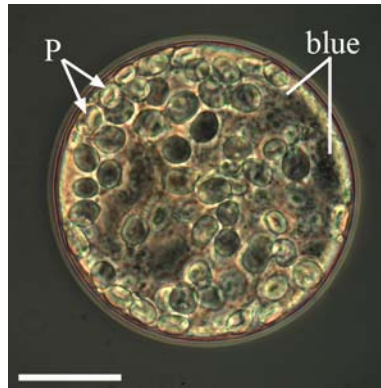


Figure AII - 2: Transient translation of lacZ-His in the microspores: Color development.

Gametophytes were treated with 10 $\mu\text{g/ml}$ RNA encoding lacZ-His and incubated in a buffer containing X-gal, the substrate for β -galactosidase. The gametophytes showed blue color indicating the expression of the β -galactosidase enzyme. **P:** Plastid. **Blue:** Blue color produced when X-gal is metabolized by β -galactosidase. The image was acquired by phase contrast light microscope. Bar= 20 μm .

Immunofluorescence staining for lacZ-His:

Gametophytes treated with lacZ-His RNA were sectioned and stained with anti- β -galactosidase (β -gal) antibody (diluted 1:40 in 1 X PBS). The secondary antibody used was an Alexa Fluor 594-conjugated goat-anti-mouse IgG. The detailed staining protocol is described in Chapter II. Gametophytes treated with lacZ-His RNA showed normal development. Untreated gametophytes showed no staining for β -gal; however, spores treated with 10, 100 and 200 μ g/ml lacZ-His RNA showed staining in both the spermatogenous and the jacket cells. This indicates that β -gal was translated throughout the microspore (Figure AII-3). Gametophytes were also stained with anti-His antibody (diluted 1: 50 in 1 X PBS). His antibody staining showed high background levels in the untreated controls. The treated gametophytes did not show specific staining higher than that observed in the controls.

Transient Translation of Centrin

Centrin constructs:

Two different types of centrin constructs were made. One type contained the centrin coding sequence, with no 3' UTR, and different tags added to the N-terminus (centrin (UTR⁻)). To generate this construct, centrin was cloned from *Mv*-centrin cDNA clone MvU336 into the PBSK vector using centrin specific primers. Later, three different centrin constructs were made with different tags, His, HA or Flag, each placed at the N-terminus. The other type of centrin construct generated included the centrin coding sequence and the 3' UTR. Similarly, His, HA or FLAG tags were added to the N-terminus (centrin (UTR⁺)).

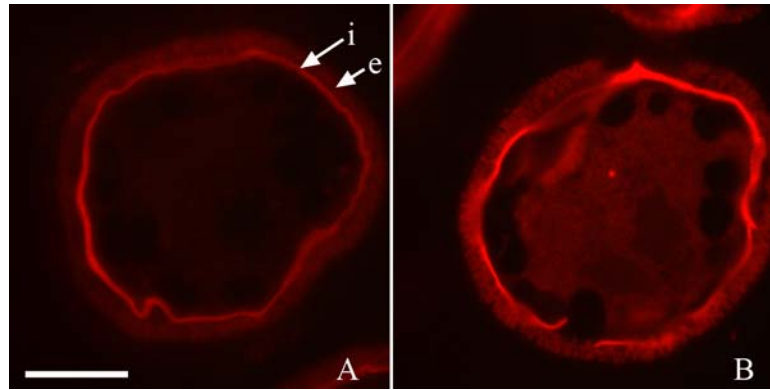


Figure AII - 3: Transient translation of lacZ-His in the microspores: immunofluorescence staining with anti- β -galactosidase antibody.

(A) Untreated controls at 4 h show no staining for β -galactosidase (B) Gametophytes were treated with 10 $\mu\text{g/ml}$ LacZ-His RNA, fixed after 4 h and embedded in Methacrylate. Development appeared normal. Low levels of β -galactosidase (red) can be detected throughout the microspore. The spore wall autofluoresces brightly (i=intine, e=exine). Bar = 20 μm .

Transient translation of centrin:

Single stranded sense RNA was transcribed with T3 *in vitro* transcription kit (Epicentre Cat# AS3103) for the centrin constructs mentioned above. In addition, capped and polyadenylated sense centrin RNA was transcribed independently with the T3 capping kit (Epicentre Cat# ACM04033) and with the tailing kit (Epicentre Cat# PAP5104H). RNA solutions of 100 µg/ml were made in DECP water and added to 4 mg of freshly isolated microspores in 2 ml tubes. Spores were allowed to hydrate in the RNA solution and to develop on a rotating orbitron shaker for different time intervals. At the desired time points, protein isolates were prepared from the developing gametophytes. The gametophytes were centrifuged in a benchtop centrifuge at max speed for 2 min. The gametophytes were transferred with 1 ml pipette tip into a dounce homogenizer and gently ground with pestles A and B on ice. The lysate was transferred into microcentrifuge tube and SDS sample buffer (62.5 mM Tris-base, pH 6.8; 2% SDS, 25% urea; 10% glycerol; 5% β-mercaptoethanol; 0.02% bromophenol blue) was added to 1 X final concentration. Protein samples were boiled for 10 min and then placed on ice for 5 min. The samples were clarified at 3000 x g for 5 min, and the supernatant was collected in a new tube. Protein concentrations were determined using the Bradford assay. To analyze translation products in the gametophytes, 50 µg of protein was loaded per lane into 15% SDS-polyacrylamide gel, 1.5 mm thick. SDS-PAGE and immunoblotting was performed as described in Tsai *et al*, (2004). Immunoblot assays were performed on blots made from these electrophoretic gels with anti-HA antibody (1:1000) (Cell Signaling), anti-Flag antibody (1:1000) (Cell Signaling), anti-His antibody (1:1000) (Abcam) and anti-centrin antibody (1:200). Secondary antibodies (antispecies horseradish

peroxidase: Amersham, Buckinghamshire, UK) were diluted 1:1500 in 0.01% PBST. Chemiluminescent detection was performed using ECF (Amersham Biosciences, Sweden) and a STORM 860 PhosphorImager (Molecular Dynamics, Sunnyvale, CA).

Results:

First, tagged centrin (UTR⁻), uncapped and unpolyadenylated, ssRNA was added to the spores at a final concentration of 100 µg/ml (Figure AII-4: A). For HA-centrin and FLAG-centrin constructs, an additional sample of 200 µg/ml RNA solution was added to the spores. Protein isolates were obtained at 2, 4, 6 and 8 h. Western blots were performed with the tag specific antibodies and then repeated with anti-centrin antibody. In control samples, centrin protein was detected in protein isolates after 4 h. In 4, 6 and 8 h samples, centrin was detected in one band of 20 KDa (Figure AII-4: B). In the protein isolates of the treated gametophytes, centrin protein was detected with anti-centrin antibody as early as 2 h in a band of approximately 21 KDa (Figure AII-4: C, D, E). In addition, centrin was detected as a single band in 4 h samples and as two bands in gametophytes homogenized at 6 or 8 h. A strong signal of two centrin bands was detected in the 6 h samples treated with 200 µg/ml RNA (Figure AII-4: D, E). Western blots were also performed with the tag specific antibodies. When anti-His and anti-FLAG antibodies were used, no bands were detected on the blots. However, when anti-HA antibody was used, a weak band was detected at 21 KDa (Figure AII-4: D). For loading controls, the blots were stained with anti- α -tubulin antibody.

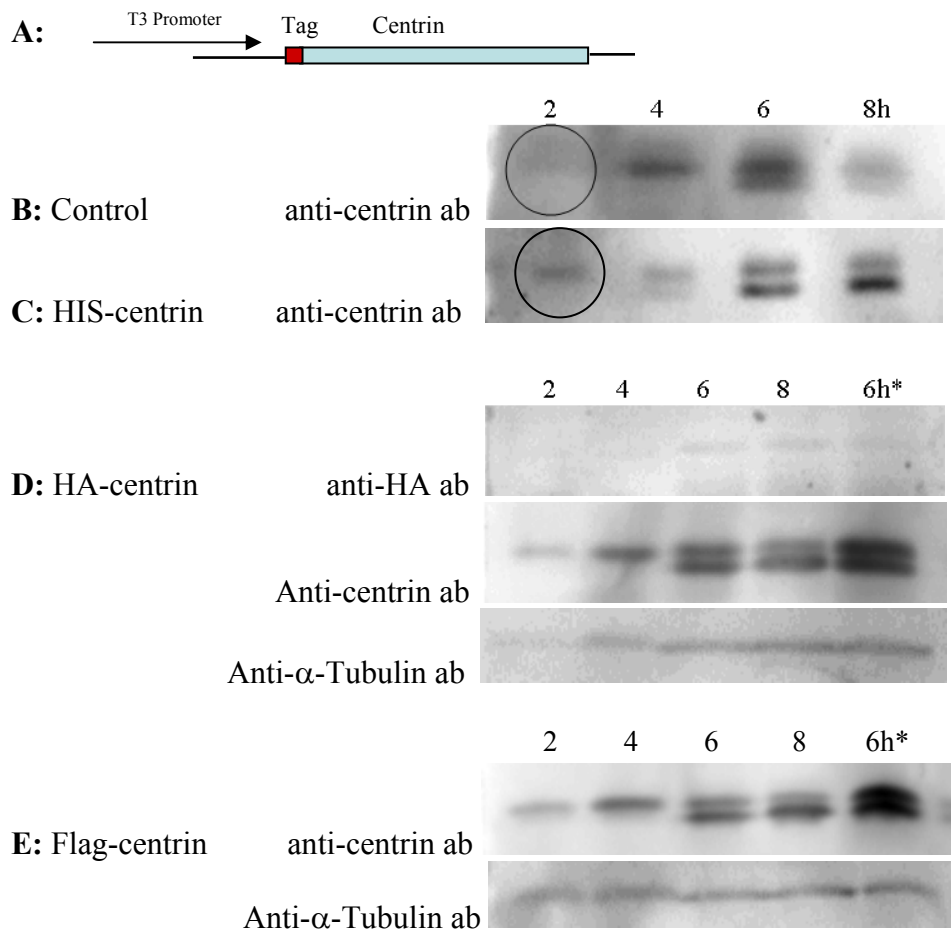


Figure AII - 4: Western blots for samples treated with ssRNA encoding tagged-centrin (UTR-) without 5'Cap and a poly(A) tail.

(A) Representation of the centrin construct used. (B) Centrin western blot for untreated samples. Centrin was detected after 4 h of development. (C) Blots for HIS-centrin. One band of centrin (21KDa) was detected in the 2 h protein sample. Two centrin bands were detected in 4, 6 and 8 h protein samples. (D) Blots for HA-centrin. A faint band of 21 KDa was detected with anti-HA antibody. (E) Blots for Flag-centrin. (D, E): One centrin band was detected in 2 and 4 h protein lysates, and two bands of 20 and 21 KDa are observed in 6, and 8 h lysates. **6 h***: Spores were treated with 200 μ g/ml RNA solution and protein lysates were obtained after 6 h of development. Two bands of centrin were detected in these samples.

Second, tagged centrin (UTR⁻), capped and polyadenylated, ssRNA was added to the spores at a final concentration of 100 µg/ml (Figure AII-4). Protein isolates were obtained at 2, 4, and 6 h. In these isolates, no bands were detected when western blots were performed with anti-HIS, anti HA or anti-FLAG antibodies (Data not presented). Blots were then stained with anti-centrin antibody where they showed a staining for one band of centrin at 20KDa (FigureAII-5: B). The data for HA-centrin only is presented.

Third, the same experiments were repeated with tagged centrin (UTR⁺). Only HA tagged constructs were transcribed and added to the spores since the other two tags, His and FLAG, were much harder to detect on the western blots. Protein isolates were obtained at 2, 4, and 6 h. Similar results were obtained for centrin (UTR⁺) construct with or without the 5' cap an poly(A)tail. No bands were detected when blots were stained with anti-HA antibody, and only one band was detected when an anti-centrin antibody was used (Figure AII-6).

Discussion and conclusions:

The purpose of this study was to develop a technique that would allow us to manipulate the expression levels and function of proteins of interest during gametophyte development. The preliminary data obtained using an exogenous mRNA encoding lacZ showed positive results. The color reaction and immunostaining indicated that we were able to induce the transient translation of lacZ mRNA even in the absence of the 5' cap and the poly(A) tail. One explanation is that when lacZ mRNA was introduced into the spores, it was not identified as foreign RNA; instead, it was capped and polyadenylated

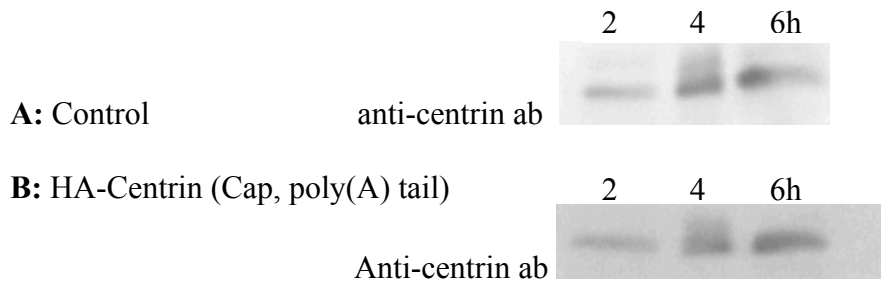


Figure AII - 5: Western blots for samples treated with ssRNA encoding tagged-centrin (UTR-) with 5'Cap and a poly(A) tail.

(A) Centrin western blot for untreated samples. Centrin is detected in one band of 20KDa (B) Blot for HA-centrin (UTR⁻) + CAP+ Poly(A) tail. Centrin is detected in one band of the same size as the control.

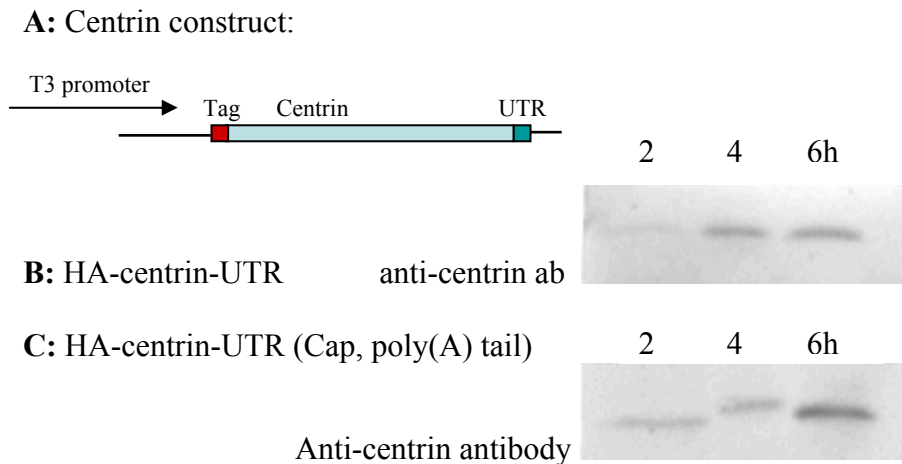


Figure AII - 6: Western blots for samples treated with ssRNA encoding tagged-centrin (UTR+).

(A) Representation of the centrin constructs used. (B) Centrin blot for samples treated with RNA encoding HA-tagged centrin with 3'UTR and without the 5'cap or a poly(A)-tail. (B) Centrin western blot for samples treated with RNA encoding HA-tagged centrin with UTR, 5'cap and poly(A)-tail. (B, C) Centrin blots show only one band of centrin of 20KDa. No bands are detected for the tagged centrin at 21KDa.

by the endogenous translational machinery. Later on, this RNA was translated at low levels. Previous studies in the lab showed that when mRNA was isolated from the spores within the first 30 min of development, no proteins were obtained by *in vitro* translation; however, an extraordinary number of protein products were obtained from samples isolated at later time points (Hart and Wolniak, 1998). This early result suggested that transcript processing precedes the rapid cell cycle phase of gametophyte development. The X-gal color reaction used in the transient translation assay showed a blue color indicating that β -galactosidase was expressed and X-gal was metabolized. This color reaction amplified the detection signal for β -galactosidase; in addition, in the absence of endogenous β -galactosidase protein, there was minimal background immunostaining.

On the other hand, the data with centrin constructs were harder to interpret. The western blots performed with antibodies directed against the epitope tags showed mostly negative results. There was only one tag that showed translation of the epitope tagged protein; the HA tag showed light staining for one centrin construct (Figure AII-3: D) but the blot revealed other unspecific light bands. Blots for centrin (UTR⁻) with no cap and poly(A) tail showed two bands of centrin (20 and 21 KDa) while blots for all of the other centrin constructs showed one centrin band of the normal size (20 KDa). This can also be interpreted that centrin (UTR⁻) mRNA was capped and polyadenylated by the translational machinery in the spores. The absence of the 3' UTR might have allowed the constitutive expression of centrin, and, therefore, centrin was detected prematurely at low levels. Since I was not able to detect the band of tagged centrin with the tag-specific antibodies, it is possible that the second (bigger) band of centrin is a modified form of

centrin that is present in the microspores and is detected on this blot. In cell culture, centrin can be phosphorylated on the C-terminus (Lutz *et al.*, 2001).

Finally, when centrin (UTR+) constructs were used with or without the cap and poly(A) tail, one band for centrin was detected, which is apparently the endogenous centrin. This can be explained in two ways. First, Centrin constructs were not translated in the microspore as a result of mRNA degradation. Second, the tagged centrin was translated at low levels that are not detected on the western blots as performed. Therefore, this protocol could be modified to ensure the stability of the RNA constructs introduced, increase the efficiency of the transient translation and improve the detection methods on western blots or *in vivo*.

APPENDIX III

M. vestita cDNA Clones Used in This Study

1. MvU89: Alignment with PRP-like protein [*Marsilea vestita*]

The closest match in GenBank database was determined using the BLASTX search parameters

GenBank accession number: gb|AAL92025.1|AF484839_1
Subject (Sbjct): PRP-like protein
Organism of Primary Identity: *Marsilea vestita*

Score = 435 bits (1118), Expect = 1e-120
Identities = 215/215 (100%), Positives = 215/215 (100%)

MvU89:	2	SQRKKRQVSQDLATPESVEKYTQLSSHPLHKTNKPGILSVDVYQSEDLILTGGVDSTAVV	181
		SQRKKRQVSQDLATPESVEKYTQLSSHPLHKTNKPGILSVDVYQSEDLILTGGVDSTAVV	
Sbjct:	1	SQRKKRQVSQDLATPESVEKYTQLSSHPLHKTNKPGILSVDVYQSEDLILTGGVDSTAVV	60
MvU89:	182	FNRSSGEIVSTLNGHSKRVNSVKFVPENGYVLTGSADKTVKIWQQKDGMYECKHTLREHT	361
		FNRSSGEIVSTLNGHSKRVNSVKFVPENGYVLTGSADKTVKIWQQKDGMYECKHTLREHT	
Sbjct:	61	FNRSSGEIVSTLNGHSKRVNSVKFVPENGYVLTGSADKTVKIWQQKDGMYECKHTLREHT	120
MvU89:	362	EEVRAVTVHATQNFVVTASTDKSWCFYDLAYGECLVQVTEPSLQEGYTSASFHPDGLILG	541
		EEVRAVTVHATQNFVVTASTDKSWCFYDLAYGECLVQVTEPSLQEGYTSASFHPDGLILG	
Sbjct:	121	EEVRAVTVHATQNFVVTASTDKSWCFYDLAYGECLVQVTEPSLQEGYTSASFHPDGLILG	180
MvU89:	542	MGTAEISLVRIWDVKSQANVAQFEGHSGPVTGLSFS	646
		MGTAEISLVRIWDVKSQANVAQFEGHSGPVTGLSFS	
Sbjct:	181	MGTAEISLVRIWDVKSQANVAQFEGHSGPVTGLSFS	215

2. MvU98: Alignment with Cyclin B [*Populus tomentosa*]

The closest match in GenBank database was determined using the BLASTX search parameters

Genbank accession number: gb|ACI89426.1|
Subject (Sbjct): Cyclin B
Organism of Primary Identity: *Populus tomentosa*

Score = 232 bits (592), Expect = 2e-59
Identities = 114/203 (56%), Positives = 153/203 (75%)

```
MvU98: 2      FKLMPETLFLTTNLIDRYLAVMPVERKNLQLVGITAMLIASKYEEIWAPEINDFIFIADN 181
          F+LM ETLFL NLIDR+L V RK LQLVG+TAML+A KYEE+ P + DF+ I+DN
Sbjct: 192    FELMDETLFLAINLIDRFLERCTVVRKKLQLVGV TAMLLACKYEEVSVPLVEDFVLISDN 251

MvU98: 182   AYTRQNIEMEKIMLNTLKFNL CIPTPYMFLVRF LKAAGSDQQMNMLAFYYVELCLVDYQ 361
          AYTR +L+MEK+M+NTL+F + +PTPYMF+ RFLKAA SD+++ +L+F+ +E+CLV+Y+
Sbjct: 252   AYTRIEVLDMEKLMVNTLQFKMSVPTPYMFMKRFLKAALSDKKLELLSFFIIEVCLVEYE 311

MvU98: 362   MVRFPSIQAAAAVYLARQTLKAGEEARWNATLKRHSGYKESQLTECVSMIVSLHQKAGE 541
          M+RF PS+ AAAA+Y A+ +L + +W+ T +RH+ Y E QL EC M+VS HQKAG
Sbjct: 312   MLRFPPSLLAAAAIYTAQCSLY--QFKQWSKT SERHTSYTEDQLECSRMMVSFHKAGY 369

MvU98: 542   GNVTVVHRKYSQSKFCVAXLKP 610
          G +T VHRKYS SKF A +P
Sbjct: 370   GKLTGVHRKYSTSKFGYAAKAEF 392
```

3. MvU 99: Alignment with Kinesin 5 [*Arabidopsis thaliana*]

The closest match in GenBank database was determined using the BLASTX search parameters

Genbank accession number: NP_192428.2
Subject (Sbjct): ATK5 (kinesin 5); microtubule motor
Organism of Primary Identity: *Arabidopsis thaliana*

Score = 114 bits (286), Expect (2) = 7e-48
Identities = 55/68 (80%), Positives = 60/68 (88%)

```
MvU99: 313 EISQLVQSALDGYKVCIFAYGQTGSGKTYTMLGQPDNESHKGLIPRSLEQIFKSSQIL*G 492
      EISQLVQSALDGYKVCIFAYGQTGSGKTYTM+G+P+ KGLIPRSLEQIFK+SQ L
Sbjct: 493 EISQLVQSALDGYKVCIFAYGQTGSGKTYTMMGRPETPEQKGLIPRSLEQIFKTSQSLST 552

MvU99: 493 QGWTFFKMQ 516
      QGW +KMQ
Sbjct: 553 QGWKYKMQ 560
```

Score = 99.8 bits (247), Expect (2) = 7e-48
Identities = 52/95 (54%), Positives = 68/95 (71%)

```
MvU99: 20 ELQLKLAEAERRLNEGELIRRKLHNTIQELKGNIRVFCRVRPXLGDE-DPEHVPAVQYPQ 196
      ELQ +LA+ ER+L EGEL+R+KLHNTI ELKGNIRVFCRVRP L D+ + + YP
Sbjct: 396 ELQDRLADTERQLFEGELLRKKLHNTILELKGNIRVFCRVRPLLPDDGGRQEASVIAYPT 455

MvU99: 197 YGDLVGRGVELVQTEGQKYTF SFDKVFGPDMKQRE 301
      + +GRG+++VQ+ G K+ F+FDKVF Q E
Sbjct: 456 STESLGRGIDVVQS-GNKHPFTFDKVFHDHGASQEE 489
```

4. MvU130: Alignment with POK1 (Phragmoplast Orienting Kinesin 1) [*Arabidopsis thaliana*]

The closest match in GenBank database was determined using the BLASTX search parameters

Genbank accession number: NP_188362.2
Subject (Sbjct): POK1 (Phragmoplast Orienting Kinesin 1);
microtubule motor
Organism of Primary Identity: *Arabidopsis thaliana*

Score = 50.8 bits (120), Expect = 6e-05
Identities = 30/80 (37%), Positives = 44/80 (55%)

```
MvU130:325 TSDKDQFCKQIIELSGQLESRLRSEDHRKLAEESEKISDALKCQLHDKETEVKLLKESI 504
+ +KDQ +I L+ +LE D +A E+ + S+A K KE EVK+LE S+
Sbjct: 1608 SDEKDQIVDEICSLNNKLELAYAIADEKEAIAVEAHQESEASKIYAEQKEEVKILEISV 1667

MvU130:505 LELEATISALETQMXIMRRE 564
ELE TI+ LE ++ M E
Sbjct: 1668 EELERTINILERRVYDMDEE 1687
```

5. MvU185: Alignment with Spermidine Synthase 1 [*Arabidopsis thaliana*]

The closest match in GenBank database was determined using the BLASTX search parameters

Genbank accession number: NP_973900.2
Subject (Sbjct): Spermidine Synthase 1
Organism of Primary Identity: *Arabidopsis thaliana*

Score = 252 bits (643), Expect = 2e-65
Identities = 123/146 (84%), Positives = 140/146 (95%)

```
MvU185: 200 ANISTIVPGWFSEVSEMWPGEAHS LQVEKILFEGKSD FQDVLV FQSATYGKVLVLDGVIQ 379
          A ST++PGWFSE+S MWPGEAHS L+VEK+LF+GKSD+QDV+VFQSATYGKVLVLDGVIQ
Sbjct: 82 ACFSTVIPGWFSEMSPMWPGEAHS LKVEKVL FQGKSDYQDVIV FQSATYGKVLVLDGVIQ 141

MvU185: 380 LTERDECAYQEMISHLPLCSIPNPKRVLVIgggdggVLREVARHKSVEQIDICEIDKMVI 559
          LTERDECAYQEMI+HLPLCSIPNPK+VLVIGGGDGGVLREVARH S+EQID+CEIDKMV+
Sbjct: 142 LTERDECAYQEMITHLPLCSIPNPKKVLVIGGGDGGVLREVARHASIEQIDMCEIDKMVV 201

MvU185: 560 DVAKQFFPDVAVG YDDPRVKLFVGDG 637
          DV+KQFFPDVA+GY+DPRV L +GDG
Sbjct: 202 DVSKQFFPDVAIGYEDPRVNLVIGDG 227
```

6. MvU271: Alignment with HSR203J [*Nicotiana tabacum*]

The closest match in GenBank database was determined using the BLASTX search parameters

Genbank accession number: emb|CAA54393.1
Subject (Sbjct): HSR203J
Organism of Primary Identity: *Nicotiana tabacum*

Score = 70.5 bits (171), Expect = 9e-11
Identities = 52/184 (28%), Positives = 90/184 (48%)

```
MvU271: 25 DPWLDPSLVYQITLLCGESTGASIIILNVALNVSPILPELQPLCIRGLVLVQPGLHTEK 204
      +PWL+   D+   L G+S+G +I+  VA+   L P+ + G + + PG   +
Sbjct  153 EPWLN-DYADFNRVFLIGDSSGGNIVHQVAVKAGE--ENLSPMRLAGAIPIHPGFVRSYR 209

MvU271: 205 RGTMLDKG---FGNMP-IDTLYDLALPIGEDLDYPPVNPLHEKSPPLTPLAAYPSIFVAA 372
      + L++   F + +D   LALP+G + D+   P+ E +P + L P ++
Sbjct  210 SKSELEQEQTFFLTLDMVDKFLGLALPVGSNKDHQITCPMGEAAPAVEELKLPYLY-CV 268

MvU271: 373 ATEDFRYDLTLIFYERIKSFCADVQLFVTEGKPHVFHLEFEPACQ-----ETLELIDRM 531
      A +D   D + FYE +K   DV+LF+ G H F+L + A +   ET +L + +
Sbjct  269 AEKDLIKDTEMEFYAMKKGEKDVELFINNGVGHSFYLNKIAVRMDPVTGSETEKLYEAV 328

MvU271: 532 ADFI 543
      A+FI
Sbjct  329 AEFI 332
```

7. MvU336: Alignment with Centrin [*Marsilea vestita*]

The closest match in GenBank database was determined using the BLASTX search parameters

Genbank accession number: gb|AAC04626.1
Subject (Sbjct): Centrin
Organism of Primary Identity: *Marsilea vestita*

Score = 332 bits (850), Expect = 2e-89
Identities = 167/167 (100%), Positives = 167/167 (100%)

```
MvU336: 4 MSNFRKGVGTGRRDKNKGRAQGLSEEQKQEIREAFDLFDTDGSGTIDAKELKVAMRALGF 183
          MSNFRKGVGTGRRDKNKGRAQGLSEEQKQEIREAFDLFDTDGSGTIDAKELKVAMRALGF
Sbjct 1 MSNFRKGVGTGRRDKNKGRAQGLSEEQKQEIREAFDLFDTDGSGTIDAKELKVAMRALGF 60

MvU336: 184 EPKKEEIKKMIADIDKDGSMTIDFEDFLQMMTTKMGERSKKEIMKAFRLFDDDETGKIS 363
          EPKKEEIKKMIADIDKDGSMTIDFEDFLQMMTTKMGERSKKEIMKAFRLFDDDETGKIS
Sbjct 61 EPKKEEIKKMIADIDKDGSMTIDFEDFLQMMTTKMGERSKKEIMKAFRLFDDDETGKIS 120

MvU336: 364 FKNLKRVAKELGENMTDEELQEMIDEADRDGDGEINEEEFYRIMKKT 504
          FKNLKRVAKELGENMTDEELQEMIDEADRDGDGEINEEEFYRIMKKT
Sbjct 121 FKNLKRVAKELGENMTDEELQEMIDEADRDGDGEINEEEFYRIMKKT 167
```


8. MvU629: Alignment with Kinesin-like protein KIF3B [*Canis familiaris*]

The closest match in GenBank database was determined using the BLASTX search parameters

Genbank accession number: XP_542954.2
 Subject (Sbjct): Kinesin-like protein KIF3B
 Organism of Primary Identity: *Canis familiaris*

Score = 45.4 bits (106), Expect = 0.007
 Identities = 37/129 (28%), Positives = 64/129 (49%)

```

MvU629: 237  KHIKELEEKADASMLKAMRLEQALEKQEELNKK-----TNEQ---LEAAYQEIATMKKKL 392
                K +++L + DA+ +   +++ A+E + + K   TNEQ  LE  QEIA  K++
Sbjct    437  KKMEDLRREKDAEMLGAKIK-AMESKLLVGGKNIVDHTNEQQKILEQKRQEIAEQKRRE 495

MvU629: 393  SSCMNALESKDGELLNLQ TALGQYYAEIEAK----DRLITELTATRSEINNLS EQLK KAY 560
                +ES+D E L L+      E++ K   +L ++L A ++EI++L E+  K
Sbjct    496  REIQQQMESRDEETLELKETYSLSLQQEVDIKTKKLLKLF SKLQAVKAEIHDLQEEHIKER 555

MvU629: 561  IALEMKDXE   587
                LE     E
Sbjct    556  QELEQTQNE   564
  
```

Score = 42.0 bits (97), Expect = 0.083
 Identities = 44/213 (20%), Positives = 92/213 (43%)

```

MvU629: 15   QQSAVTE DNNVSKQAADILKEAESAFDVERK KYQDRVNTLSVEkdka lrdlkr l kQH LI 194
                ++ A+ ED++ V+++ +LKE E + R++ +D  L +      L  ++++
Sbjct    413  EKRAIVEDHSLVAEEKMRL LKEKEKKMEDLRRE-KDAAEMLGAKIKAMESKLLVGGKNIV 471

MvU629: 195  ekeesesekmeQDCKHIKELEEKADASMLKAMRLEQALEKQEELNKK TNEQLEAAYQEIA 374
                +   + + +EQ + I E + +      ++Q +E ++E + E +  QE+
Sbjct    472  DHTNEQQKILEQKRQEIAEQKRRE-----REIQQQMESRDEETLELKETYSLSLQQEVD 524

MvU629: 375  TMKKKLS SCMNALESKDGELLNLQ TALGQYYAEIEAKDRLITELTATRSEINNLS EQLK K 554
                KKL + L++ E+ +LQ      E  K+R  E T      N L+ +LK
Sbjct    525  IKTKKLLKLF SKLQAVKAEIHDLQ-----EEHIKERQELEQTQ-----NELTRELK L 571

MvU629: 555  AYIALEMKDXEKXDLMERLALQQKKFTDSDHKH 653
                ++ +E      L E+ + + F D + H
Sbjct    572  KHLIIE----NFIPLEEKSKIMNRSFFDEEEDH 600
  
```

9. MvU951: Alignment with ARK1, kinesin1 [*Arabidopsis thaliana*]

The closest match in GenBank database was determined using the BLASTX search parameters

Genbank accession number: dbj|AB290928.1|
Subject (Sbjct): ARK1, kinesin1
Organism of Primary Identity: *Arabidopsis thaliana*

Score = 152 bits (327), Expect = 3e-34
Identities = 67/126 (53%), Positives = 85/126 (67%)

```
MvU951: 658 EGGIRAXLRMARLGYVDVQAQVARGIANFAKXEYRRVSQEDVKSRSLXEDGVLPPVVTN 479
          E GI+ L MA+ G +D+ AQVARG+ANFAK E R + Q K RSLLE+GVL W+ +N
Sbjct 2791 EEGIKGLLTMAQSGNIDIIAQVARGMANFAKCETREIMQGRRKGRSLLLEEGVLEWLTSN 2970

MvU951: 478 VDNDHVSIRRHLELAMCHLAQNEANSRDLLNGGAVHELARISAEGSREDIRDLAGRILNA 299
          D S +RH+ELA+CHLAQNE N+ D G+V E+ RIS E SR+DIR LA +IL
Sbjct 2971 SHIDSASTQRHIELALCHLAQNEENANDFKRTGVSVEIVRISVSSRDIRSLAKKILKT 3150

MvU951: 298 IPLFQA 281
          P F +
Sbjct 3151 NPYFSS 3168
```

Score = 91.3 bits (193), Expect = 8e-16
Identities = 52/122 (42%), Positives = 62/122 (50%)

```
MvU951: 294 GIAFRIRPARSRMSSLEPSADIRASSCTAPPLSKSLELASFCAK*HIASSKWRLMDT*SL 473
          G I A+ R+SSL S DI S T P L KS +SF AK ASS R +D S+
Sbjct 3155 GFVLSIFFAKLRISLLDSTDILTISVTLPLVLLKSFAFSSF*AKWQSASSM*RCVDAESI 2976

MvU951: 474 STFVTTQGKTPSSMSNDLDFTSSETRYSHLAKFAIPRATCAWTSTYPSLAILRXALIP 653
          F +TPSS + F C R SH AKFAIP AT A S +P AI+ L+P
Sbjct 2975 CEFVNHRSRTPSSNRERPFRLRPCIISRVSHFAKFAIPLAT*AMISMFPDCAIVSSPLMP 2796

MvU951: 654 PS 659
          S
Sbjct 2795 SS 2790
```

10. MvU 1647: Alignment with Atkinesin-13A/Kinesin-13A [*Arabidopsis thaliana*]

The closest match in GenBank database was determined using the BLASTX search parameters

Genbank accession number: NP_850598.1
Subject (Sbjct): Atkinesin-13A/Kinesin-13A; microtubule motor
Organism of Primary Identity: *Arabidopsis thaliana*

Score = 126 bits (317), Expect = 2e-27
Identities = 67/86 (77%), Positives = 77/86 (89%)

```
MvU1647: 636 DNNISAILeeeEDLIAAHRLEVEDTMELVREEMRLLTEVDQPGSRIDKYVSQLSYVLSRK 457
          D N+ A+LEEEE LIAAHR E+EDTME+VREEM+LL EVDQPGS I+ YV+QLS+VLSRK
Sbjct    704 DENLDALLEEEEEALIAAHRKEIEDTMEIVREEMKLLAEVDQPGSMIENYVTQLSFVLSRK 763

MvU1647: 456 AAGIVNLQARLARFQRHLKEQEILSR 379
          AAG+V+LQARLARFQ LKEQEILSR
Sbjct    764 AAGLVSLQARLARFQHRHLKEQEILSR 789
```

**11. MvU 2336: Alignment with POK2 (Phragmoplast Orienting Kinesin 2)
[*Arabidopsis thaliana*]**

The closest match in GenBank database was determined using the BLASTX search parameters

Genbank accession number: NM_112791.4
 Subject (Sbjct): POK2 (Phragmoplast Orienting Kinesin 2);
 microtubule motor
 Organism of Primary Identity: *Arabidopsis thaliana*

Score = 95.9 bits (203), Expect = 4e-17
 Identities = 43/104 (41%), Positives = 69/104 (66%)

```
MvU2336: 66 LSRQINFEMDEELYSNRRRIQELEDIAASRQKEIFHLSKKLGEAESMTGDVIRDLLGVKH 245
          +++Q+ E DEEL + R RI+ELE + ++RQKEIF L+ KL + +SMT D+ R LLGVK
Sbjct 7270 ITQQMRSEKDEELAAARLRIEELETVVSTRQKEIFLLNSKLAKVDSMTHDINRVLLGVKQ 7449

MvU2336: 246 DFVNNRVSLDPQQIEEMSNA LCHLQKESRAKEKELEALRKQYDQ 377
          + N LD QQ+ +++ L H +SR ++ E+ L++Q ++
Sbjct 7450 NVTNCASF LDSQQVLKIAEMLQHNSSDSRERDLEVSHLKQQLNE 7581
```

Score = 47.8 bits (98), Expect = 0.014
 Identities = 30/74 (40%), Positives = 38/74 (51%)

```
MvU2336: 295 ISSIC*GSRDTLLLT K SCLTPSKSLMTSPVIDSASPSFLLKWKISF*RDAAISSSS*MRR 116
          I + C* S++ CLTPSK+ + S V+ S SF ISF R SSS +R
Sbjct 7499 IFNTC*LSKNDAQFVTFCLTPSKTRLISCVMLSTLASFEFNKNISFCRVETTVSSSSIRS 7320

MvU2336: 115 LFEYNSSSISKFIC 74
          L +SSS S IC
Sbjct 7319 LAAASSSFSDLIC 7278
```

12. MvU2357: Alignment with kinesin-like protein [*Arabidopsis thaliana*]

The closest match in GenBank database was determined using the BLASTX search parameters

Genbank accession number: gb|AF159052.1|AF159052
Subject (Sbjct): kinesin-like protein
Organism of Primary Identity: *Arabidopsis thaliana*

Score = 163 bits (351), Expect = 1e-37
Identities = 72/132 (54%), Positives = 92/132 (69%)

```
MvU2357: 658 EGGIRAXLRMARLGYVDVQAQVARGIANFAKXEYRRVSQEDVKSRSLXEDGVLPPVVVN 479
          EGGI A L M R G+ DV AQVARGIANFAK E R +Q + +SLL EDG L W+V N
Sbjct 2557 EGGIAALLGMVRCGHPDVLAQVARGIANFAKCESRASTQGTKRGKSLLIEDGALSWIVQN 2736

MvU2357: 478 VDNDHVSIRRHLELAMCHLAQNEANSRDLLNGGAVHELARISAEGSREDIRDLAGRILNA 299
          + +IRRH+ELA+CHLAQ+E N+++++ GA+ EL RIS + SREDIR LA R L +
Sbjct 2737 AKTETAAIRRHIELALCHLAQHEGNAKEMVKEGAMWELVRISRDCSREDIRSLAHRRLTS 2916

MvU2357: 298 IPLFQAE LQNLQ 263
          P F EL+ L+
Sbjct 2917 SPTFLTELRLR 2952
```

**13. MvU2596: Alignment with Spermidine ABC Transporter, PotC subunit.
[*Shigella flexneri*]**

The closest match in GenBank database was determined using the BLASTX search parameters

Genbank accession number: NP_707037.1
 Subject (Sbjct): spermidine/putrescine ABC transporter membrane protein, potC
 Organism of Primary Identity: *Shigella flexneri* 2a str. 301

Score = 294 bits (752), Expect = 4e-78
 Identities = 168/189 (88%), Positives = 170/189 (89%)

MvU2596:	3	MIGRLLRGGFMTAiyxylyipiiliivNSFNSSRFGINWQGFTTKWYSLLMNNDSSLQAA	182
		MIGRLLRGGFMTAIY YLYIPIIILIVNSFNSSRFGINWQGFTTKWYSLLMNNDSSLQAA	
Sbjct	1	MIGRLLRGGFMTAIYAYLYIPIIILIVNSFNSSRFGINWQGFTTKWYSLLMNNDSSLQAA	60
MvU2596:	183	QHSLTMAVFSATFATLIGSLTAVALYRYRFRGKPFVSGMLFVMMSPDIVMAISLLVLFM	362
		QHSLTMAVFSATFATLIGSLTAVALYRYRFRGKPFVSGMLFVMMSPDIVMAISLLVLFM	
Sbjct	61	QHSLTMAVFSATFATLIGSLTAVALYRYRFRGKPFVSGMLFVMMSPDIVMAISLLVLFM	120
MvU2596:	363	LLGIQLGFWSLLFSHITFCLPFVVVTVYSRLKGF DVRMLEAGXRSRCPANLPFCEKSFCH	542
		LLGIQLGFWSLLFSHITFCLPFVVVTVYSRLKGF DVRMLEA + + K	
Sbjct	121	LLGIQLGFWSLLFSHITFCLPFVVVTVYSRLKGF DVRMLEAA-KDLGASEFTILRKIILP	179
MvU2596:	543	WAMPAVGAG 569	
		AMPAV AG	
Sbjct	180	LAMPAVAAG 188	

Bibliography

- Banan, A., McCormack, A., and Johnson, L. R. (1998). Polyamines are required for microtubule formation during gastric mucosal healing. *Am. J. Physiol. Gastrointest. Liver Physiol.* *274*: 879-885.
- Baskin, T. I., and Wilson, J. E. (1997). Inhibitors of protein kinases and phosphatases alter root morphology and disorganize cortical microtubules. *Plant Physiol.* *113*, 493–502.
- Beauchemin, R., Harnois, L., Rouillon, R., Tajmir-Riahi, H. A. and Carpentier, R. (2007). Interaction of polyamines with proteins of photosystem II: Cation binding and photosynthetic oxygen evolution. *Jour. Mol. Struc.* *833*, 13: 169-174.
- Bertrand, E., Chartrand, P., Schaefer, M., Shenoy, S. M., Singer, R. H., and Long, R. M. (1998). Localization of ASH1 mRNA particles in living yeast. *Mol. Cell.* *2*, 437-445.
- Betley, J. N., Heinrich, B., Vernos, I., Sardet, C., Prodon, F., and Deshler, J. O. (2004). Kinesin II mediates Vg1 mRNA transport in *Xenopus* oocytes. *Curr. Biol.* *14*, 219–224.
- Bloomfield, V. A. (1997). DNA condensation by multivalent cations. *Biopolymers.* *44*, (3): 269-282.
- Brendza, R. P., Serbus, L. R., Duffy, J. B., and Saxton, W. M. (2000). A function for kinesin I in the posterior transport of *oskar* mRNA and staußen protein. *Science.* *289*, (5487): 2120 – 2122.
- Brown, J. M., Marsala, C., Kosoy, R., and Gaertig, J. (1999). Kinesin-II is preferentially targeted to assembling cilia and is required for ciliogenesis and normal cytokinesis in *Tetrahymena*. *Mol. Biol. Cell.* *10*, 3081–3096.
- Callan, H. G. (1986). Lampbrush chromosomes. Springer, Berlin, Heidelberg, New York.
- Capco, D. G., and Jeffery, W.R. (1979). Origin and spatial distribution of maternal messenger RNA during oogenesis of an insect *Oncopeltus fasciatus*. *J. Cell Sci.* *39*, 63-76.
- Carothers, Z. B. 1975. Comparative studies on spermatogenesis in bryophytes. In: Duckett JG, Racey PA, editors. The biology of the male gamete. *Biol. J. Linn. Soc. Suppl.* *1*. London: Academic Press. p 71–84.
- Cleary, A. L., and Smith, L. G. (1998). The Tangled1 gene is required for spatial control of cytoskeletal arrays associated with cell division during maize leaf development. *Plant Cell.* *10*, 1875-1888.
- Clément, S., Delcros, J. G., Basu, H. S., Quash, G., Marton, L. J., and Feuerstein, B. G. (1995). The structure of polyamine analogues determines haemoglobin production and cytotoxicity in murine erythroleukaemia cells. *The Biochemical Journal.* *309*, 787-91.
- Cole, D. G. (2003). The intraflagellar transport machinery of *Chlamydomonas reinhardtii*. *Traffic.* *4*, 435-442.
- Curtis, D., Lehman, R., and Zamore P. D. (1995). Translational regulation in development. *Cell.* *81*, 171-178.
- Davidson, E. H. (1986). Gene activity in early development. 3rd Ed. Academic press, New York. 670 pp.

- Davies, E., Larkins, B., and Knight, R. (1972). Polyribosomes from Peas: An Improved Method for Their Isolation in the Absence of Ribonuclease Inhibitors. *Plant Physiol.* *50*, 581-584.
- Deacon, S. W., Serpinskaya, A. S., Vaughan, P. S., Lopez Fanarraga, M., Vernos, I., Vaughan, K. T., and Gelfand, V. I. (2003). Dynactin is required for bidirectional organelle transport. *J. Cell Biol.* *160*, 297-301.
- Didier D. K., Schiffenbauer, J., Woulfe, S. L., Sacheis, M., and Schwartz, B. D. (1988). Characterization of the cDNA encoding a protein binding to the major histocompatibility complex class II Y box. *Proc. Natl. Acad. Sci.* *85*, 7322-7326.
- Dure, L. S. and Waters, L. (1965), Long-lived messenger RNA: Evidence from cotton seed germination. *Science.* *147*, 410-413.
- Dworkin, M. B., and Dworkin-Rastl, E. (1990). Functions of maternal mRNA in early development. *Mol. Rep. Dev.* *26*, (3): 261-297.
- Eiben, R. (1982). Storage of embryonically transcribed poly(A) RNA and its utilization during metamorphosis of *Hydractinia echinata*. *Roux's Arch. Dev. Biol.* *191*, 270-276.
- Gallie, D. R. (1991). The cap and poly(A) tail function synergistically to regulate mRNA translational efficiency. *Genes Dev.* *5*, 2108-2116.
- Gandolfi, T. A. L. B. and Gandolfi, F. (2001). The maternal legacy to the embryo: Cytoplasmic components and their effects on early development. *Theriogenology.* *55*, (6): 1255-1276.
- Geall, A. J., Eaton, M. A.W., Baker, T., Catterall, C., and Blagbrough, I. S. (1999). The regiochemical distribution of positive charges along cholesterol polyamine carbamates plays significant roles in modulating DNA binding affinity and lipofection. *FEBS Letters.* *459*, 337-342.
- Hachet, O., and Ephrussi, A. (2001). *Drosophila* Y14 shuttles to the posterior of the oocyte and is required for *oskar* mRNA transport. *Curr. Biol.* *11*, 1666-1674.
- Hakovirta, H., Keiski, A., Toppari, J., Halmekeyto, M., Alhonen, L., Janne, J., and Parvinen, M. (1993). Polyamines and regulation of spermatogenesis: selective stimulation of late spermatogonia in transgenic mice overexpressing the human ornithine decarboxylase gene. *Mol. Endocrinol.* *7*, 1430-1436.
- Hammett, J. R. and Katterman, F. R. (1975). Storage and metabolism of poly(adenylic acid)-mRNA in germinating cotton seeds. *Biochemistry.* *14*, (20): 4375-4379
- Han, Y. G., Kwok, B. H., and Kernan, M. J. (2003). Intraflagellar transport is required in *Drosophila* to differentiate sensory cilia but not sperm. *Curr. Biol.* *13*, 1679-1686.
- Hardin, S., and Wolniak, S. M. (1998). Molecular cloning and characterization of maize ZmMEK1, a protein kinase with a catalytic domain homologous to mitogen- and stress-activated protein kinase kinases. *Planta.* *206*, 577-584.
- Hart, P. E., and Wolniak, S. M. (1998). Spermiogenesis in *Marsilea vestita*: a temporal correlation between centrin expression and blepharoplast differentiation. *Cell Motil. Cytoskelet.* *41*, 39-48.
- Hart, P. E., and Wolniak, S. M. (1999). Molecular cloning of a centrin homolog from *Marsilea vestita* and evidence for its translational control during spermiogenesis. *Biochem. Cell Biol.* *77*, 101-108.
- Hepler, P. K. (1976). The blepharoplast of *Marsilea*: its *de novo* formation and spindle association. *J. Cell Sci.* *21*, 361-390.

- Hershey, J. W. B. (1991). Translational control in mammalian cells. *Annu. Rev. Biochem.* *60*, 717-755.
- Hochstrasser, M. (1996). Ubiquitin-dependent protein degradation. *Annu. Rev. Genet.* *30*, 405-439.
- Hoffman, J. C., and Vaughn, K.C. (1995). Using developing spermatogenous cells of *Ceratopteris* to unlock the mysteries of the plant cytoskeleton. *Int. J. Plant Sci.* *156*, 346-358.
- Hoyt, M. A., Broun, M., and Davis, R. H. (2000). Polyamine Regulation of Ornithine decarboxylase Synthesis in *Neurospora crassa*. *Mol. Cell Biol.* *20*, (8): 2760-2773.
- Hyams, J. S., Vondy, K. P., Luba, A., and Bell, P. R. (1983). Structural and macromolecular events associated with basal body morphogenesis in *Marsilea*. *J. Submicrosc. Cytol.* *15*, 133-138.
- Igarashi, K., and Kashiwagi, K. (1999). Polyamine transport in bacteria and yeast. *J. Biochem.* *344*, (3): 633-642.
- Igarashi, K., and Kashiwagi, K. (2000). Polyamines: Mysterious modulators of cellular functions. *Biochem. Biophys. Res. Comm.* *271*, (3): 559-564.
- Jänne, J., Pösö, H., and Raina A. (1978). Polyamines in rapid growth and cancer. (1978). *Biochim Biophys Acta.* *473*, 241-293.
- Jorstad, C. M., Harada, J. J., and Morris, D. R. Structural Specificity of the Spermidine Requirement of an Escherichia Coli Auxotroph. *J. Bacteriol.* *141*, 456-463 (1980).
- Kaipia, A., Toppari, J., Mali, P., Kangasniemi, M., Alcivar, A. A., Hecht, N.B., and Parvinen, M. (1990). Stage- and cell-specific expression of the ornithine decarboxylase gene during rat and mouse spermatogenesis. *Mol. Cell Endocrinol.* *73*, 45-52.
- Kaur-Swahney, R., Tiburcio, A.F., Atlabells, T., and Galston, A. W. (2003). Polyamines in plants: An overview. *Jour. Cell. Mol. Biol.* *2*, 1-12.
- Kleene, K. C. (1995). Patterns of translational regulation in the mammalian testis. *Mol. Reprod. Dev.* *43*, (2): 268 - 281.
- Klink, V. P. and Wolniak, S. M. (2000). The utility of RNAi in the study of the plant cytoskeleton. *J. Pl. Gr. Reg.* *19*, 371-384.
- Klink, V. P. and Wolniak, S. M. (2001). Centrin is necessary for the formation of the motile apparatus in spermatids of *Marsilea*. *Mol. Biol. Cell.* *12*, 761-776.
- Klink, V. P. and Wolniak, S. M. (2003). Changes in the abundance and distribution of conserved centrosoma, cytoskeletal and ciliary proteins during spermiogenesis in *Marsilea vestita*. *Cell Mot. Cyto.* *56*, 57-73.
- Kloc, M., Zearfoss, N. R. and Etkin, L. (2002). Mechanisms of subcellular mRNA Localization. *Cell.* *108*, 533-544.
- Kozak, M. (1989). Circumstances and mechanisms of inhibition of translation by secondary structure in eucaryotic mRNAs. *Mol. Cell Biol.* *9*, 5134-5142.
- Kreis, T. and Vale, R. (1993). *Guidbook to the Cytoskeleton and Motor Proteins*. Oxford: Oxford University Press, Inc, pp. 175-212.
- Kwon, Y. K. and Hecht, N. B. (1991). Cytoplasmic protein binding to highly conserved sequences in the 38 untranslated region of mouse protamine 2 mRNA, a translationally regulated transcript of male germ cells. *Proc. Natl. Acad. Sci.* *88*, 3584-3598.
- Laetsch, W. M. (1967). Ferns. In: Methods in Developmental Biology, eds. Fred H. Wiltand Norman K. Wessells, pp.319-328. Tomas Y. Crowell Co.: New York.

- Lamond, A. I., and Spector, D. L. (2003). Nuclear speckles: a model for nuclear organelles. *Nat. Rev. Mol. Cell Biol.* 4, 605–612.
- Le Bot, N., Antony, C., White, J., Karsenti, E., and Vernos, I. (1998). Role of xklp3, a subunit of the *Xenopus* kinesin II heterotrimeric complex, in membrane transport between the endoplasmic reticulum and the Golgi apparatus. *J. Cell Biol.* 143, 1559–1573.
- Le Hir, H., Gatfield, D., Izaurralde, E., and Moore, M. J. (2001b). The exon-exon junction complex provides a binding platform for factors involved in mRNA export and nonsense-mediated mRNA decay. *EMBO J.* 20, 4987–4997.
- Lopez de Heredia, M., and Jansen, R.P. (2004). mRNA localization and the cytoskeleton. *Curr. Opin. Cell Biol.* 16, 80-85.
- Luo, M. J., and Reed, R. (1999). Splicing is required for rapid and efficient mRNA export in metazoans. *Proc. Natl. Acad. Sci. USA* 96, 14937–14942.
- MacIndoe, J. H., and Turkington, R.W. (1973). Hormonal regulation of spermidine formation during spermatogenesis in the rat. *Endocrinology.* 92, 595-605.
- Marc, J., and Gunning, B.E.S. (1986). Immunofluorescent localization of cytoskeletal tubulin and actin during spermatogenesis in *Pteridium aquilinum* (L.) Kuhn. *Protoplasma.* 134, 163–177.
- Mark S. Miller, M. S., Esparza, J. M., Lippa, A. M., Lux, III, F. G., Cole, D. G., and Dutcher, S. K. (2005). Mutant Kinesin-2 Motor Subunits Increase Chromosome Loss. *MCB.* 16, 8: 3810-3820.
- Masumori, M., Yamamoto, N., and Sasaki, S. (1992). Stored mRNA in Pine Seeds: Prolonged Preservation in Dry Seeds and Disappearance during Germination. *Plant and Cell Physiology.* 33, (4): 485-488.
- Matsuzaki, S., Tanaka, S., Suzuki, M., Hamana, K. (1981). A possible role of cadaverine in the biosynthesis of polyamines in the Japanese newt testis. *Endocrinol Jpn.* 28, (3): 305-12.
- Mayer, U., and Jurgens, G. (2002). Microtubule cytoskeleton: a track record. *Curr. Opin. Plant Biol.* 5, 494-501.
- McDonald, P.M., and Smibert, C.A. (1996). Translational regulation of maternal mRNAs. *Curr. Opin. Genet. Dev.* 6, (4):403-407.
- McIntish, J. R., and Porter, K. R. (1967). Microtubules in the spermatids of domestic fowl. *J. Cell Biol.* 35, 153-173.
- Miller, M. S., Esparza, J. M., Lippa, A. M., Lux, III, F. G., Cole, D.G., and Dutcher, S.K. (2005). Mutant Kinesin-2 Motor Subunits Increase Chromosome Loss. *MCB.* 16, (8): 3810-3820.
- Mizukami, I., and Gall, J., (1966). Centriole replication II. Sperm formation in the fern *Marsilea*, and the cycad *Zamia*. *J. Cell Biol.* 29, 97-111.
- Molk, J. N., and Wolniak, S. M. (2000). Spermatid formation in *Marsilea vestita* involves Myosin Light Chain Kinase (MLCK). *Mol. Biol. of the Cell.* 11s: 352a.
- Morris, R. L., and Scholey, J. M. (1997). Heterotrimeric kinesin-II is required for the assembly of motile 9_2 ciliary axonemes on sea urchin embryos. *J. Cell Biol.* 138, 1009–1022.
- Müller, S., Han, S., and Smith, L. (2006). Two kinesins are involved in the spatial control of cytokinesis in *Arabidopsis thaliana*. *Curr. Biol.* 16, 9: 888-894.

- Myles, D. G., and Bell, P. R. (1975). An ultrastructural study of the spermatozoid of the fern, *Marsilea vestita*. *J. Cell Sci.* 17, 633-645.
- Myles, D. G., and Hepler, P. K. (1977). Spermiogenesis in the fern *Marsilea vestita*: microtubules, nuclear shaping, and cytomorphogenesis. *J. Cell Sci.* 23, 57-83.
- Myles, D. G., and Hepler, P. K. (1982). Shaping of the sperm nucleus in *Marsilea*: a distinction between factors responsible for shape generation and shape determination. *Develop. Biol.* 90, 238-252.
- Needleman, D. J., Ojeda-Lopez, M. A., Raviv, U., Miller, H. P., Wilson, L., and Safinya, C. R. (2004). Higher order assembly of microtubules by counterions: From hexagonal bundles to living necklaces. *PNAS.* 101, (46): 16099-16103.
- O'Brien, T. P., and McCully, M. E. (1981). *The Study of Plant Structure. Principles and Selected Methods*, Melbourne, Australia: Termarcaphi Pty. Ltd.
- Oliva, R., Vidal, S., and Mezquita, C. (1982). Cellular content and biosynthesis of polyamines during rooster spermatogenesis. *Biochem J.* 208, (2): 269-273.
- Palacios, I. M., Gatfield, D., St. Johnston, D., and Izaurralde, E. (2004). An eIF4AIII-containing complex required for mRNA localization and nonsensemediated mRNA decay. *Nature.* 427, 753-757.
- Paris, J., K. Swenson, H. Piwnica Worms, and J. D. Richter. (1991). Maturation-specific polyadenylation: *In vitro* activation by p34cdc2 and phosphorylation of a 58-kD CPE-binding protein. *Genes & Dev.* 5, 1697-1708.
- Parkin, N. T., Cohen, E. A., Darveau, A., Rosen, C., Haseltine, W., and Sonenberg, N. (1988). Mutational analysis of the 5' non-coding region of human immunodeficiency virus type 1: effects of secondary structure on translation. *EMBO J.* 7, 2831-2837.
- Pegg A. E., Poulin, R., and Coward, J. K. (1995). Use of aminopropyltransferase inhibitors and non-metabolized analogs to study polyamine regulation and function. *Int. J. Biochem. Cell Biol.* 27, 425-42.
- Pennelle, R., Hyams, J. S., and Bell, R. P. (1986). The blepharoplast of *Marsilea*: a structure concerned with basal body assembly lacking tubulin. *Eur. J. Cell Biol.* 40, 238-241.
- Pennelle, R., Vondy, K.P., Bell, R.P., and Hyams, J.S. (1988). Composition and function of the blepharoplast of *Marsilea vestita*. *Eur. J. Cell Biol.* 46, 51-60.
- Pohjanpelto, P., Virtanen, I., and Holta, E. (1981). Polyamine starvation causes disappearance of actin filaments and microtubules in polyamine-auxotrophic CHO cells. *Nature.* 293, 475 - 477.
- Pollard, K. J., Samuels, M. L., Crowley, K. A., Hansen, J. C., and Peterson, C. L. Functional interaction between GCN5 and polyamines: a new role for core histone acetylation. (1999). *EMBO. J.* 18, (20): 5622-33.
- Proweller, A. and Butler, S. (1994). Efficient translation of poly(A)-deficient mRNAs in *Saccharomyces cerevisiae*. *Genes & Dev.* 8, 2629-2640.
- Quemener, V., Blanchard, Y., Lescoat, D., Havouis, R., and Moulinoux, J. P. (1992). Depletion in nuclear spermine during human spermatogenesis, a natural process of cell differentiation. *Am. J. Physiol. Cell Physiol.* 263, 343-347
- Raff, R. A., Collot, H. V., Selvig, S. E., and Gross, P. R. (1972). Oogenetic origin of messenger RNA for embryonic synthesis of microtubule proteins. *Nature.* 235, 211-214.

- Ray, K., Perez, S. E., Yang, Z., Xu, J., Ritchings, B. W., Steller, H., and Goldstein, L. S. (1999). Kinesin-II is required for axonal transport of choline acetyltransferase in *Drosophila*. *J. Cell Biol.* *147*, 507–518.
- Reddy, A. S. (2001). Molecular motors and their functions in plants. *Int. Rev. Cytol.* *204*, 97-178.
- Richter, J. D. (1991) Translational control in early development. *BioEssays.* *13*, 179-183.
- Richter, J. D. and Smith, L. D. (1984). Reversible inhibition of translation by *Xenopus* oocyte-specific proteins. *Nature.* *309*, 378-380.
- Rosenthal, E. T., Bahr, M., and Wilt, F. H. (1993). Regulation of maternal messenger RNA translation during oogenesis in *Urechis caupo*. *Dev. Biol.* *155*, 297-306.
- Sarpal, R., Todi, S. V., Sivan-Loukianova, E., Shirolkar, S., Subramanian, N., Raff, E. C., Erickson, J. W., Ray, K., and Eberl, D. F. (2003). *Drosophila* KAP interacts with the kinesin II motor subunit KLP64D to assemble chordotonal sensory cilia, but not sperm tails. *Curr. Biol.* *13*, 1687–1696.
- Scheer, U. and Dabauvalle, M-C. (1895). Functional organization of the oocyte nucleus. In Browder L.R. (ed). *Developmental Biology*, vol 1. Plenum, New York, pp 385-430.
- Shakir, M. A., Fukushige, T., Yasuda, H., Miwa, J., and Siddiqui, S. S. (1993). *C. elegans* *osm-3* gene mediating osmotic avoidance behavior encodes a kinesin-like protein. *Neuroreport.* *4*, 891–894.
- Sharp, L. W. (1914). Spermatogenesis in *Marsilea*. *Bot. Gaz.* *58*, 419-432.
- Shibuya, T., Tange, T. O., Sonenberg, N., and Moore, M. J. (2004). eIF4AIII binds spliced mRNA in the exon junction complex and is essential for nonsense-mediated decay. *Nat. Struct. Mol. Biol.* *11*, 346–351.
- Sible, J. C., Marsh, A. G., Walker, C. W. (1990). Effect of extrinsic polyamines on post-spawning testes of the sea star, *Asterias vulgaris* (Echinodermata) : implications for the seasonal regulation of spermatogenesis. *Invert. Reprod.Develop.* *19*, (3): 257-264.
- Slocum, R. B., and Flores, H. E. (1991). Biochemistry and Physiology of Polyamines in Plants. CRC Press.
- Sommerville, J. (1981). Immunological and structural organization of nascent RNP. In: Bussch H (ed). *The cell nucleus*. Vol 8. Academic Press, New York, pp 1-57.
- Sommerville, J. (1992). RNA binding proteins: masking proteins revealed. *BioEssays.* *14*, 337-339.
- Sommerville, J. and Ladomery, M. (1995). Transcription and masking of mRNA in germ cells: involvement of Y-box proteins. *Chromosoma.* *104*: 469-478.
- Sommerville, J. and Ladomery, M. (1996). Masking of mRNA by Y-box proteins. *The FASEB Journal.* *10*, 435-443.
- Spirin, A. S. (1994). Storage of messenger RNA in Eukaryotes: Envelopment with protein, translational barrier at 5' side, or conformational masking by 3' side. *Mol. Rep. and Develop.* *38*, 107-117.
- St. Johnston, D. Driever, W., Berleth, T., Riehlstein, S. and Nüsslein-Volhard, C. (1989). Multiple steps in the localization of *bicoid* RNA to the anterior pole of the *Drosophila* oocyte. *Development.* *107*, 13-19.
- Stavy, L., and Gross, P. R. (1969). Availability of mRNA for translation during normal and transcription-blocked development. *Biochimica et Biophysica Acta.* *182*: 203-213.
- Tabor, C. W., and Tabor, H. (1976). 1,4-Diaminobutane (Putrescine), Spermidine, and Spermine. *Annu. Rev. Biochem.* *45*, 285-306.

- Tabor, C. W., and Tabor, H. (1984). Polyamines. *Annu. Rev. Biochem.* *53*, 749-790.
- Tafari, S. R., Familiari, M., and Wolffe, A. P. (1993). A mouse Y-Box protein, MSY1, is associated with paternal mRNA in spermatocytes. *J. Biol. Chem.* *268*, 12213-12220.
- Tange, T. O., Nott, A., and Moore, M. J. (2004). The ever-increasing complexities of the exon junction complex. *Curr. Opin. Cell Biol.* *16*, 279–284.
- Tange, T. O., Shibuya, T., Jurica, M. S., and Moore, M. J. (2005). Biochemical analysis of the EJC reveals two new factors and a stable tetrameric protein core. *RNA.* *11*, 1869–1883.
- Telford, N. A., Watson, A. J., Schultz, G. A. (1990). Transition from maternal to embryonic control in early mammalian development: A comparison of several species. *Mol. Rep. Dev.* *26*, (1): 90-100.
- Tsai, C. W., and Wolniak, S. M. (2001). Cell cycle arrest allows centrin translation but not basal body formation during spermiogenesis in *Marsilea*. *J. Cell Sci.* *114*, 4265-4272.
- Tsai, C. W., Van der Weele, C. M., and Wolniak, S.M. (2004). Differential segregation and modification of mRNA during spermiogenesis in *Marsilea vestita*. *Dev. Biol.* *269*, 319-330.
- Tuma, M. C., Zill, A., Le Bot, N., Vernos, I., and Gelfand, V. (1998). Heterotrimeric kinesin II is the microtubule motor protein responsible for pigment dispersion in *Xenopus melanophores*. *J. Cell Biol.* *143*, 1547–1558.
- Turner, F. R. (1970). The effects of colchicine on spermatogenesis in *Nitella*. *J. Cell Biol.* *46*, 220-234.
- Van der Weele, C. M., Tsai, C. W., Wolniak, S.M. (2007). Mago Nashi is essential for spermatogenesis in *Marsilea*. *MBC.* *18*, (10): 3711-3722.
- Vaughn, K. C., Sherman, T. D., Renzaglia, K.S. (1993). A centrin homologue is a component of the multilayered structure in bryophytes and pteridophytes. *Protoplasma.* *174*, 1-2: 58-66.
- Verhey, K. J., Meyer, D., Deehan, R., Blenis, J., Schnapp, B. J., Rapoport, T. A., and Margolis, B. (2001). Cargo of kinesin identified as JIP scaffolding proteins and associated signaling molecules. *J. Cell Biol.* *152*, (5): 959-970.
- Walker, J., Dale, M. and Standart, N. (1996). Unmasking mRNA in clam oocytes: Role of phosphorylation of a 38 UTR masking element-binding protein at fertilization. *Dev. Biol.* *173*, 292–305.
- Wolniak, S. M. and Swamy, R. N. (2004). Microfilaments and spermatid differentiation in *Marsilea*. *MBC.* *15*(Suppl. S): 90A–91A
- Wolniak, S. M., V.P. Klink, P. E. Hart and C. W. Tsai. (2000). Control of Development and motility in the spermatozooids of lower plants. *Grav. Sp. Biol. Bull.* *13*, 85-93.
- Yamazaki, H., Nakata, T., Okada, Y., and Hirokawa, N. (1995). KIF3A/B: a heterodimeric kinesin superfamily protein that works as a microtubule plus end-directed motor for membrane organelle transport. *J. Cell Biol.* *130*, 1387–1399.
- Yang, Z., Roberts, E. A., and Goldstein, L. S. (2001). Functional analysis of mouse kinesin motor Kif3C. *Mol. Cell. Biol.* *21*, 5306–5311.
- Yatin, M. (2002). Polyamines in living organisms. *J. Cell and Mol. Biol.* *1*, 57-67.
- Zhou, Z., Luo, M. J., Straesser, K., Katahira, J., Hurt, E., and Reed, R. (2000). The protein Aly links pre-messenger-RNA splicing to nuclear export in metazoans. *Nature* *407*, 401–405.